The natural product sulforaphane inhibits breast cancer stem cell targets in triple negative and trastuzumab-resistant breast cancers

By

Joseph Burnett

A dissertation submitted in partial fulfillment
of the requirements for the degree of
Doctor of Philosophy
(Pharmaceutical Science)
in the University of Michigan
2015

Doctoral Committee:

Professor Duxin Sun, Chair

Professor Kyung-Dall Lee

Professor David E. Smith

Professor Max S. Wicha

To my parents, Rick and Donna Burnett, who taught me to follow my dreams and the work ethic required to achieve them. Further, to my siblings Jessi, Beth, Abbe, Jake, and Rick whose love and support made this possible.

Acknowledgements

I would like to thank my advisor, Dr. Duxin Sun, for his guidance through the years of my training. His mentorship has helped me develop not only as a scientist, but as a human being. With his consistently positive attitude he leads by example, demonstrating the importance of humility, honesty, and integrity in both scientific research and life in general.

I would also like to give a special thank you to my committee members. Dr. Max Wicha welcomed me into his lab group and was instrumental in cultivating my understanding of the root causes of cancer. Dr. David Smith was always available to convey the importance of obtaining a truly in-depth knowledge of the intricacies required to conduct scientific research. Dr. Kyung-Dall Lee was able to help me understand the broader picture of how my research fits into the wide body of scientific knowledge. I would also like to acknowledge the talented people who I have had the pleasure to work with: Lichao Sun, Mari Gasparyan, Bryan Newman, Hayley Paholak, Jamie Connarn, Hebao Yuan, Fangying Xu, Miao-Chia Lo, Hongwei Chen, Yiqun Jiang, Tao Zhang, Yanyan Li, Hsiu-Fang Lee, Sarah Williams, Hui Jiang, Yasuhiro Tsume, Ronak Shah, Hasan Korkaya, Maria Ouzounova, Sarah Conley, Sean McDermott, Yajing Liu, Tahra Luther, Shawn Clouthier and all other past and present members of the Sun and Wicha labs.

Table of Contents

List of Figures

Abstract

The cancer stem cell (CSC) hypothesis provides a hierarchical model which explains the observed heterogeneity of cancers cells within a tumor. CSCs sit at the apex of the tumor hierarchy and are uniquely capable of initiating tumor formation. These cells retain two key properties: self-renewal, which allows for long term proliferation potential and the capability to differentiate into the heterogeneous cell lineages found within a tumor. In order to truly cure patients it is necessary to not only reduce tumor volume but eliminate all cell populations within the cancer. Accumulating evidence suggests that breast cancers are driven by CSCs and that this model can address two critical needs associated with drug resistance in patients to improve overall survival. In this report we demonstrate that in triple negative breast cancers (TNBCs) current chemotherapy fails to eliminate, and may even expand, breast CSCs through activation of the NF-kB signaling node. Similarly, we demonstrate in HER2+ breast cancers with PTEN inactivation that the generation of trastuzumab resistance results in the dependence on an IL6/STAT3/NF-kB positive feedback loop. Activation of this signaling loop induced the epithelial to mesenchymal transition, expanded BCSCs, and results in a subtype conversion from HER2+ to TNBC. In these contexts, current treatment strategies are simply delaying disease progression rather than attacking the roots of breast cancer. Using the natural product sulforaphane (SF) which has been demonstrated to inhibit NF-kB signal transduction, we demonstrate that this compound can be used to address these issues. In

this report SF preferentially inhibited TNBC cell lines and CSCs. Due to its inhibition of NF-kB, SF reduced IL6-mediated BCSC expansion induced by docetaxel treatment. Consequently, combination of the two therapies dramatically reduced both tumor volume and CSCs. In trastuzumab resistant, PTEN deficient, breast cancers NF-kB inhibition by SF was sufficient to eliminate both of these populations. By analyzing the transcriptional landscape of trastuzumab sensitive and resistant cell lines in the presence of SF with RNA sequencing, MEOX1 was identified as a novel drug target capable of regulating bulk cell line proliferation and breast CSC self-renewal in trastuzumab resistant breast cancer and a subset of TNBCs.

Chapter 1

Background

Abstract

The cancer stem cell (CSC) hypothesis presents a fundamentally different paradigm for cancer treatment. CSCs reflect a small fraction of tumor initiating cells capable of sustained self-renewal and differentiation to form the heterogeneous tumor bulk. In order to cure cancer, it is necessary to eliminate CSCs in addition to differentiated cancer cells to decrease metastasis, reduce recurrence, and improve patient survival. In this chapter, we review signaling pathways which regulate CSCs, including Wnt, Hedgehog, and Notch, as well as interactions of CSCs with the tumor microenvironment. Further, we discuss methods to isolate CSCs and demonstrate ways to identify therapeutic efficacy toward eliminating these cells. Natural products which regulate key signaling pathways with CSCs are also highlighted. Applying the CSC model to breast cancers we identify specific clinical issues which can be addressed by inhibition of these cells. Finally, using the natural product sulforaphane we propose three specific aims which can be used to overcome such issues.

Introduction

Currently, cancer is the second leading cause of death in the United States and is estimated to be the leading cause of death worldwide by the World Health Organization.

Tumorigenesis occurs when normal cells accumulate sufficient mutations to allow for sustained proliferation, evasion of apoptosis, and ultimately tissue invasion and metastasis (1). Substantial progress has been made with respect to the treatment of primary tumors using surgery, chemotherapy, radiation therapy, and radiofrequency ablation. However, the advancement of cancer to an invasive or metastatic stage is frequently associated with a poor patient prognosis and remains a critical hurdle in the treatment of the disease (2). The heterogeneity of the cancer cells pose great challenges for effective treatment using conventional therapy as all cancer cells do not respond to therapy homogeneously, leaving the potential for recurrence (3).

A mechanistic understanding of the observed heterogeneity in tumors has yet to be fully elucidated, and has historically been a subject of controversy within the cancer research field (4). Since the observation that a single murine leukemia cell was capable of generating a tumor graft, there have been numerous reports illustrating that the capacity for tumor initiation is heterogeneous within subpopulations of cancer cell lines and primary tumors. Strikingly, in a human autotransplantation study by Southam and Brunschwig, it was demonstrated that a minimum of one million unsorted cells from primary tumors were required to form secondary engraftments and that the frequency of initiation varied by the form of carcinoma (5). The stochastic model predicts that phenotypic differences among tumor cells are influenced by random intrinsic and extrinsic factors and that every cell has an equal likelihood of tumorigenic transformation(6). Interestingly, a recent breast cancer study argues that this model may still have some relevance today (7). However, over the past 50 years, mounting evidence in leukemias as well as several solid cancers including brain, breast, colon, head/neck,

liver, pancreas, prostate, and ovarian indicate that tumors are organized in a hierarchical manner somewhat paralleling their organ of origin (8-11).

Advances in hematopoietic stem cell (HSC) research established that HSCs are capable of sustained self-renewal, proliferation, and differentiation (6). These results were later confirmed after the isolation of mouse hematopoietic stem cells based on a variety of phenotypic markers (12). Analogous studies in Acute Myeloid Leukemia (AML) (13, 14) ultimately led to the discovery of AML cancer stem cells (CSCs) in 1994 by John Dick's group (15). The hierarchical CSC model proposes only a small fraction (typically <10%) of cells within the cancer, known as CSCs, are capable of tumor initiation and unlimited self-renewal through asymmetric division(4). Furthermore, these populations are responsible for differentiation into the other heterogeneous lineages found within a tumor. Current studies have shown, using this functional definition, that CSCs are resistant to conventional cancer treatments such as radiotherapy and chemotherapy (16). This model then requires a paradigm shift in the way in which cancer is treated. In order to effectively eliminate the roots of cancer, CSC specific inhibitors must be developed.

Epidemiological studies have shown strong correlations between consumption of certain dietary products and herbal remedies with reduced risk of developing a host of cancers (17-19). As a result natural produces with known mechanisms of action and, those recently discovered to be biologically active, have gained considerable attention as agents capable of modulating CSCs (20). Here we briefly review CSC biology and the mechanisms by which natural products modulate essential CSC pathways. The potential of combining these CSC targeting natural products with conventional chemotherapy agents known to eradicate more differentiated cancer cells will also be discussed.

Therapeutic Implications of the CSC Model

While many advances have been made in terms of surgical treatment and diagnosis, recurrence and metastasis still remain as major obstacles to overcome (21, 22). Applying the CSC model not only provides significant insight into why conventional therapy fails, but also provides druggable targets which may unlock the key to curing this debilitating disease (23). Clinical trial endpoints for the approval of chemotherapy drugs have historically been based on improvements in overall survival or more commonly by direct tumor assessments (24). With respect to direct tumor assessments, three common methods exist for quantifying results: objective response rate (ORR), time to progression (TTP), and progression-free survival (PFS) (25). The RECIST criteria can be used to measure therapeutic response, although together, all of these results are predominantly based on tumor size (26). Using these statistics as endpoints of clinical trials has resulted in identification of compounds which can reduce the size of primary tumors, but may have little to no effect on CSCs.

The CSC model predicts that the bulk of a tumor is made up of differentiated tumor cells while only a small fraction are CSC (27, 28) responsible for metastasis, recurrence, and drug resistance (29, 30). However, because of the inherent differences in drug response between these two populations, it is possible that currently approved chemotherapeutics are only effective against the more differentiated tumor cells representing the bulk of the tumor (Fig. 1.1). Indeed, recent literature suggests that most current chemotherapeutics (such as cisplatin, doxorubicin, and docetaxel) and radiation therapy lack the ability to kill CSCs (31-33). Alarmingly, these conventional therapies have been demonstrated to even expand the population of CSCs (34, 35). Consequently, tumor regression may be

an inadequate endpoint for clinical trials because the remaining CSCs, either from the primary tumor or at sites of micrometastases can simply initiate new tumors, and potentially pass on a drug resistant phenotype (16). Therefore, strategies which inhibit CSCs by targeting critical CSCs signaling pathways (36-38) are essential to treatment.

While the CSC model predicts that elimination of CSCs will prevent recurrence and metastasis, the removal of the bulk tumor mass is also beneficial. Cancer cells that are more differentiated than CSCs may retain limited proliferation potential, indicating that tumor growth may still occur. It is also plausible that these genetically unstable tumor cells could obtain additional mutations, or stochastic influence (7), sufficient to regain self-renewal capacity, consequently little would be done to cure the cancer. Bulk tumor volume is also responsible for unwanted symptoms in patients. For instance, solid neoplasms of the brain lead to increased intracranial pressure while tumor size in patients diagnosed with renal angiomyolipoma is correlated with aneurysm formation (39). Thus, to improve the overall quality of life and reduce future risk elimination of both CSCs as well as the more differentiated cancer cells within a tumor is required.

Identifying CSCs and Evaluating Therapeutic Efficacy

With the successful demonstration that AML stem cells could be identified using monoclonal antibodies targeted to the cell surface markers (CD34+/CD38-) (12) and isolated using fluorescent activated cell sorting (40), the CSC model was rapidly applied to solid tumors. While a complete review of all CSC markers is beyond the scope of this review, table 1 summarizes markers used to identify CSCs in a variety of solid tumors as well as the number of cells needed for engraftment in immunocompromised mice. It is

important to note that these cell surface markers vary based on the origin of tumor as well as the molecular subtype of the cancer. For instance, CD44+/CD24-/lin- cells isolated from primary breast cancer patients preferentially initiate tumors in NOD/SCID mice with as few as 100 cells (11). When comparing the expression of these markers in basal and luminal type breast cancer cell lines Fillmore and Kuperwasser maintain that this population more accurately describes a basal cellular phenotype (41). It was further shown that the CD44+/CD24-/ESA+ fraction better reflect the CSC properties of tumor initiation, quiescence, tumorsphere formation, and chemo-resistance in basal type cell lines. These results demonstrate a need for general molecular markers of CSCs.

Aldehyde dehydrogenase (ALDH) has gained considerable attention and has demonstrated utility in identifying stem and progenitor cells in both normal and malignant tissue, as well as across species. The activity of this enzyme is responsible for intracellular detoxification of aliphatic and aromatic aldehydes via the oxidation to carboxylic acids (42). One such substrate, retinaldehyde is a critical precursor to retinoic acid, which can further direct differentiation of stem cells via GSK3-β signaling (43). ALDH positive cells contain normal murine and human hematopoietic (44, 45), neural (46), and mammary stem cells (28). Furthermore, in primary tumors as well as cell lines, ALDH+ sorting, alone or in conjunction with cell surface markers can be used to isolate CSCs for head and neck (47), mammary (28), pancreatic (48), and ovarian cancers (49).

At the root of defining these populations as CSCs is the observation that in all cases, the ALDH+ cells preferentially initiate tumor formation *in vivo* (using serial dilution analysis in a murine xenograft model), are capable of sustained self-renewal (demonstrated by serial passages in immunocompromised mice), and differentiation to form the bulk of

tumor mass (ALDH+ cells regenerate heterogeneity of primary tumor as opposed to ALDH- cells) (28, 50). In breast cancer cell lines, Charafe-Jauffret *et al*. utilized Affymetrix microarrays to illustrate that ALDH+ cells overexpress known stem cell self-renewal genes such as NOTCH2 and NFYA (51). Conversely, ALDH- populations exhibited higher levels of genes responsible for apoptosis and differentiation.

Table 1. Prospective Identification of CSC markers in solid tumors.

Origin of tumor	CSC Marker	CSCs required for initiation	Reference
Brain	CD 133+	100	(57, 58)
Breast	CD44+CD24-(EpCAM+) ALDH+ CD44+CD24-ALDH+	100 500 20	(11, 28, 41)
Colon	EpCAM+CD44+	200	(59)
Head and Neck	CD44+ ALDH+	5000 500	(9, 60, 61)
Pancreas	CD44+CD24+ESA+ ALDH+	100 100	(48, 50)
Prostate	CD44+	100-1000	(62)
Ovaries	CD133+(ALDH+)	2000	(63)

While the search for a universal CSC marker is appealing, it is essential to note that the term CSC is a functional definition, as these cells may arise from any number of mutagenic transformations. Consequently, monitoring the efficacy of CSC-targeted drugs may not be possible with the use of surface markers or enzymatic activity alone. Neuronal stem cell studies demonstrated that primitive neuronal cells are anchorage

independent and produce floating colonies called neurospheres when grown in non-adherent conditions (52). Similarly, the self-renewal capacity of CSCs can be demonstrated *in vitro* through tumor sphere formation (53). Primary tumors or cell lines are dissociated into single cell suspensions and placed in serum free media containing bFGF and VEGF. In these nonadherent culture conditions differentiated cells will undergo anoikis, while CSCs survive, self-renew, and differentiate to produce a spherical cluster enriched in stem and progenitor cells (54). Under no external stress, tumorspheres can be dissociated and passaged to further generations. In the presence of therapeutics that inhibit CSCs, sphere size and formation frequency will be reduced (55). Treated spheres are then dissociated and passaged for a second generation in the absence of therapeutic; alterations in sphere formation then reflect the self-renewal capacity changes in the CSCs.

The "gold standard" for assessing CSC inhibition is demonstrating a reduction in xenograft take when tumors cells are implanted in NOD/SCID mice (56). In contrast, reduction in tumor growth in vivo is not an appropriate measurement to quantify CSC reduction by therapeutics. In a model of advanced carcinogenesis, where tumors are already fully established, the CSC population represents typically less than 10% of tumor bulk. Thus, even complete abolition of CSCs may not result in reduced tumor volume. In order to evaluate a therapeutics effect on CSCs, it is necessary to dissociate the primary tumor and engraft the serially diluted cells in secondary animals. Therapeutic response of the CSCs can then be seen through reduction in tumor initiation and growth.

Targeting CSC signal transduction

Developmental biology studies have revealed three major signaling pathways, Wnt, hedgehog (Hh), and Notch, are essential for the self-renewal and differentiation properties of stem cells. Due to the phenotypic similarities of CSCs to their normal stem cell counterparts, it is no surprise that these pathways also regulate CSCs and targeting each one has demonstrated efficacy toward eliminating cancers. Several key signaling nodes also act as points of cross talk between these pathways and are known to be regulated by natural products. Furthermore, dynamic interactions of CSCs with the tumor microenvironment reveal a niche which can be exploited for drug discovery. Figure 1.2 summarizes the critical components of each pathway and demonstrates the interconnected nature of signaling in CSCs. Figure 1.3 highlights natural produces capable of inhibiting these pathways.

The WNT signaling pathway

Purified Wnt3A from mouse L cells, as well as up regulation of downstream transcription factor β-catenin, has shown an increase in HSC proliferation and reduced differentiation *in vitro* (64, 65). In the intestinal epithelium, Wnt target gene Lgr5 is exclusively expressed by stem cells in the crypt base capable of generating all epithelial lineages, additionally similar results were found in the colon and pyloric glands (66, 67). Prolonged culture of mammary SC enriched populations, in the presence of Wnt3A, were capable of regenerating the cleared fat pads of recipient mice whereas those without Wnt proteins were not (68). Additionally, a cell-surface glycoprotein known as CD44 implicated in hematopoiesis (69) and tumor progression is modulated by Wnt signaling components APC and Tcf4 (70, 71).

Enhanced activation of Wnt signaling has also been observed in a host of cancers including both acute myeloid and chronic lymphoid leukemias (72, 73). One of the most well studied changes in Wnt signaling is the loss of function of the APC gene leading to Familial Adenomatous Polyposis (74). Furthermore, one of the most common genetically engineered mouse models for breast cancer study (MMTV-Wnt-1) develops mammary tumors via deregulation of Wnt signaling leading to aberrant β-catenin activation. Consistent with reports of human breast cancer, these mice contain a subpopulation of highly tumorigenic CSCs (75). To assess targets within the Wnt pathway it is essential to know the mechanism by which signal transduction occurs (76-78).

The conical Wnt signaling pathways contains two receptors, the seven transmembrane domain Wnt binding protein Frizzled (Fz) and its co-receptor low density lipoprotein receptor-related protein (LRP). Associated with the intracellular domain of Fz is the scaffold protein Dishevelled (Dvl), which serves as a platform for assembly of signal transduction proteins (79). In the absence of Wnt stimulation a cytoplasmic protein complex exists in which transcriptional activator and cytoskeletal linker β-catenin is phosphorylated and subsequently eliminated by ubiquitination and proteasomal degradation. Within this complex are the scaffold protein Axin, the human tumor suppressor adenomatosis polyposis coli (APC) protein, and the kinase regulating β-catenin degradation GSK-3β. In the event of Wnt protein binding to Fz, LRP and Dvl become phosphorylated by GSK-3β and casein kinase (CK) proteins (80). Axin also associates with LRP at the cell surface and consequently β-catenin is no longer degraded.

Translocation of β-catenin to the nuclease occurs, where it acts with LEF/Tcf transcription factors to regulate Wnt target gene expression.

Natural products that modulate Wnt signaling have proven to be effective at targeting CSCs. Piperine, an alkaloid derived from black and long peppers, has been shown to reduce lung metastasis in a melanoma mouse model (81) as well as prevent chemically induced lung carcinogenesis (82). Prevention of metastasis and tumor initiation by this compound indicates an effect on CSCs. These results were confirmed in both primary breast tissue and breast cancer cell lines by Kakarala *et al*. using mammospheres formation and the BCSC marker ALDH1 (83). In this study, the observation that little response was shown in differentiated cells indicates a mechanism of action primarily important in SCs. A LEF/Tcf green fluorescence protein reporter was used in the luminal cell line MCF7 to indicate that inhibition of Wnt signaling was mediating piperine's effect.

High-throughput screening (HTS) has also been used to identify natural products that block Wnt signaling. Lepourcelet et.al. demonstrate that high-throughput ELIZA can be utilized to determine the binding of β-catenin to Tcf4 (84). After screening approximately 7,000 natural products and 45,000 synthetic compounds, Eight natural products were capable of obtaining IC50 values less than 10 μM whereas no synthetic compounds produced the same results. Selective inhibitors of BCSCs have also been identified by HTS. Immortalized human mammary epithelial cells undergoing an epithelial to mesenchymal transition (EMT) adopt SC-like properties and markers (85). By inducing this phenomenon Gupta *et al*. identified four compounds with consistent selectivity toward the EMT-induced cells and one compound salinomycin was confirmed

to eradicate BCSCs (35). Recent studies in chronic lymphocytic leukemia demonstrate that this potassium ionophore downregulates LRP, preventing its activating phosphorylation as well as reducing Wnt target gene expression with nanomolar efficacy.

The Hedgehog signaling pathway

The Hedgehog (Hh) signaling pathway has been known for some time to regulate tissue polarity, embryonic patterning, and organ development. Experiments in the development of Drospohila demonstrated that cells in posterior limb compartments release Hg to mediate development in anterior compartments indirectly through Wnt signaling (86). In mammals three secreted proteins known as Desert hedgehog (Dhh), Indian hedgehog (Ihh), and Sonic hedgehog (Shh) are endogenous activators of the Hh signaling cascade (87). Of these, Shh facilitates differentiation in the mouse neural tube in a gradient fashion via production and secretion from the notochord and floor plate (87). Additionally, activation of the Gli2 transcription factor by Hh signaling in mammary stroma supports normal ductal formation (88).

The influence of Hh on cell fate indicates that it is a key factor in differentiation and plays a role in SC and CSC biology. Using primarily neurosphere culture and BrdU labeling to monitor quiescence, Palma and Altaba demonstrated embryonic and postnatal neocortical cells from mice contained stem cell like properties (89). Furthermore, these cells were reliant upon Shh-Gli and EGF to maintain self-renewal. In a companion study Palma *et al*. demonstrated that the Shh-Gli signaling is critical for the regulation of stem cells in the adult mouse subventricular zone (90). The generation of $Ihh^{-/-}$ embryonic mice also demonstrated a reduction in the size of intestinal microvilli, and was attributed

to lower proliferation rates in the stem cell compartment(91). With respect to BCSCs, primary human tumors produce higher mRNA levels of Hedgehog signaling receptors (PTCH/SMO) and transcription factors (GLI1/GLI2) (92). Further, in glioma CSCs pharmacological inhibition of Hh-Gli signaling prevents self-renewal *in vitro* and tumor growth in xenograft models (53).

The Hh signaling pathway exists typically "off state", and like the Wnt pathway contains two receptors smoothened (SMO) and patched (PTCH). In the absence of one of the three hedgehog ligands, PTCH binds and prevents association of SMO with the cell membrane. The off state is also characterized by the sequestration of GLI transcription factors to microtubules by SuFu and Kif7. This state allows for GLI phosphorylation by PKA, CK, and GSK-3β subsequently followed by degradation. Binding of Hh ligands to PTCH relieves inhibition of SMO, allowing for translocation to the microtubule. SMO then prevents the action of kinases on GLI, allowing it to translocate to the nucleus and activate transcription (93-95).

The natural product cyclopamine (CYC), derived from *Veratrum Californicum*, has been showed to target the Hedgehog pathway and inhibit transcription. Previous work has shown CYC acts as an antagonist to SMO by direct binding, altering the macromolecular conformation. Inhibition of SMO with CYC locks the Hh pathway in the "off state" preventing transcription (96). With glioblastoma cell lines CYC reduces neurosphere formation and prevents engraftment in mice (97). In an advanced model of pancreatic cancer CYC alone was insufficient to deplete the CSC compartment. However, when combined with conventional chemotherapy agent gemcitabine and mTOR inhibitor rapamycin the CSC levels were virtually undetectable both in vitro and in vivo (98).

The Notch signaling pathway

Notch receptors are key cell coordination proteins that help create complex tissue organization and patterning. In early developmental systems, Notch signaling drives cell fate determination between contacting cell dimers, in which both cells initially carry equal propensity for lineage specialization (99). For example, during neurogenesis, contacting cells expressing both Notch receptors and ligands have equal pull towards a given differentiation pathway. Local variations in expression will cause one cell to express higher levels of Notch ligands, thereby causing Notch mediated inhibition of neuronal development in the neighboring cell (100, 101). This "lateral inhibition" helps to drive local distinctions in cell specialization, creating tissue complexity that is seen in a variety of organ systems, such as the retina in flies and tip-cell formation during angiogenesis (102-104).

The Notch protein is a transmembrane receptor heterodimer, with each monomer containing either the extracellular or intracellular domain. Comprised of four receptors (Notch1-4), the Notch family can interact with any of the five Notch transmembrane ligands: Jagged1 and 2, Delta-like 1, 3, and 4. The extracellular domain of these ligands, expressed on the signaling cell, interacts with the extracellular domain of the Notch receptors. Binding of effector ligand induces a conformational change in the Notch protein allowing for cleavage by the membrane bound metalloprotease TACE/ADAM17. The Notch receptor is further processed by γ-secretase enzymes, which release the Notch Intracellular Domain (NICD) for translocation to the nucleus. In the nucleus, the NICD facilitates conversion of the CSL repressor complex into active transcriptional complex

after recruitment of the MAML1 co-activator protein, leading to a wide assortment of downstream signaling (105-107).

Aberrant regulation of Notch signaling can arise through different mechanisms. Overexpression of Notch ligands, such as Jagged1, have been linked to enhanced Notch activity and correlated with poorer prognosis in breast cancers (108-110). Loss of the negative regulator of Notch signaling, Numb, has also been observed, correlating with a higher tumor grade (111). Constitutive activation of Notch can also occur, although this is more common in hematological cancers where cell-cell interactions are less frequent (112-114). Increased Notch activity influences a number of tumorigenic processes, such as cell-cycle progression, inhibition of apoptosis, and enhanced drug resistance. Notch activation has been shown to stimulate both Cyclin D1 and c-Myc, potent cell cycle regulators (115-117). Upregulation of Hes-1, a downstream Notch target gene, drives several changes to other regulatory pathways. Hes-1 potentiates cell-cycle progression by repressing transcription of cell-cycle kinase inhibitors (118-120). Hes-1 mediated repression of PTEN can lead to inhibition of apoptosis and enhanced survival signaling via PI3K/Akt in different cancer cells (121-123).

Notch activity has been implicated in cell fate determination for both stem and cancer stem cells. Normal mammary stem cells stimulated with a DSL peptide (a surrogate Notch ligand) had an increased capacity for generating mammospheres (124). Neuronal precursor cells were maintained in an undifferentiated state through interaction of Notch with HIF1a (125). Both brain and breast CSCs were shown to require Notch activity for self-renewal, as treatment with gamma secretase inhibitors (GSI) reduced the ability of these CSCs to form spheroid colonies (126, 127). Notch activity has also been observed

during EMT, a process believed to bestow stem-like qualities on differentiated cells. The downstream Notch target gene SLUG was shown to induce EMT in breast cancer cells stimulated with Jagged1 (128).

Disruption of Notch activity with natural products has been demonstrated in a variety of cancer cell types. Both curcumin, a polyphenol found in turmeric, and genistein, a soy isoflavone, were found to disrupt Notch1 mediated activation of NF-κB, leading to increased apoptosis in pancreatic cancer cells (129-131). Resveratrol, another well-known polyphenol, induced apoptosis in MOLT4 acute lymphoblastic leukaemia cells by Notch1 inhibition and subsequent activation of p53 (132). Withaferin-A and Celastrol, triterpenes known for their anti-inflammatory properties, have also been reported to block Notch1 activity in cancer cells (133, 134). Further, both are known to inhibit the function of BCSCs, albeit with varying reported mechanisms of action which may be a result of the importance of certain signaling nodes in multiple CSC signal transduction pathways (135, 136).

Targeting signaling nodes involved in crosstalk between pathways

Critical pathways within CSCs are interconnected and converge at several key regulatory nodes. Mutations in the tumor suppressor phosphatase and tensin homolog (PTEN) gene are common in a host of human cancers. Without the function of PTEN to turn off phosphoinositide-3 kinase (PI3K) signaling the kinase Akt can be constitutively activated, resulting in cellular changes in survival and metabolism (137). Furthermore, Akt is capable of inactivating GSK-3β through phosphorylation(138) and as a consequence relieving inhibition of both Wnt and Notch signaling. Korkaya *et al*. have

utilized this principle to demonstrate that inhibition of Akt with the alkylphospholipid perifosine prevents β-catenin activation and subsequently eliminates BCSCs *in vivo* (139). Perifosine is currently in phase III clinical trials in combination with Capecitabine for the treatment of patients with refractory advanced colorectal cancer.

Previous work in our laboratory has shown that the dietary isothiocyanate sulforaphane (SF) selectively eliminates BCSCs *in vitro* at concentrations as low as 1 μM (55). Further study into the regulation of CSCs with SF revealed a reduction in the level of Akt, phospho-GSK-3β, and β-catenin. Introduction of a GFP β-catenin reporter into the luminal B cell line MCF7, cultured as mammospheres, was used to confirm the reduction in β-catenin mediated transcription. *In vivo*, SF significantly reduced primary tumor growth and prevented tumor engraftment into secondary mice demonstrating that BCSCs were eliminated.

The molecular chaperone heat shock protein 90 (Hsp90) has become a promising target for eliminating multiple forms of cancer. Due to the role of assisting protein maturation and the staggering number its oncogenic clients, such as those in the PI3K/Akt pathway, inhibition of HSP90 may serve as one target that can disrupt multiple pathways. The prototypical HSP90 inhibitor geldanamycin was isolated from *Streptomyces hygroscopicus* and demonstrated efficacy across many forms of cancer (140). However, *in vivo* toxicity limited its potential use and derivatives such as 17-AAG were created (141). This compound has been shown to preferentially inhibit glioma stem cell growth, indicating the potential use HSP90 inhibitors as CSC therapeutics (142). Recently, we have shown that SF synergistically block HSP90 function with 17-AAG through simultaneous disruption of the co-chaperone complex and antagonism of the N-terminal

ATP binding pocket respectively (143). Consequently, client proteins Akt, mutant p53, Raf-1, and Cdk4 were all down regulated, suggesting another possible mechanism for SF function in pancreatic cancer.

Preventing CSC-Microenvironment Interactions

The transcription factor NF-κB, has been shown to be critical to the function of AML CSCs (144). In addition to the conical tumor necrosis factor activation, NF-κB is a key signaling molecule in the pathways responsible for mediating interactions of CSCs with the tumor microenvironment. *In vivo*, mesenchymal stem cells from bone marrow traffic to the site of tumor formation and regulate BCSC by releasing cytokines (145). Two of these, IL-6 and IL-8, bind to their respective receptors IL-6R/gp-130 and CXCR1 on tumor cells producing a signaling cascade through NF-κB (146). This in turn stimulates further cytokine production, generating a positive feedback loop that can then perpetuate CSC self-renewal (147). Inhibition of NF-κB has been accomplished using the sesquiterpene lactone parthenolide, which induces apoptosis in leukemia stem cells *in vitro* and inhibits tumor initiation in NOD/SCID mice with minimal damage to normal hematopoietic cells (148). These promising results have led to the exploration of orally active analogs of parthenolide.

Hypoxia-inducible factors (HIFs) regulate many cellular processes including cell metabolism and stem cell differentiation in hypoxic environments. With respect to CSCs, Keith and Simon proposed that HIFs may play a critical role by enhancing expression or activity of critical signaling pathways such Notch (149). In a recent study it was demonstrated that in human AML samples HIF-1α is selectively activated in the CSC

compartment (150). Confirming the hypothesis of Keith and Simon, pharmacological inhibition of HIF activity reduced Notch mediated production of Hes1. This was accomplished in part through the use of echinomycin, a cyclic peptide isolated from *Streptomyces echinatus*. Echinomycin, originally discovered by high-throughput screening, prevents HIF-1 binding to DNA preventing hypoxia induced gene expression (151). Treatment of primary AML from human with echinomycin in xenograft mice remarkably eliminates virtually all CSCs, preventing serial transplantation (150). These results were obtained at doses 50 times lower than those tolerable in human phase II clinical trials and prompt further investigation into the use of echinomycin as a CSC targeting therapeutic (152).

Addressing Critical Needs for Breast Cancer Therapy with Sulforaphane and the Cancer Stem Cell Model

Breast cancer remains the second leading cause of cancer related deaths among women in the United States with 232,670 new cases diagnosed each year and 40,000 annual deaths (153). This disease progresses through a multistage process characterized by the development of a hyperplasia which progresses to an in situ carcinoma that ultimately invades surrounding tissue and spreads throughout the body causing distant metastasis (154). Advances in surgical techniques, radiation therapy, and novel therapeutics have led to an increase of overall survival rates (155). Unfortunately metastatic breast cancer remains largely an incurable disease with on average a 25% five-year survival rate. Like most cancers this disease is highly variable from patient to patients but can be classified into four major subtypes based on the expression of the estrogen (ER), progesterone

(PR), and HER2 receptor expression within a given malignancy, which can guide the use of small molecule or biologic intervention(156).

The most commonly diagnosed breast cancer (42-59% of patients) is referred to as Luminal A, which expresses ER and/or PR with low expression of the proliferation marker Ki-67(157). Luminal A breast cancers are tend to have the best prognosis for patients and are susceptible to targeted endocrine therapies. Like Luminal A breast cancers, Luminal B breast cancers express ER and/or PR but are characterized by higher proliferation as evident by Ki-67 and are less prevalent (6-19%). While these diseases tend to have an overall worse prognosis still several targeted treatment options are available to patients. Diseases exhibiting the worst prognosis are the HER2+ and triple negative breast cancer (TNBC) subtypes. HER2+ breast cancers account for 7-12% of patients and is diagnosed by either high HER2 staining by immunohistochemistry (3+, IHC), or boarder line IHC staining (2+) with a demonstrated HER2 gene amplification identified by fluorescence in situ hybridization. Patients with this disease will most commonly be treated with a combination of HER2 targeted therapy with conventional cytotoxic chemotherapy(158). Finally, TNBC is characterized by the lack of ER, PR, and HER2 and predominantly expresses basal/myoepithelial cytokeratins. Due to the lack of expression of receptors that can be targeted by therapy these breast cancers are limited to treatment with some combination of cytotoxic chemotherapy. Further, by definition the term TNBCs is exclusionary in nature, meaning that any form of breast cancer which does not express ER, PR, or HER2 is combined into this one subtype. Thus, this group is highly heterogeneous and one report suggest is should be further divided into 6 additional subtypes (159).

Treatment of advanced TNBCs

Systemic therapies for the treatment of breast cancer is given in either the adjuvant setting (after primary therapy i.e. surgery) or neoadjuvant setting (before primary therapy) (160, 161). Due to the aggressive nature of TNBCs neoadjuvant chemotherapy is increasing in frequency. Further, recent evidence has suggested that TNBC patients tend to achieve better response to chemotherapy in the neoadjuvant setting relative to luminal breast cancers with regard to pathologic complete response (pCR)(162). However, following neoadjuvant therapy in TNBC patients those who did not initially achieve pCR had an overall worse overall survival than those with luminal subtypes (163, 164). This discrepancy between initial response rates of TNBCs in the neoadjuvant setting has been termed the "Triple Negative Paradox". The implication of the CSC model (Fig 1.) suggests that in the patients that did not respond it is possible that the system therapy was able to only reduce bulk tumor volume, allowing CSCs to produce a rapid relapse at primary and metastatic sites. *In order to overcome this potential problem it may be necessary to combine conventional chemotherapy with a compound capable of selectively inhibiting CSCs*.

Treatment of Trastuzumab Resistant Breast Cancers

The ERBB family of receptors (EGFR, HER2, HER3 and HER4) is characterized as transmembrane proteins which dimerise to elicit downstream signaling(165). Of these receptors only HER2 lacks a ligand for activation and canonically signals through activation of PI3K and further downstream to AKT. Four major targeted therapies are clinically used for the treatment of HER2+ breast cancers (166). First and foremost is

trastuzumab which is an antibody capable of binding HER2 to inhibit downstream signal transduction. As a first line therapy trastuzumab may be combined with a second targeted therapy known as pertuzumab. Like trastuzumab, pertuzumab is an antibody which targets the extracellular domain of HER2, although it primarily functions by preventing ERBB family dimerization. HER2+ breast cancers may also be treated in second line therapy by the use of ado-trastuzumab emtansine (T-DM1), which consists of the monoclonal antibody trastuzumab conjugated to the cytotoxic agent DM1 which inhibits of tubulin(167). Finally, small molecule lapatinib may also be employed for HER2 targeted therapy as it is a reversible small molecule tyrosine kinase inhibitor effecting both HER2 and EGFR. Unfortunately, while these four targeted therapies exist no cure is available for the treatment of metastatic HER2+ breast cancer. Further, in one clinical trial less than 30% of metastatic HER2+ breast cancer patients initially responded to single agent trastuzumab and patients who respond to trastuzumab initially are likely to develop acquired resistance within 1-2 years(168, 169). Therefore, it is necessary to identify new strategies for the treatment of HER2+ breast cancer patients after trastuzumab resistance develops. Recently our collaborators have demonstrated that within PTEN deficient HER2+ breast cancers the generation of trastuzumab resistance leads to the induction of the epithelial to mesenchymal transition (EMT) and expansion of CSCs by activation of an IL-6/NF-kB positive feedback loop. *Therefore, in order to treat trastuzumab resistant breast cancers it may be advantageous to inhibit NF-kB signaling to inhibit both bulk tumor volume and eradicate CSCs.*

Using Sulforphane for the treatment of TNBCs and Trastuzumab Resistant Breast Cancers

As mentioned above, our laboratory has identified that the natural product sulforaphane (SF) is capable of inhibiting breast CSCs at concentrations well below its respective IC50 in bulk cell lines (20). While these results were attributed to inhibition of Akt/β-catenin signaling, a variety of different signaling pathways have been proposed for the bioactivity of SF (170). However, accumulating literature across several types of cancers suggests that SF may be capable of reducing the function of NF-kB in multiple malignancies including leukemia, breast, and pancreatic cancer (171-173). In addition to the role of NF-kB in regulating CSCs and trastuzumab resistance as mentioned above, this signaling node and the cytokines it produces have been reported to regulate TNBCs (174, 175). Docetaxel, a front line neo-adjuvant cytotoxic agent for the treatment of TNBCs, has been shown to increase circuiting cytokines which are produced from, and may further activate, NF-kB in breast CSCs (176). Taken together this suggests that blockade of NF-kB signaling lead to inhibition of breast CSCs, TNBCs, and trastuzumab resistant breast cancers. *Therefore, we hypothesize that SF will prevent docetaxel mediated cytokine production to provide clinical benefit to TNBC patients, as well as, disrupt the positive feedback loop driving trastuzumab resistant breast cancers to create a novel therapeutic option*.

In order to evaluate this hypothesis we propose the following specific aims:

Specific Aims

Aim 1 To combine docetaxel with sulforaphane for elimination of both bulk tumors and CSCs in TNBC

Objectives: A) To demonstrate that docetaxel expands breast CSCs by upregulation of IL-6 in TNBC cell lines in vitro and in vivo. B) To identify that sulforaphane preferentially inhibits TNBCs and their CSCs by inhibiting NF-kB signal transduction in vitro and in vivo. C) To demonstrate that the combination of docetaxel and sulforaphane suppresses both bulk cell line proliferation and CSCs in vitro and in vivo.

Aim 2 To identify the efficacy of sulforaphane over the course of trastuzumab resistance in PTEN- breast cancers

Objectives: A) To evaluate changes in bulk cell line phenotype and signal transduction pathways following the generation of trastuzumab resistance in PTEN- cells. B) To demonstrate increased NF-kB activity and IL-6 expression following trastuzumab resistance can be inhibited by SF. C) To evaluate the efficacy of SF to inhibit bulk cell line proliferation and CSCs within trastuzumab resistant breast cancers with PTEN in activation in vitro and in vivo.

Aim 3 To determine additional potential mechanism of action of SF in trastuzumab resistant breast cancers with PTEN inactivation

Objectives: A) To use unbiased global mRNA expression analysis to determine alterations in signal transduction between trastuzumab sensitive and resistant cell lines. B) To identify novel genes which are inhibited by SF preferentially with trastuzumab resistant cells. C) To validate the functional relevance of the gene target in trastuzumab resistant breast cancers with PTEN inactivation.

References

1. Hanahan D & Weinberg RA (2000) The Hallmarks of Cancer. *Cell* 100(1):57-70.
2. Jemal A, *et al.* (2009) Cancer Statistics, 2009. *CA: A Cancer Journal for Clinicians* 59(4):225-249.
3. Gottesman MM (2002) MECHANISMS OF CANCER DRUG RESISTANCE. *Annual Review of Medicine* 53(1):615-627.
4. Dick JE (2008) Stem cell concepts renew cancer research. *Blood* 112(13):4793-4807.
5. Southam CM & Brunschwig A (1961) Quantitative studies of autotransplantation of human cancer. Preliminary report. *Cancer* 14(5):971-978.
6. Till JE, McCulloch EA, & Siminovitch L (1964) A STOCHASTIC MODEL OF STEM CELL PROLIFERATION, BASED ON THE GROWTH OF SPLEEN COLONY-FORMING CELLS. *Proc Natl Acad Sci U S A* 51(1):29-36.
7. Gupta Piyush B, *et al.* (Stochastic State Transitions Give Rise to Phenotypic Equilibrium in Populations of Cancer Cells. *Cell* 146(4):633-644.
8. Sarkar B, Dosch J, & Simeone DM (2009) Cancer Stem Cells: A New Theory Regarding a Timeless Disease. *Chemical Reviews* 109(7):3200-3208.
9. Prince ME, *et al.* (2007) Identification of a subpopulation of cells with cancer stem cell properties in head and neck squamous cell carcinoma. *Proceedings of the National Academy of Sciences* 104(3):973-978.
10. Fong M (2010) The role of cancer stem cells and the side population in epithelial ovarian cancer. *Histol Histopathol* 25(1):113-120.
11. Al-Hajj M, Wicha MS, Benito-Hernandez A, Morrison SJ, & Clarke MF (2003) Prospective identification of tumorigenic breast cancer cells. *Proc Natl Acad Sci U S A* 100(7):3983-3988.
12. Spangrude G, Heimfeld S, & Weissman I (1988) Purification and characterization of mouse hematopoietic stem cells. *Science* 241(4861):58-62.
13. Hillen H, Wessels T, & Haanen C (1975) BONE-MARROW-PROLIFERATION PATTERNS IN ACUTE MYELOBLASTIC LEUKAMIA DETERMINED BY PULSE CYTOPHOTOMETRY. *The Lancet* 305(7907):609-611.
14. Buick R, Minden M, & McCulloch E (1979) Self-renewal in culture of proliferative blast progenitor cells in acute myeloblastic leukemia. *Blood* 54(1):95-104.
15. Lapidot T, *et al.* (1994) A cell initiating human acute myeloid leukaemia after transplantation into SCID mice. *Nature* 367(6464):645-648.
16. Dean M, Fojo T, & Bates S (2005) Tumour stem cells and drug resistance. *Nat Rev Cancer* 5(4):275-284.
17. Franceschi S BE, La Vecchia C, Talamini R, D'Avanzo B, Negri E (1994) Tomatoes and risk of digestive-tract cancers. *Int J Cancer* 59(2):181-184.
18. De Stefani E, *et al.* (2000) Tomatoes, tomato-rich foods, lycopene and cancer of the upper aerodigestive tract: a case-control in Uruguay. *Oral Oncology* 36(1):47-53.
19. Steinmetz KA & Potter JD (1991) Vegetables, fruit, and cancer. I. Epidemiology. *Cancer Causes and Control* 2(5):325-357.

20. Ginestier C, *et al.* (ALDH1 Is a Marker of Normal and Malignant Human Mammary Stem Cells and a Predictor of Poor Clinical Outcome. *Cell Stem Cell* 1(5):555-567.
21. Jemal A, Siegel R, Xu J, & Ward E (Cancer Statistics, 2010. *CA: A Cancer Journal for Clinicians* 60(5):277-300.
22. Keshtgar M, Davidson T, Pigott K, Falzon M, & Jones A (Current status and advances in management of early breast cancer. *International Journal of Surgery* 8(3):199-202.
23. McDermott SP & Wicha MS (Targeting breast cancer stem cells. *Molecular Oncology* 4(5):404-419.
24. FDA US (2007) Clinical Trial Endpoints for the Approval of Cancer Drugs and Biologics. *Guidance for Industry*.
25. Therasse P, *et al.* (2000) New Guidelines to Evaluate the Response to Treatment in Solid Tumors. *Journal of the National Cancer Institute* 92(3):205-216.
26. Eisenhauer EA, *et al.* (2009) New response evaluation criteria in solid tumours: Revised RECIST guideline (version 1.1). *European Journal of Cancer* 45(2):228-247.
27. Reya T, Morrison SJ, Clarke MF, & Weissman IL (2001) Stem cells, cancer, and cancer stem cells. *Nature* 414(6859):105-111.
28. Ginestier C, *et al.* (2007) ALDH1 is a marker of normal and malignant human mammary stem cells and a predictor of poor clinical outcome. *Cell Stem Cell* 1(5):555-567.
29. Zhou B-BS, *et al.* (2009) Tumour-initiating cells: challenges and opportunities for anticancer drug discovery. *Nat Rev Drug Discov* 8(10):806-823.
30. Sakariassen PO, Immervoll H, & Chekenya M (2007) Cancer stem cells as mediators of treatment resistance in brain tumors: status and controversies. *Neoplasia (New York, N.Y.)* 9(11):882-892.
31. Hirsch HA, Iliopoulos D, Tsichlis PN, & Struhl K (2009) Metformin Selectively Targets Cancer Stem Cells, and Acts Together with Chemotherapy to Block Tumor Growth and Prolong Remission. *Cancer Research* 69(19):7507-7511.
32. Shafee N, *et al.* (2008) Cancer Stem Cells Contribute to Cisplatin Resistance in Brca1/p53â€“Mediated Mouse Mammary Tumors. *Cancer Research* 68(9):3243-3250.
33. Bao S, *et al.* (2006) Glioma stem cells promote radioresistance by preferential activation of the DNA damage response. *Nature* 444(7120):756-760.
34. Tanei T, *et al.* (2009) Association of Breast Cancer Stem Cells Identified by Aldehyde Dehydrogenase 1 Expression with Resistance to Sequential Paclitaxel and Epirubicin-Based Chemotherapy for Breast Cancers. *Clinical Cancer Research* 15(12):4234-4241.
35. Gupta PB, *et al.* (2009) Identification of Selective Inhibitors of Cancer Stem Cells by High-Throughput Screening. *Cell* 138(4):645-659.
36. Katoh M & Katoh M (2007) WNT Signaling Pathway and Stem Cell Signaling Network. *Clinical Cancer Research* 13(14):4042-4045.
37. Liu S, *et al.* (2006) Hedgehog Signaling and Bmi-1 Regulate Self-renewal of Normal and Malignant Human Mammary Stem Cells. *Cancer Research* 66(12):6063-6071.

38. Dontu G, *et al.* (2004) Role of Notch signaling in cell-fate determination of human mammary stem/progenitor cells. *Breast Cancer Res* 6(6):R605 - R615.
39. Yamakado K, *et al.* (2002) Renal Angiomyolipoma: Relationships between Tumor Size, Aneurysm Formation, and Rupture1. *Radiology* 225(1):78-82.
40. Bonner W A HHR, Sweet G R, and Herzenberg L A (1972) Fluorescence Activated Cell Sorting. *Rev. Sci. Instrum.* 43(3):404.
41. Fillmore C & Kuperwasser C (2008) Human breast cancer cell lines contain stem-like cells that self-renew, give rise to phenotypically diverse progeny and survive chemotherapy. *Breast Cancer Research* 10(2):R25.
42. Vasiliou V, Pappa A, & Petersen DR (2000) Role of aldehyde dehydrogenases in endogenous and xenobiotic metabolism. *Chemico-Biological Interactions* 129(1-2):1-19.
43. Duester G, Mic FA, & Molotkov A (2003) Cytosolic retinoid dehydrogenases govern ubiquitous metabolism of retinol to retinaldehyde followed by tissue-specific metabolism to retinoic acid. *Chemico-Biological Interactions* 143-144(0):201-210.
44. Armstrong L, *et al.* (2004) Phenotypic Characterization of Murine Primitive Hematopoietic Progenitor Cells Isolated on Basis of Aldehyde Dehydrogenase Activity. *STEM CELLS* 22(7):1142-1151.
45. Hess DA, *et al.* (2004) Functional characterization of highly purified human hematopoietic repopulating cells isolated according to aldehyde dehydrogenase activity. *Blood* 104(6):1648-1655.
46. Corti S, *et al.* (2006) Identification of a Primitive Brain–Derived Neural Stem Cell Population Based on Aldehyde Dehydrogenase Activity. *STEM CELLS* 24(4):975-985.
47. Clay MR, *et al.* (2010) Single-marker identification of head and neck squamous cell carcinoma cancer stem cells with aldehyde dehydrogenase. *Head & Neck* 32(9):1195-1201.
48. Kim MP, *et al.* (2011) ALDH Activity Selectively Defines an Enhanced Tumor-Initiating Cell Population Relative to CD133 Expression in Human Pancreatic Adenocarcinoma. *PLoS ONE* 6(6):e20636.
49. Silva IA, *et al.* (2011) Aldehyde Dehydrogenase in Combination with CD133 Defines Angiogenic Ovarian Cancer Stem Cells That Portend Poor Patient Survival. *Cancer Research* 71(11):3991-4001.
50. Ginestier C, *et al.* (2007) ALDH1 Is a Marker of Normal and Malignant Human Mammary Stem Cells and a Predictor of Poor Clinical Outcome. *Cell Stem Cell* 1(5):555-567.
51. Charafe-Jauffret E, *et al.* (2009) Breast cancer cell lines contain functional cancer stem cells with metastatic capacity and a distinct molecular signature. *Cancer Res* 69(4):1302-1313.
52. Bez A, *et al.* (2003) Neurosphere and neurosphere-forming cells: morphological and ultrastructural characterization. *Brain Research* 993(1-2):18-29.
53. Clement V, Sanchez P, de Tribolet N, Radovanovic I, & Ruiz i Altaba A (2007) HEDGEHOG-GLI1 Signaling Regulates Human Glioma Growth, Cancer Stem Cell Self-Renewal, and Tumorigenicity. *Current Biology* 17(2):165-172.

54. Ponti D, *et al.* (2005) Isolation and In vitro Propagation of Tumorigenic Breast Cancer Cells with Stem/Progenitor Cell Properties. *Cancer Research* 65(13):5506-5511.
55. Li Y, *et al.* (2010) Sulforaphane, a dietary component of broccoli/broccoli sprouts, inhibits breast cancer stem cells. *Clin Cancer Res* 16(9):2580-2590.
56. Charafe-Jauffret E, Ginestier C, & Birnbaum D (2009) Breast cancer stem cells: tools and models to rely on. *BMC Cancer* 9(1):202.
57. Singh SK, *et al.* (2003) Identification of a cancer stem cell in human brain tumors. *Cancer Res* 63(18):5821-5828.
58. Singh AV, Xiao D, Lew KL, Dhir R, & Singh SV (2004) Sulforaphane induces caspase-mediated apoptosis in cultured PC-3 human prostate cancer cells and retards growth of PC-3 xenografts in vivo. *Carcinogenesis* 25(1):83-90.
59. Dalerba P, *et al.* (2007) Phenotypic characterization of human colorectal cancer stem cells. *Proceedings of the National Academy of Sciences* 104(24):10158-10163.
60. Clay MR, *et al.* (Single-marker identification of head and neck squamous cell carcinoma cancer stem cells with aldehyde dehydrogenase. *Head & Neck* 32(9):1195-1201.
61. Prince ME, *et al.* (2007) Identification of a subpopulation of cells with cancer stem cell properties in head and neck squamous cell carcinoma. *Proc Natl Acad Sci U S A* 104(3):973-978.
62. Patrawala L, *et al.* (2006) Highly purified CD44+ prostate cancer cells from xenograft human tumors are enriched in tumorigenic and metastatic progenitor cells. *Oncogene* 25(12):1696-1708.
63. Kryczek I, *et al.* (Expression of aldehyde dehydrogenase and CD133 defines ovarian cancer stem cells. *International Journal of Cancer* 130(1):29-39.
64. Willert K, *et al.* (2003) Wnt proteins are lipid-modified and can act as stem cell growth factors. *Nature* 423(6938):448-452.
65. Reya T, *et al.* (2003) A role for Wnt signalling in self-renewal of haematopoietic stem cells. *Nature* 423(6938):409-414.
66. Barker N, *et al.* (2007) Identification of stem cells in small intestine and colon by marker gene Lgr5. *Nature* 449(7165):1003-1007.
67. Barker N, *et al.* (Lgr5+ve Stem Cells Drive Self-Renewal in the Stomach and Build Long-Lived Gastric Units In Vitro. *Cell Stem Cell* 6(1):25-36.
68. Zeng YA & Nusse R (Wnt Proteins Are Self-Renewal Factors for Mammary Stem Cells and Promote Their Long-Term Expansion in Culture. *Cell Stem Cell* 6(6):568-577.
69. Miyake K, *et al.* (1990) Monoclonal antibodies to Pgp-1/CD44 block lympho-hemopoiesis in long-term bone marrow cultures. *The Journal of Experimental Medicine* 171(2):477-488.
70. Wielenga VJM, *et al.* (1999) Expression of CD44 in Apc and TcfMutant Mice Implies Regulation by the WNT Pathway. *The American Journal of Pathology* 154(2):515-523.
71. Sy MS, Guo YJ, & Stamenkovic I (1992) Inhibition of tumor growth in vivo with a soluble CD44-immunoglobulin fusion protein. *The Journal of Experimental Medicine* 176(2):623-627.

72. Müller-Tidow C, *et al.* (2004) Translocation Products in Acute Myeloid Leukemia Activate the Wnt Signaling Pathway in Hematopoietic Cells. *Molecular and Cellular Biology* 24(7):2890-2904.
73. Lu D, *et al.* (2004) Activation of the Wnt signaling pathway in chronic lymphocytic leukemia. *Proceedings of the National Academy of Sciences of the United States of America* 101(9):3118-3123.
74. Kinzler KW & Vogelstein B (1996) Lessons from Hereditary Colorectal Cancer. *Cell* 87(2):159-170.
75. Cho RW, *et al.* (2008) Isolation and Molecular Characterization of Cancer Stem Cells in MMTV-Wnt-1 Murine Breast Tumors. *STEM CELLS* 26(2):364-371.
76. Reya T & Clevers H (2005) Wnt signalling in stem cells and cancer. *Nature* 434(7035):843-850.
77. Polakis P (2000) Wnt signaling and cancer. *Genes & Development* 14(15):1837-1851.
78. Klaus A & Birchmeier W (2008) Wnt signalling and its impact on development and cancer. *Nat Rev Cancer* 8(5):387-398.
79. Gao C & Chen Y-G (Dishevelled: The hub of Wnt signaling. *Cellular Signalling* 22(5):717-727.
80. Bernatik O, *et al.* (Sequential activation and inactivation of dishevelled in the Wnt/Î²-catenin pathway by casein kinases. *Journal of Biological Chemistry*.
81. Pradeep CR & Kuttan G (2002) Effect of piperine on the inhibition of lung metastasis induced B16F-10 melanoma cells in mice. *Clinical and Experimental Metastasis* 19(8):703-708.
82. Selvendiran K, Banu SM, & Sakthisekaran D (2004) Protective effect of piperine on benzo(a)pyrene-induced lung carcinogenesis in Swiss albino mice. *Clinica Chimica Acta* 350(1-2):73-78.
83. Kakarala M, *et al.* (Targeting breast stem cells with the cancer preventive compounds curcumin and piperine. *Breast Cancer Research and Treatment* 122(3):777-785.
84. Lepourcelet M, *et al.* (2004) Small-molecule antagonists of the oncogenic Tcf/β-catenin protein complex. *Cancer Cell* 5(1):91-102.
85. Mani SA, *et al.* (2008) The Epithelial-Mesenchymal Transition Generates Cells with Properties of Stem Cells. *Cell* 133(4):704-715.
86. Basler K & Struhl G (1994) Compartment boundaries and the control of Drosopfiffa limb pattern by hedgehog protein. *Nature* 368(6468):208-214.
87. Echelard Y, *et al.* (1993) Sonic hedgehog, a member of a family of putative signaling molecules, is implicated in the regulation of CNS polarity. *Cell* 75(7):1417-1430.
88. Lewis MT, *et al.* (2001) The Gli2 Transcription Factor Is Required for Normal Mouse Mammary Gland Development. *Developmental Biology* 238(1):133-144.
89. Palma Vn & Altaba ARi (2004) Hedgehog-GLI signaling regulates the behavior of cells with stem cell properties in the developing neocortex. *Development* 131(2):337-345.
90. Palma Vn, *et al.* (2005) Sonic hedgehog controls stem cell behavior in the postnatal and adult brain. *Development* 132(2):335-344.

91. Ramalho-Santos M, Melton DA, & McMahon AP (2000) Hedgehog signals regulate multiple aspects of gastrointestinal development. *Development* 127(12):2763-2772.
92. Liu S, *et al.* (2006) Hedgehog signaling and Bmi-1 regulate self-renewal of normal and malignant human mammary stem cells. *Cancer Res* 66(12):6063-6071.
93. Marini KD, Payne BJ, Watkins DN, & Martelotto LG (2011) Mechanisms of Hedgehog signalling in cancer. *Growth Factors* 29(6):221-234.
94. Theunissen J-W & de Sauvage FJ (2009) Paracrine Hedgehog Signaling in Cancer. *Cancer Research* 69(15):6007-6010.
95. Wang Y, McMahon AP, & Allen BL (2007) Shifting paradigms in Hedgehog signaling. *Current Opinion in Cell Biology* 19(2):159-165.
96. Chen JK, Taipale J, Cooper MK, & Beachy PA (2002) Inhibition of Hedgehog signaling by direct binding of cyclopamine to Smoothened. *Genes & Development* 16(21):2743-2748.
97. Bar EE, *et al.* (2007) Cyclopamine-Mediated Hedgehog Pathway Inhibition Depletes Stem-Like Cancer Cells in Glioblastoma. *STEM CELLS* 25(10):2524-2533.
98. Mueller MT, *et al.* (2009) Combined Targeted Treatment to Eliminate Tumorigenic Cancer Stem Cells in Human Pancreatic Cancer. *Gastroenterology* 137(3):1102-1113.
99. Artavanis-Tsakonas S, Rand MD, & Lake RJ (1999) Notch signaling: cell fate control and signal integration in development. *Science* 284(5415):770-776.
100. Cabrera CV (1990) Lateral inhibition and cell fate during neurogenesis in Drosophila: the interactions between scute, Notch and Delta. *Development* 110(1):733-742.
101. Lewis J (1998) Notch signalling and the control of cell fate choices in vertebrates. *Semin Cell Dev Biol* 9(6):583-589.
102. Cagan RL & Ready DF (1989) Notch is required for successive cell decisions in the developing Drosophila retina. *Genes Dev* 3(8):1099-1112.
103. Claxton S & Fruttiger M (2004) Periodic Delta-like 4 expression in developing retinal arteries. *Gene Expr Patterns* 5(1):123-127.
104. Hellstrom M, *et al.* (2007) Dll4 signalling through Notch1 regulates formation of tip cells during angiogenesis. *Nature* 445(7129):776-780.
105. Bray SJ (2006) Notch signalling: a simple pathway becomes complex. *Nat Rev Mol Cell Biol* 7(9):678-689.
106. Kopan R & Ilagan MX (2009) The canonical Notch signaling pathway: unfolding the activation mechanism. *Cell* 137(2):216-233.
107. Fortini ME (2009) Notch signaling: the core pathway and its posttranslational regulation. *Dev Cell* 16(5):633-647.
108. Reedijk M, *et al.* (2005) High-level coexpression of JAG1 and NOTCH1 is observed in human breast cancer and is associated with poor overall survival. *Cancer Res* 65(18):8530-8537.
109. Dickson BC, *et al.* (2007) High-level JAG1 mRNA and protein predict poor outcome in breast cancer. *Mod Pathol* 20(6):685-693.

110. Reedijk M, *et al.* (2008) JAG1 expression is associated with a basal phenotype and recurrence in lymph node-negative breast cancer. *Breast Cancer Res Treat* 111(3):439-448.
111. Pece S, *et al.* (2004) Loss of negative regulation by Numb over Notch is relevant to human breast carcinogenesis. *J Cell Biol* 167(2):215-221.
112. Ellisen LW, *et al.* (1991) TAN-1, the human homolog of the Drosophila notch gene, is broken by chromosomal translocations in T lymphoblastic neoplasms. *Cell* 66(4):649-661.
113. Weng AP, *et al.* (2004) Activating mutations of NOTCH1 in human T cell acute lymphoblastic leukemia. *Science* 306(5694):269-271.
114. Ranganathan P, Weaver KL, & Capobianco AJ (Notch signalling in solid tumours: a little bit of everything but not all the time. *Nat Rev Cancer* 11(5):338-351.
115. Cohen B, *et al.* (Cyclin D1 is a direct target of JAG1-mediated Notch signaling in breast cancer. *Breast Cancer Res Treat* 123(1):113-124.
116. Sharma VM, *et al.* (2006) Notch1 contributes to mouse T-cell leukemia by directly inducing the expression of c-myc. *Mol Cell Biol* 26(21):8022-8031.
117. Weng AP, *et al.* (2006) c-Myc is an important direct target of Notch1 in T-cell acute lymphoblastic leukemia/lymphoma. *Genes Dev* 20(15):2096-2109.
118. Murata J, *et al.* (2009) Notch-Hes1 pathway contributes to the cochlear prosensory formation potentially through the transcriptional down-regulation of p27Kip1. *J Neurosci Res* 87(16):3521-3534.
119. Monahan P, Rybak S, & Raetzman LT (2009) The notch target gene HES1 regulates cell cycle inhibitor expression in the developing pituitary. *Endocrinology* 150(9):4386-4394.
120. Riccio O, *et al.* (2008) Loss of intestinal crypt progenitor cells owing to inactivation of both Notch1 and Notch2 is accompanied by derepression of CDK inhibitors p27Kip1 and p57Kip2. *EMBO Rep* 9(4):377-383.
121. Palomero T, Dominguez M, & Ferrando AA (2008) The role of the PTEN/AKT Pathway in NOTCH1-induced leukemia. *Cell Cycle* 7(8):965-970.
122. Ristorcelli E, Beraud E, Mathieu S, Lombardo D, & Verine A (2009) Essential role of Notch signaling in apoptosis of human pancreatic tumoral cells mediated by exosomal nanoparticles. *Int J Cancer* 125(5):1016-1026.
123. Wang Z, *et al.* (Down-regulation of Notch-1 and Jagged-1 inhibits prostate cancer cell growth, migration and invasion, and induces apoptosis via inactivation of Akt, mTOR, and NF-kappaB signaling pathways. *J Cell Biochem* 109(4):726-736.
124. Dontu G, *et al.* (2004) Role of Notch signaling in cell-fate determination of human mammary stem/progenitor cells. *Breast Cancer Res* 6(6):R605-615.
125. Pistollato F, *et al.* (Interaction of hypoxia-inducible factor-1alpha and Notch signaling regulates medulloblastoma precursor proliferation and fate. *Stem Cells* 28(11):1918-1929.
126. Farnie G & Clarke RB (2007) Mammary stem cells and breast cancer--role of Notch signalling. *Stem Cell Rev* 3(2):169-175.
127. Farnie G, *et al.* (2007) Novel cell culture technique for primary ductal carcinoma in situ: role of Notch and epidermal growth factor receptor signaling pathways. *J Natl Cancer Inst* 99(8):616-627.

128. Leong KG, *et al.* (2007) Jagged1-mediated Notch activation induces epithelial-to-mesenchymal transition through Slug-induced repression of E-cadherin. *J Exp Med* 204(12):2935-2948.
129. Wang Z, Zhang Y, Banerjee S, Li Y, & Sarkar FH (2006) Notch-1 down-regulation by curcumin is associated with the inhibition of cell growth and the induction of apoptosis in pancreatic cancer cells. *Cancer* 106(11):2503-2513.
130. Wang Z, Zhang Y, Banerjee S, Li Y, & Sarkar FH (2006) Inhibition of nuclear factor kappab activity by genistein is mediated via Notch-1 signaling pathway in pancreatic cancer cells. *Int J Cancer* 118(8):1930-1936.
131. Wang Z, *et al.* (2006) Down-regulation of Notch-1 contributes to cell growth inhibition and apoptosis in pancreatic cancer cells. *Mol Cancer Ther* 5(3):483-493.
132. Cecchinato V, *et al.* (2007) Resveratrol-induced apoptosis in human T-cell acute lymphoblastic leukaemia MOLT-4 cells. *Biochem Pharmacol* 74(11):1568-1574.
133. Koduru S, Kumar R, Srinivasan S, Evers MB, & Damodaran C (Notch-1 inhibition by Withaferin-A: a therapeutic target against colon carcinogenesis. *Mol Cancer Ther* 9(1):202-210.
134. Wang XN, *et al.* (Effects of Celastrol on growth inhibition of U937 leukemia cells through the regulation of the Notch1/NF-kappaB signaling pathway in vitro. *Chin J Cancer* 29(4):385-390.
135. Kim S-H & Singh SV (2014) Mammary Cancer Chemoprevention by Withaferin A Is Accompanied by In Vivo Suppression of Self-Renewal of Cancer Stem Cells. *Cancer Prevention Research* 7(7):738-747.
136. Rajasekhar VK, Studer L, Gerald W, Socci ND, & Scher HI (2011) Tumour-initiating stem-like cells in human prostate cancer exhibit increased NF-[kappa]B signalling. *Nat Commun* 2:162.
137. Sansal I & Sellers WR (2004) The Biology and Clinical Relevance of the PTEN Tumor Suppressor Pathway. *Journal of Clinical Oncology* 22(14):2954-2963.
138. Cross DAE, Alessi DR, Cohen P, Andjelkovich M, & Hemmings BA (1995) Inhibition of glycogen synthase kinase-3 by insulin mediated by protein kinase B. *Nature* 378(6559):785-789.
139. Korkaya H, *et al.* (2009) Regulation of mammary stem/progenitor cells by PTEN/Akt/beta-catenin signaling. *PLoS Biol* 7(6):e1000121.
140. Supko JG, Hickman RL, Grever MR, & Malspeis L (1995) Preclinical pharmacologic evaluation of geldanamycin as an antitumor agent. *Cancer Chemotherapy and Pharmacology* 36(4):305-315.
141. Schulte TW & Neckers LM (1998) The benzoquinone ansamycin 17-allylamino-17-demethoxygeldanamycin binds to HSP90 and shares important biologic activities with geldanamycin. *Cancer Chemotherapy and Pharmacology* 42(4):273-279.
142. Sauvageot CM-E, *et al.* (2009) Efficacy of the HSP90 inhibitor 17-AAG in human glioma cell lines and tumorigenic glioma stem cells. *Neuro-Oncology* 11(2):109-121.
143. Li Y, Zhang T, Schwartz SJ, & Sun D (Sulforaphane Potentiates the Efficacy of 17-Allylamino 17-Demethoxygeldanamycin Against Pancreatic Cancer Through

Enhanced Abrogation of Hsp90 Chaperone Function. *Nutrition and Cancer* 63(7):1151-1159.
144. Guzman ML, *et al.* (2001) Nuclear factor-κB is constitutively activated in primitive human acute myelogenous leukemia cells. *Blood* 98(8):2301-2307.
145. Liu S, *et al.* (Breast Cancer Stem Cells Are Regulated by Mesenchymal Stem Cells through Cytokine Networks. *Cancer Research* 71(2):614-624.
146. Korkaya H, Liu S, & Wicha MS (2011) Regulation of Cancer Stem Cells by Cytokine Networks: Attacking Cancer's Inflammatory Roots. *Clinical Cancer Research* 17(19):6125-6129.
147. Ginestier C, *et al.* (2010) CXCR1 blockade selectively targets human breast cancer stem cells in vitro and in xenografts. *The Journal of Clinical Investigation* 120(2):485-497.
148. Guzman ML, *et al.* (2005) The sesquiterpene lactone parthenolide induces apoptosis of human acute myelogenous leukemia stem and progenitor cells. *Blood* 105(11):4163-4169.
149. Keith B & Simon MC (2007) Hypoxia-Inducible Factors, Stem Cells, and Cancer. *Cell* 129(3):465-472.
150. Wang Y, Liu Y, Malek SamiÂ N, Zheng P, & Liu Y (2011) Targeting HIF1a Eliminates Cancer Stem Cells in Hematological Malignancies. *Cell Stem Cell* 8(4):399-411.
151. Kong D, *et al.* (2005) Echinomycin, a Small-Molecule Inhibitor of Hypoxia-Inducible Factor-1 DNA-Binding Activity. *Cancer Research* 65(19):9047-9055.
152. Muss HB, Blessing JA, & Malfetano J (1990) Echinomycin (NSC 526417) in squamous-cell carcinoma of the cervix. A phase II trial of the gynecologic oncology group. *American Journal of Clinical Oncology: Cancer Clinical Trials* 13(3):191-193.
153. Siegel R, Ma J, Zou Z, & Jemal A (2014) Cancer statistics, 2014. *CA: a cancer journal for clinicians* 64(1):9-29.
154. Bombonati A & Sgroi DC (2011) The Molecular Pathology of Breast Cancer Progression. *The Journal of pathology* 223(2):307-317.
155. Edwards BK, *et al.* (2014) Annual Report to the Nation on the status of cancer, 1975-2010, featuring prevalence of comorbidity and impact on survival among persons with lung, colorectal, breast, or prostate cancer. *Cancer* 120(9):1290-1314.
156. Sørlie T, *et al.* (2001) Gene expression patterns of breast carcinomas distinguish tumor subclasses with clinical implications. *Proceedings of the National Academy of Sciences* 98(19):10869-10874.
157. Sims AH, Howell A, Howell SJ, & Clarke RB (2007) Origins of breast cancer subtypes and therapeutic implications. *Nat Clin Prac Oncol* 4(9):516-525.
158. Slamon DJ, *et al.* (2001) Use of Chemotherapy plus a Monoclonal Antibody against HER2 for Metastatic Breast Cancer That Overexpresses HER2. *New England Journal of Medicine* 344(11):783-792.
159. Lehmann BD, *et al.* (2011) Identification of human triple-negative breast cancer subtypes and preclinical models for selection of targeted therapies. *The Journal of Clinical Investigation* 121(7):2750-2767.

160. Joensuu H & Gligorov J (2012) Adjuvant treatments for triple-negative breast cancers. *Annals of Oncology* 23(suppl 6):vi40-vi45.
161. von Minckwitz G & Martin M (2012) Neoadjuvant treatments for triple-negative breast cancer (TNBC). *Annals of Oncology* 23(suppl 6):vi35-vi39.
162. Huober J, *et al.* (2010) Effect of neoadjuvant anthracycline–taxane-based chemotherapy in different biological breast cancer phenotypes: overall results from the GeparTrio study. *Breast Cancer Research and Treatment* 124(1):133-140.
163. Carey LA, *et al.* (2007) The Triple Negative Paradox: Primary Tumor Chemosensitivity of Breast Cancer Subtypes. *Clinical Cancer Research* 13(8):2329-2334.
164. von Minckwitz G, *et al.* (2012) Definition and Impact of Pathologic Complete Response on Prognosis After Neoadjuvant Chemotherapy in Various Intrinsic Breast Cancer Subtypes. *Journal of Clinical Oncology* 30(15):1796-1804.
165. Alroy I & Yarden Y (1997) The ErbB signaling network in embryogenesis and oncogenesis: signal diversification through combinatorial ligand-receptor interactions. *FEBS Letters* 410(1):83-86.
166. Gajria D & Chandarlapaty S (2011) HER2-amplified breast cancer: mechanisms of trastuzumab resistance and novel targeted therapies. *Expert review of anticancer therapy* 11(2):263-275.
167. Lewis Phillips GD, *et al.* (2008) Targeting HER2-Positive Breast Cancer with Trastuzumab-DM1, an Antibody–Cytotoxic Drug Conjugate. *Cancer Research* 68(22):9280-9290.
168. Vogel CL, *et al.* (2002) Efficacy and Safety of Trastuzumab as a Single Agent in First-Line Treatment of HER2-Overexpressing Metastatic Breast Cancer. *Journal of Clinical Oncology* 20(3):719-726.
169. Rexer BN & Arteaga CL (2012) Intrinsic and Acquired Resistance to HER2-Targeted Therapies in HER2 Gene-Amplified Breast Cancer: Mechanisms and Clinical Implications. 17(1):1-16.
170. Juge N, Mithen R, & Traka M (2007) Molecular basis for chemoprevention by sulforaphane: a comprehensive review. *Cellular and Molecular Life Sciences* 64(9):1105-1127.
171. Moon D-O, Kim M-O, Kang S-H, Choi YH, & Kim G-Y (2009) Sulforaphane suppresses TNF-α-mediated activation of NF-κB and induces apoptosis through activation of reactive oxygen species-dependent caspase-3. *Cancer Letters* 274(1):132-142.
172. Lee Y-R, *et al.* (2013) Sulforaphane controls TPA-induced MMP-9 expression through the NF-κB signaling pathway, but not AP-1, in MCF-7 breast cancer cells. *BMB Reports* 46(4):201-206.
173. Kallifatidis G, *et al.* (2009) Sulforaphane targets pancreatic tumour-initiating cells by NF-κB-induced antiapoptotic signalling. *Gut* 58(7):949-963.
174. Kim G, *et al.* (2015) SOCS3-mediated regulation of inflammatory cytokines in PTEN and p53 inactivated triple negative breast cancer model. *Oncogene* 34(6):671-680.

175. Hartman ZC, *et al.* (2013) Growth of triple-negative breast cancer cells relies upon coordinate autocrine expression of the pro-inflammatory cytokines IL-6 and IL-8. *Cancer Research* 73(11):10.1158/0008-5472.CAN-1112-4524-T.
176. Tsavaris N, Kosmas C, Vadiaka M, Kanelopoulos P, & Boulamatsis D (2002) Immune changes in patients with advanced breast cancer undergoing chemotherapy with taxanes. *Br J Cancer* 87(1):21-27.

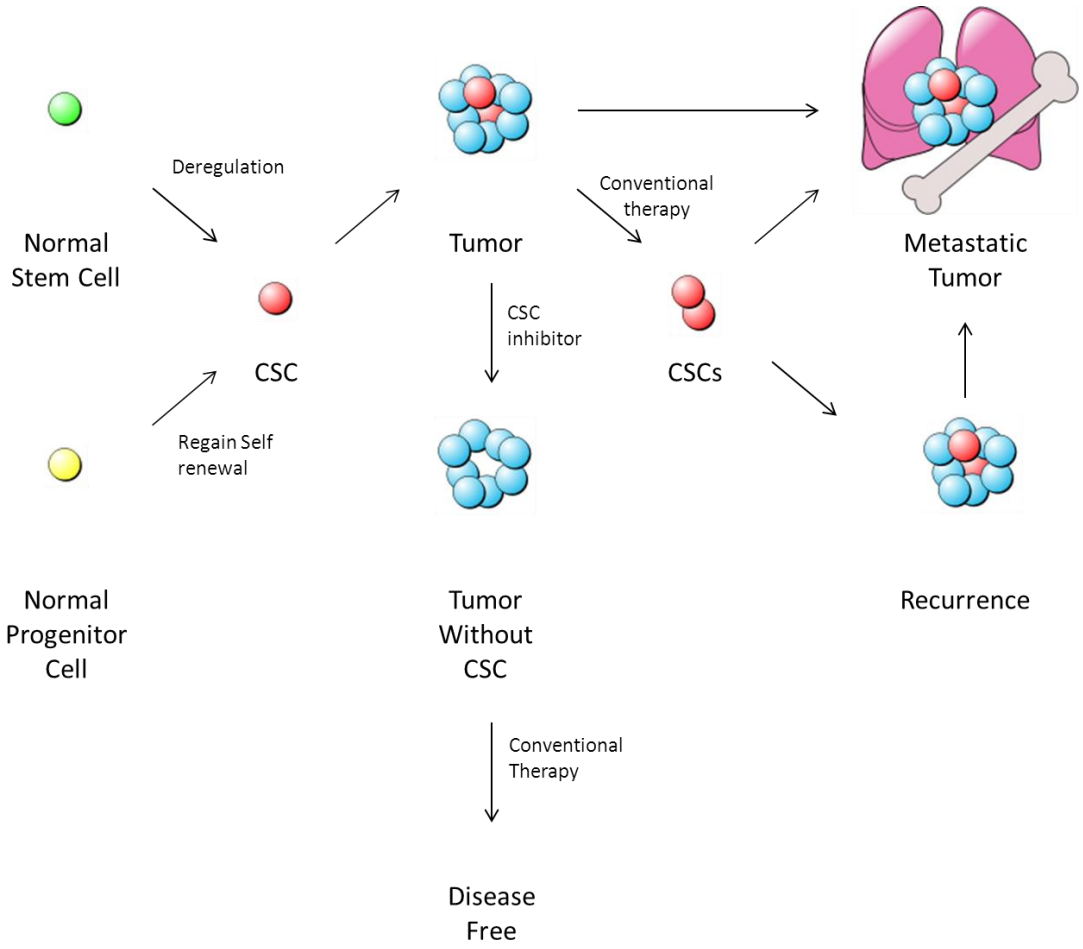

Figure 1.1 Therapeutic implications of the cancer stem cell model. Normal stem or progenitor cells give rise to CSCs through deregulation or regained self-renewal capacity. CSCs are then capable of self-renewal and differentiation to form tumors, which left untreated can form new metastasis. Conventional therapy will eliminate the bulk of the tumor mass leaving behind CSCs that then initiate recurrence and dislodge, spreading to distant organs. Given a CSC inhibitor tumors will lose the ability for sustained growth and metastasis. In combination with conventional therapy this will likely lead to disease-free survival.

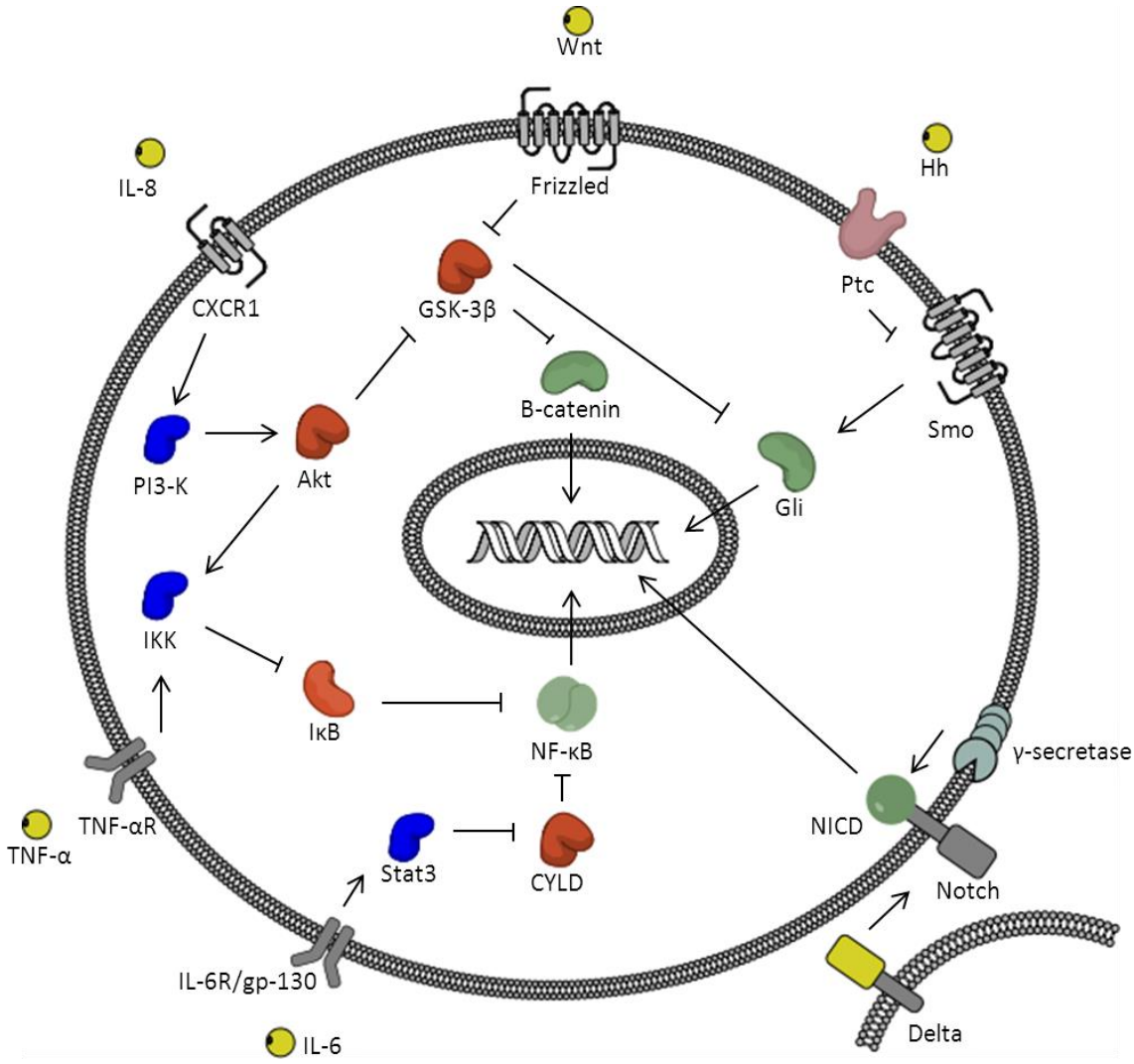

Figure 1.2 Critical signal transduction pathways essential for CSC function. Wnt signaling in stem cells is initiated by binding of Wnt to its receptor frizzled, ultimately leading to translocation of β-catenin to initial transcription. Similarly, binding of the Hh ligands to Ptc relieves inhibition of the Gli family of transcription factor. Extracellular ligands on neighboring cells activate the Notch pathway, causing cleavage of the NICD which translocate to the nucleus. Interaction of inflammatory cytokines or endogenous receptors such as HER2 activates the key signaling nodes Akt and NF-κB. Post-translational modification of Akt and GSK-3β represent the generation of proteins capable of modulating multiple pathways including Wnt and Hh.

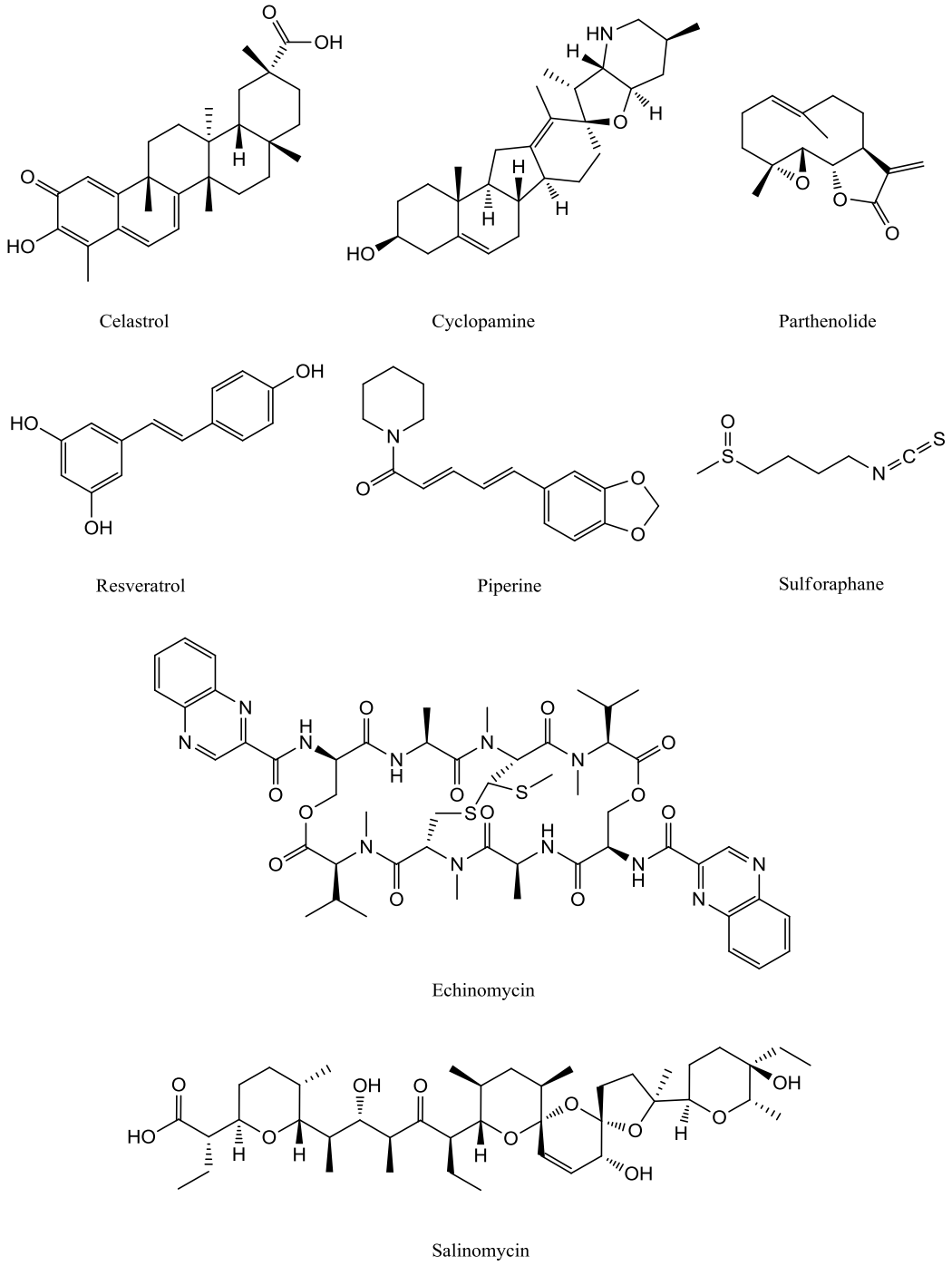

Figure 1.3 Natural products with demonstrated efficacy toward modulating targets critical to CSC function. Successful inhibition of Wnt signaling has been shown using the compounds piperine and salinomycin. The SMO antagonist cyclopamine prevents activation of the Hedgehog pathway, which is critical for the differentiation process. Inhibitors of the juxtacrine Notch signaling pathway include resveratrol and celastrol. Multiple pathways are targeted by the natural product sulforaphane, through inhibition of the molecular chaperone HSP-90 and the Akt signaling node. Interactions of CSCs with

the surrounding microenvironment may be modulated by both parthenolide and echinomycin.

Chapter 2

Combination of Docetaxel with Sulforaphane Synergistically Inhibits Triple Negative Breast Cancer and Cancer Stem Cells

Abstract

Triple negative breast cancer (TNBC) (ER-, PR-, Her2-), constituting 10-20% of all breast cancers, is a heterogeneous disease that has limited treatment options, exhibits rapid progression, and results in overall poor patient prognosis. The cancer stem cell (CSC) model provides an attractive explanation for relapse of TNBC after primary therapy since these cells demonstrate resistance to conventional chemotherapy and are thought to be responsible for tumor relapse and metastasis. Docetaxel is a commonly utilized therapeutic for the treatment of metastatic TNBCs, although no cure is ultimately available for these patients. While docetaxel has been demonstrated to effectively reduce tumor volume accumulating evidences suggests it may fail to eliminate CSCs, possibly due to enhanced intratumoral cytokine expression. Expressions of several cytokines, including IL-6, have been shown to regulate CSCs, and their own expression is determined in part by the activity of the NF-kB transcription factor. Therefore, we propose that combination therapy with docetaxel and a CSC inhibitor capable of inhibiting NF-kB would be ideally suited for the treatment of TNBC patients receiving chemotherapy. Our in vitro results demonstrate that docetaxel treatment increases the proportion of ALDH+ and CD44+/CD24-/EpCAM+ breast CSCs in TNBC cell lines.

Further, we identify that the natural product sulforaphane is capable of preferentially inhibiting breast CSCs and TNBCs in general by reducing NF-kB function in vitro. Addition of sulforaphane to docetaxel treatment potentiates its therapeutic effect in bulk cells lines. This combination is also able to effectively eliminate breast CSCs in vitro through sulforaphane-mediated inhibition of IL-6, as evident by flow cytometry analysis, mammosphere formation, and reduced IL-6 secretion. Using an orthotopic mouse xenograft model we demonstrate that docetaxel significantly reduces bulk tumor growth while increasing CSC frequency. Conversely, sulforaphane (SF) treatment modestly inhibits bulk tumor volume but reveals a potent reduction in CSCs. In vivo, the combination of docetaxel and SF exhibits a greater reduction in primary tumor volume and breast CSCs relative to either treatment alone. These results suggest that SF-mediated inhibition of breast CSCs and IL-6 provide a scientific rationale for using this agent in combination with docetaxel for the treatment of TNBC patients.

Introduction

Triple negative breast cancers (TNBCs) (ER-, PR-, Her2-), which represent the vast majority of basal and claudin-low subtypes, are an aggressive form of breast cancer with limited treatment options and poor prognosis in contrast to the other three types of breast cancers (luminal A, B, Her2+) (1-4). The use of neoadjuvant chemotherapy has increased in recent years with several clinical trials demonstrating more frequent pathologic complete responses (pCR) in TNBC patients relative to other subtypes (5-8). Therapies in the neoadjuvant setting typically consist of a taxane, paclitaxel or docetaxel, with other chemotherapeutic agents such as anthracyclines or cyclophosphamide (9).

However, with respect to patients who do not exhibit pCR, overall survival is often worse in TNBC patients relative to non-TNBC patients due in part to higher rates of metastasis (6). Strikingly, in advanced TNBC the duration of response to first line palliative chemotherapy has been reported to be less than 12 weeks and the response to secondary and tertiary therapies even shorter (9 and 4 weeks, respectively) (10).

While considerable effort has been given to identify new therapeutic targets or prognostic markers which may predict response to chemotherapy in TNBC, an obvious strategy for treating these patients is not clear and is due largely to the heterogeneity of the subtype (11-14). The breast cancer stem cell (BCSC) model provides an attractive explanation for the relapse of TNBC after primary chemotherapy (15-17). This small population of BCSCs in tumors exhibits two key properties; self-renewal, which allows for long term proliferation potential, and differentiation to form the heterogeneous tumor bulk (18-24). With these properties BCSCs are thought to be responsible for tumor initiation and metastasis, and their relative abundance is correlated with poor patient survival (23, 25-28). In addition, these cells are have been shown to rely on alternative signal transduction pathways relative to their more differentiated counterparts, including Wnt/β-catenin, Sonic Hedgehog (SHH), Notch, PTEN/AKT, and NF-kB (29-33). Due to several reported resistance mechanisms the efficacy of cytotoxic chemotherapy in BCSCs may be reduced, thereby allowing residual BCSCs within a TNBC patient to repopulate primary and metastatic tumors following neoadjuvant therapy.

Docetaxel is commonly prescribed to TNBC patients and has established efficacy toward reducing tumor volume in preclinical and clinical settings. However, several reports in a preclinical setting suggest that this therapy may actually fail to inhibit or even increase

the frequency of BCSCs (34-36). In addition, docetaxel had been demonstrated to increase production of IL-6 and IL8 in patients (37). Direct stimulation of breast cancer cell lines in vitro with IL-6 and IL-8 has been shown to increase BCSCs (35, 36, 38). Production of these cytokines is regulated by the activity of the transcription factor NF-kB, which has been demonstrated to be of critical importance in the regulation of BCSCs (33, 39, 40). Therefore, we hypothesize that the combination of docetaxel with a BCSC inhibitor capable of NF-kB inhibition would be ideally suited for therapy in TNBC patients.

In this report we demonstrate that docetaxel treatment increases the proportion of BCSCs and enhances IL-6 production in TNBC cell lines. Conversely, the natural product sulforaphane, which is capable of preferentially inhibiting TNBCs and ALDH+ BCSCs, reduces production of IL-6 through inhibition of NF-kB nuclear translocation and transcriptional activity. Combination of these therapeutics not only elicits a synergistic response in bulk cell lines but SF suppresses docetaxel-mediated IL-6 production and BCSC expansion in vitro. Finally, using an orthotopic mouse xenograft model with extreme limiting dilution analysis (ELDA) of serially reimplanted tumors, we demonstrate that docetaxel increases BCSCs while the combination of SF and docetaxel demonstrates greater efficacy in primary tumors and reduces BCSC frequency. These results provide a strong rationale for future studies aimed to utilize novel combination therapies for the treatment of TNBC patients.

Results

Docetaxel increases IL-6 expression and expands breast cancer stem cells in TNBC cell lines.

The role of IL-6 expression with regard to expanding the breast cancer stem cell population in vitro has been shown in many breast cancer cell lines (36, 38, 41, 42). In addition, previous clinical trials have demonstrated that administration of taxanes (paclitaxel and docetaxel) to patients increases IL-6 in circulation (37); however, it is unknown if this circulating IL-6 is due primarily to secretion from cancerous cells or normal tissues. In order to evaluate in vitro if these two phenomena are linked, we treated TNBC cell lines in vitro with docetaxel at increasing concentrations. Following 72 hour incubation with SUM149 (Basal) and SUM159 (Claudin-low) cells, the MTS proliferation assay was performed to identify the sensitivity of either cell line to docetaxel. The efficacy of docetaxel was more pronounced in SUM149, with an IC50 of 0.5 nM, relative to SUM159, which exhibited an IC50 of 3 nM (Fig 2.1 A). In addition, the maximum effect at the highest dose tested was greater in SUM149 cells (89.5% vs 76% at 100 nM). At therapeutic concentrations which inhibited greater than 50% of bulk cell lines docetaxel increased the percentage of cells expressing BCSC markers CD44+/CD24-/Epcam+, as evident by FACS analysis, with maximum fold changes observed at 3.7 (5 nM) in SUM149 and 8.2 in SUM159 (Fig 2.1 B top and C). In addition, in SUM149 72 hour treatment with docetaxel increased cells expressing the BCSC marker ALDH by 2.7 fold (Fig 2.1B bottom). This suggests that BCSCs exhibit enhanced docetaxel resistance relative to non-BCSCs. Next we sought to demonstrate a link between BCSC expansion and IL-6 secretion. We treated SUM149 cells with the same concentrations that expanded BCSCs but for only 8 hours, replaced the medium, and performed ELISA to quantify the secretion of IL-6 after an additional 64 hours (Fig 2.1C). These results show a maximum of 9.2 fold increase in IL-6 secreted into the cell

culture medium relative to control treated cells with minimal alterations in cell viability. This suggests that release of IL-6 to expand BCSCs is a response of the tumor to external therapies.

Sulforaphane preferentially inhibits TNBC cell lines and ALDH+ breast cancer stem cells in vitro.

The anticancer efficacy of sulforaphane has been studied in many types of cancer (43-49). However, most of these studies showed that sulforaphane only exhibits modest inhibition of bulk cancer cell lines at relatively high concentrations. Further, it is unknown if different subtypes of a given cancer will demonstrate varying responses to sulforaphane. To identify if SF exhibits differential efficacy based on breast cancer subtype, the effect of SF on in vitro proliferation of 10 different breast cancer cell lines was carried out by MTS assay. In the triple negative cell lines SUM149, SUM159, MDA-MB-231, and MDA-MB436 sulforaphane exhibits the lowest predicted IC50s, ranging from 7.63 to 10.63 μM, and produces a high predicted maximum effect (Fig. 2.2A). In luminal cell lines, which express the estrogen and/or progesterone receptors, SF sensitivity is decreased, as demonstrated by higher IC50 values of 14.5 μM for MCF7 and 27.46 μM for ZR-75-1 cells (Fig. 2.2B). In contrast to TNBC cell lines the HER2 amplified cell lines SKBR3 and BT474 demonstrate the lowest efficacy, even at concentrations of sulforaphane up to 50 μM (Fig. 2.2C). Interestingly, while MDA-MB-453 and MDA-MB-361 cells have previously been shown to express HER2 the efficacy of SF in these cells is similar to that of the TNBC cell lines (Fig 2.2D), with IC50s of 9.14 and 16.15 μM respectively. MDA-MB-361 contains an activating mutation in the

PIK3CA gene; in addition to this mutation, MDA-MB-453 has reduced PTEN activity (50). It has previously been shown that expression of HER2 with activation of the AKT signaling pathway by PTEN deletion or PI3K activation results in cross talk, ultimately simulating the NF-κB signaling node (36, 51).

Our laboratory has previously demonstrated that within the SUM159 cell line ALDH+ BCSCs show enhanced sensitivity to SF compared to bulk cells (the opposite of docetaxel efficacy) (43). In order to evaluate this in additional breast cancer cell lines (SUM149 TNBC, ZR75-1 Luminal) we performed the Aldefluor assay after 72 hours of SF treatment. FACS analysis shows similar results to those previously published, with a 2-fold reduction in the percent of ALDH+ BCSCs with as little as 1 μM SF in SUM149 cells (Fig 2.2E, bars). SF reduces not only the percentage of residual BCSCs but also the absolute number of cells in this population at a concentration >7–fold lower than the bulk cell line IC50 (Fig 2.2E, line). Additionally, Aldefluor analysis in luminal ZR-75-1 cells shows a significant reduction in ALDH+ BCSCs following 5 and 10 μM SF treatment. Again, inhibition of ALDH+ cells occurs at a >5-fold lower concentration relative to bulk cell line IC50. These results confirm that SF is capable of preferentially reducing BCSCs across multiple subtypes of breast cancer, although the exact concentration may be dependent on the relative sensitivity of the bulk cell line to SF.

Sulforaphane reduces NF-kB nuclear translocation and transcriptional activity.

Reports of potential mechanisms of action for SF vary greatly between cancer cell lines derived from different organs of origin as well as within those derived from the same tissue but of different molecular subtype. One potential theme emerging from the

literature is the function of SF to inhibit NF-κB signaling across various forms of cancer. Inhibition of NF-κB signaling is known to induce apoptosis in primitive AML CSCs (CD34+) but not in the same population of normal cord blood cells (52). Further, this signaling node has been implicated in the formation of mammospheres and the production of cytokines which regulate BCSCs (53). The growth of triple-negative breast cancer (TNBC) cell lines has also been shown to rely on autocrine expression of IL-6 and IL-8, which are regulated by NF-κB (54, 55). With SF able to preferentially regulate TNBCs, and the BCSCs within them, we sought to determine if NF-KB inhibition is responsible for its efficacy.

Canonical activation of the NF-kB transcription factor is accomplished by a signal which results in translocation of the NF-kB subunits from the cytoplasm to the nucleus after dissociating from its endogenous inhibitor IκB. In order to elucidate if SF is able to prevent this translocation SUM159 cells were incubated with increasing concentrations of SF, followed by stimulation with TNF-α. The absence of SF and presence of TNF-α causes the NF-kB p65 subunit to translocate into the nucleus of SUM159 cells (Fig 2.3A, left two columns). The addition of SF results in reduced nuclear NF-kB p-65 staining two hours after TNF-α addition (Fig 2.3 A, right columns). In order to determine if blockade of translocation by sulforaphane translates to inhibition of transcriptional activity, TNBC cells (SUM159, MDA-MB-231) were stably transfected with a reporter construct which produces luciferase mediated by a NF-kB response element. Following stimulation of transcription by TNF-α for six hours in the presence of increasing concentrations of SF, luciferase activity was determined (Fig 2.3B). Stimulation with TNF-α in SUM159 and MDA-MB-231 cells results in a 4.0 and 4.4 fold increase in

luciferase activity, respectively, which was reduced in a dose-dependent manner by SF. This increase of NF-kB activity by TNF-α is not only completely repressed by SF in both cell lines, but in the case of 10 and 15 μM in SUM159 cells SF reduced luciferase activity relative to unstimulated levels in SUM 159 (10 μM p=0.011, 15 μM p=0.0002). With this observation we sought to determine if SF would reduce endogenous NF-kB targets within the parental cell line in the absence of any stimulator factor. Consequently, SUM159 cells were treated with concentrations of SF for 72 hours and the levels of secreted IL-6 and IL-8 were determined by ELISA (Fig. 2.3C). Interestingly, SF reduces IL-6 expression at concentrations as low as 1 μM, which is sufficient to only inhibit BCSCs in terms of therapeutic efficacy. A maximum total inhibition of 68% is observed. SF reduces IL-8 by a maximum of 74%, albeit at a concentration which inhibits bulk cell line proliferation. Taken together, these results suggest that SF is capable of reducing NF-kB function at therapeutically relevant concentrations in TNBCs, with IL-6 suppression correlated with BCSC inhibition.

Combination of Sulforaphane and Docetaxel synergistically inhibit bulk TNBC cell lines.

The major benefit of combining docetaxel with sulforaphane is a rational combination of drugs to inhibit multiple cell populations within a heterogeneous tumor, both BCSCs and differentiated cells. Another potential benefit is that the combination may be more effective than either drug alone (either additive or synergistic) within a given cell line. These scenarios allow for a reduction in doses while achieving the same therapeutic effect. However, combination therapy may also produce an antagonistic relationship

which could potentially limit therapeutic efficacy. In order to explore the potential of SF and docetaxel to enhance or reduce the efficacy of one another we first utilize a broad range of concentration combinations for either drug. Then we apply the combination index (CI) theorem, developed by Chou and Talalay, based on the Median-Effect Equation (56). Using this theorem, generally accepted values for CI indicate the relationship as follows: 0-0.9 is synergistic, 0.9–1.1 is additive, and CI values from 1.1 to infinity are antagonistic (57).

As previously demonstrated, the therapeutic efficacy of docetaxel varies between the TNBC cell lines SUM149 and SUM159 (Fig 2.1A, IC50 0.5 vs 3 nM, respectively). However, the variability of these cell lines to SF is very slight (Fig 2.2A, IC50 7.4 vs 7.8 μM, respectively). Therefore, we sought to determine the therapeutic efficacy of different combinations of SF and docetaxel concentration by the MTS proliferation assay in both cell lines. The SUM159 cell line was treated for 72 hours with increasing concentrations of docetaxel (0, 0.1, 0.5, 1, 5, 1, and 100 nM) alone or with fixed concentrations of SF (Fig 2.4A, left). Addition of 5 μM SF was sufficient to synergistically inhibit bulk cell line growth at all but the highest concentration of docetaxel, which reduced viability to 70%. Automated analysis of CI values was performed using Compusyn (ComboSyn, Inc.) and revealed that all of the tested combined doses (36 total), which ultimately inhibit 50% of cells, experience a synergistic effect (Fig 2.4A, right). Interestingly, in SUM149 cells many of concentration combinations of docetaxel with SF led to an additive effect at 1 nM docetaxel and below (Fig 2.4B), while concentrations of docetaxel above its IC50 (red symbols) resulted in a strong antagonistic response in the bulk cell line (Fig 2.4B, right). These results suggest

that if the goal of future studies is aimed at synergistically inhibiting bulk tumor volume then optimizing dose regimens may be critically important.

Combination of Sulforaphane and Docetaxel inhibits BCSCs in vitro and reduces IL-6 expression.

In order to effectively eliminate breast cancers it is necessary to eliminate the BCSCs which are responsible for tumor initiation, recurrence, and metastasis. As demonstrated above, SF and docetaxel elicit the opposite effect in BCSCs: SF inhibits but docetaxel increases the percentage of this population. However, it is unknown if the inhibitory effect of SF is sufficient to overcome BCSC expansion by docetaxel. Consequently, we performed the Aldefluor assay in vitro to monitor the relative levels of ALDH+ BCSCs in the TNBC cell line SUM149 following treatment with SF and docetaxel alone or in combination (Fig 2.5A). Consistent with previous results (Fig 2.1C), 5 nM docetaxel alone increases the percentage of ALDH+ BCSCs by 71% following 72 hour treatment. Conversely, 2.5 μM SF alone is capable of reducing this population 2 fold, consistent with previous results (Fig 2.2E). Strikingly, the combination of 2.5 μM SF with 5 nM docetaxel not only prevents BCSC expansion but actually reduces the population to the same extent as SF treatment alone. This effect from combination is also observed with 10 nM docetaxel treatment which, taken with results from Figure 2.1C, suggests SF inhibition of the ALDH+ BCSCs is likely to occur to the same extent regardless of docetaxel concentration.

To further support our findings, we performed an additional functional assay to determine the effect of treatment on BCSCs. Normal breast stem and progenitor cells, and their

cancerous counterparts, possess a unique ability of being resistant to anoikis (58). Therefore, when a heterogeneous population of breast-derived cells is placed into serum free and non-adherent conditions, the majority of cells will undergo a programmed cell death. This leaves only the stem and progenitor cells able to proliferate, generating free floating spheres referred to as mammospheres. By evaluating the effect of treatment on the frequency of cells in parental cell lines capable of forming these spheres and also the sphere size, we can infer if a drug is inhibiting stem and progenitor cells. Further, by collecting primary treated cells and passaging for another generation grown in the absence of drug, it is possible to determine if long term self-renewal of these populations is altered. In the presence of 1 nM docetaxel, the primary sphere formation rate is unaltered (Fig 2.5B, bars) relative to the vehicle treated control cells; however upon passaging in the absence of additional drug treatment, more secondary spheres form (Fig 2.5B, line). Conversely, 2.5 μM SF and the combination of 2.5 μM SF with 1 nM docetaxel both inhibit primary sphere formation and alter the long term self-renewal of BCSCs and progenitors, as evident by decreasing the ability to form secondary spheres. For all drug treatments, the size of spheres is reduced relative to control (Fig 2.5B, Bottom).

Due to the observed increase in BCSCs by docetaxel and decrease by SF and their respective regulation of NF-kB signaling, we hypothesize that SF was preventing docetaxel-mediated IL-6 production. In order to test this hypothesis SUM149 cells were cultured in the presence of docetaxel, SF, or different combinations of the two as previously described (Fig 2.1D and Fig 2.3C). In line with our previous experiments 2.5 μM SF reduces IL-6 protein secretion 2-fold whereas docetaxel increases IL-6 secretion

3.5-fold, as measured by ELISA (Fig 2.5C, white bars). Further, the addition of 1, 2.5, and 5 μM SF is sufficient to abrogate IL-6 production induced by docetaxel (Fig 2.5C, red bars). These results suggest that a low dose sulforaphane in combination with therapeutically relevant concentrations of docetaxel effectively eliminates BCSCs by preventing NF-kB signal transduction.

Combination of Sulforaphane and Docetaxel significantly inhibit tumor growth and BCSCs in vivo.

Elimination of BCSCs is critical to ultimately curing patients. It is also necessary to eliminate the more differentiated cells, which are responsible for the majority of a tumor's volume, in order to reduce symptoms of disease progression. Further, due to the genetically unstable nature of cancer cells it is possible that overtime a more differentiated cell could acquire mutations or experience enough environmental or stochastic influence to reactivate genes responsible for self-renewal. These potential problems could then lead to the acquisition of BCSC characteristics and little would be done to eliminate the disease. Accordingly, we sought to evaluate the ability of SF and docetaxel combination treatment to inhibit bulk tumor volume and BCSCs. We utilized an advanced treatment orthotopic mouse xenograft model and performed extreme limiting dilution analysis (ELDA) in secondary mice using residual primary tumors (59).

After implantation of 1.5 million SUM149 cells into the fourth mammary pad of NOD/SCID mice, tumors were allowed to reach an average volume of 50 mm^3 before randomizing the mice into four separate treatment groups (Fig 2.6A). Treatments included 0.9% saline (control), 50 mg/kg SF daily, 10 mg/kg docetaxel weekly, and 50

mg/kg SF daily with 10 mg/kg docetaxel weekly. All treatments were administered via intraparitoneal (I.P.) injection. Treatment efficacy on primary tumor volume was evaluated when control tumors reached the protocol specific endpoint. Our data show that SF treatment reduces bulk tumor volume by 37.4% ($p=0.011$), while docetaxel and the combination reduce tumor volume by 83.2% and 92.5%, respectively. Interestingly, only the combination of SF and Docetaxel cause significant ($p=0.039$) tumor regression relative to the maximum tumor volume for that treatment group (day 27 vs 51). Mouse body weight was consistent throughout the course of study, demonstrating no obvious toxicity at the indicated dose regimens (Fig 2.6B).

In order to evaluate the therapeutic efficacy of the given treatment groups with respect to BCSCs, primary tumors were harvested and dissociated into a single cell suspension to obtain residual live human cells (DAPI-, H2KD-) with FACS. Three separate dilutions of cells from each treatment group were implanted into recipient secondary mice, which had not received any therapy, to quantify the frequency of tumor initiating BCSCs by ELDA (Fig 2.6C). After 7 weeks tumor formation rates demonstrate that one in 1514 control-treated cells was capable of tumor initiation. Docetaxel significantly increased this frequency to one in 330 cells, whereas both SF and combination therapy reduced the number of tumor initiating cells (one in 3181 and one in 4245 cells, respectively). Taken together, these in vivo results suggest that the combination of SF and docetaxel is the most effective treatment to reduce both bulk tumor volume and the BCSC population.

Discussion

Treatment options for breast cancer vary depending on the subtype. Luminal A (ER or PR+, Her2-) and luminal B (ER or PR+, Her2-, Ki-67 high or ER-PR+, Her2+) breast cancers have multiple treatment options, including endocrine, anti-HER2, and conventional cytotoxic chemotherapy. Her2+ (ER and PR-, Her2+) breast cancers may respond well to anti-HER2 therapy in combination with cytotoxic chemo-therapy (60). However, triple negative breast cancers (TNBC) (ER-, PR-, Her2-), which represent the vast majority of basal and claudin-low subtypes, are resistant to most current treatment options and are largely restricted to treatment with conventional cytotoxic chemotherapy (61). The preclinical methods and clinical trial endpoints by which these compounds are evaluated tend to be focused on reducing tumor volume to delaying disease progression. With these endpoints, it is possible that conventional therapies only reduce bulk tumor volume and fail to eliminate the BCSCs which may make up only a small portion of the heterogeneous tumor.

In order to cure TNBCs there is a critical need to develop effective strategies that eliminate both BCSCs, responsible for metastasis and relapse after therapy, as well as the more differentiated cancer cells which may cause unwanted symptoms, particularly at metastatic sites. However, accumulating preclinical evidence suggest that many anticancer agents such as paclitaxel, sunitinib, doxorubicin, and gemcitabine only inhibit the growth of differentiated cancer cells but fail to eliminate or may even expand CSC populations (62-65). In this report we demonstrate that the conventional cytotoxic chemotherapy docetaxel, which inhibits microtubule polymerization to shrink bulk tumor volume, actually enhances IL-6 production, thereby increasing BCSCs. This data is consistent with previous reports demonstrating that docetaxel increases IL-6 and IL8

production both in vitro and in patients and that direct stimulation with IL-6 and IL-8 has been shown to increase BCSCs (35-38). Production of both these cytokines is regulated by the activity of the transcription factor NF-kB, which has been demonstrated to be of critical importance in the regulation of CSCs (33, 39, 40, 52, 53). Furthermore, IL-6 is known to regulate NF-kB through STAT3, an interaction capable of establishing a positive feedback loop (36, 42).

The anticancer efficacy of sulforaphane has been shown in a variety of cancers including those from breast, colon, leukemia, prostate, and pancreatic cell lines (66-69). However, in most cases the IC50 of this compound is above 5 μM and is reported with high variability depending upon the cell lines used. Our group first reported that SF selectively inhibits self-renewal of BCSCs at relatively low concentrations (0.5-5 μM) relative to the bulk cell line IC50 (43). These results were subsequently confirmed by the Herr and Shankar groups, where it was demonstrated that SF eliminates pancreatic and prostate CSCs (69, 70). In order to establish a greater understanding of SF efficacy, and how it varies among breast cancer subtypes, we demonstrate two key features of SF therapy. First, TNBCs are the most sensitive subtype to SF treatment, with HER2+ breast cancers tending to be resistant. Second, within a given cell line, the ALDH+ BCSCs are more sensitive than the heterogeneous bulk. This information provides a rationale for further studies which seek to utilize SF treatment in breast cancer because it identifies a clear population of patients who are likely to consistently respond (TNBCs).

A staggering number of potential mechanisms of action have reported to explain SF's efficacy; regulation of Nrf2, HDAC, Chk2, p21, MAPK, death receptor, NF-kB, Stat3, and Hsp90 (44, 71, 72). While SF may indeed regulate these molecules it is unclear what

their relative contributions are to efficacy and in what contexts each are relevant. In this report we identify that SF inhibits NF-kB function by preventing intracellular translocation and transcriptional activity. Noting that both BCSCs and TNBCs in general are more dependent on cytokine-NF-kB signaling and that we have shown SF preferentially inhibits all of these factors, we hypothesize that in TNBCs NF-kB inhibition is the major mechanism of action for efficacy. This is consistent with the report by Kallifatidis et. al. demonstrating pancreatic cancer cell lines and their respective CSC population are sensitive to SF-mediated NF-kB inhibition (73).

As identified above our results indicate that docetaxel treatment increases both ALDH+ and CD44+/CD24-/EpCAM+ BCSCs as well as IL-6, while SF inhibits BCSCs across multiple subtypes of breast cancer and also NF-kB. Therefore we postulate that SF is well suited for combination with docetaxel to overcome induction of BCSCs through regulation of IL-6. In vitro, therapeutically relevant doses in which docetaxel which would inhibit the majority of differentiated cells in combination with a low dose of SF capable of inhibiting BCSCs result in SF-mediated inhibition of IL-6 production. Consequently, not only does the combination block docetaxel-mediated CSC expansion but also actually reduces BCSC levels to that of SF treatment alone. In bulk TNBC cell lines in vitro this combination leads to an additive (SUM149) or synergistic (SUM159) response when 50% of cells are inhibited, for instance when concentrations below the IC50 are used for both drugs. However, when docetaxel concentrations well above the IC50 are combined with concentrations of SF near its IC50, an antagonist response is observed. While this does not alter the conclusion that SF and docetaxel should be

combined to target both BCSCs and reduce bulk tumor volume, it does indicate that there may be a need for future studies to identify an optimum dosing regimen.

Using an orthotopic mouse xenograft tumor model, I.P. administration of daily SF in combination with weekly docetaxel leads to a dramatic reduction in primary tumor growth and begins to cause tumor regression. Furthermore, ELDA of secondary tumor formation with residual cells from the primary tumors illustrates that docetaxel indeed increases the BCSC frequency, whereas the combination treatment dramatically reduces it. These results are similar to those reported by Herr's research group in which the combination of SF with gemcitabine in pancreatic cancer reduced CSCs and enhanced gemcitabine-mediated cytotoxicity (69). However, in our study no observable reductions in body weight occurred, even in the combination treatment group. Taken together, these results demonstrate that treatment of TNBCs with cytotoxic chemotherapy would greatly benefit from the addition of SF to prevent expansion of and eliminate BCSCs.

Material and methods

Cell Lines and Reagents. SUM159 and SUM149 cell lines were cultured under a 5% CO_2 environment in F12 medium (Invitrogen, Carlsbad, CA) supplemented with 5% fetal bovine serum (Fisher Scientific, Pittsburgh, PA), 1% antibiotic-antimycotic (Invitrogen, Carlsbad, CA), 5 μg/ml insulin (Sigma-Aldrich, St Louis, MO), 1 μg/ml hydrocortisone (Sigma-Aldrich, St Louis, MO), and 4 μg/ml gentamicin (Invitrogen, Carlsbad, CA). MCF-7 was maintained in RPMI-1640 supplemented with 10% fetal bovine serum, 1% antibiotic-antimycotic, and 5 μg/ml insulin. HER2 amplified SKBR-3 and BT474 were cultured in DMEM supplemented with 10% fetal bovine serum and 1% antibiotic-

antimycotic. ZR75-1, MDA-MB-436, and MDA-MB-231 were cultured in RPMI-1640 supplemented with 10% fetal bovine serum, and 1 % antibiotic-antimycotic

MTS Cell Proliferation Assay. Cell lines were seeded at a density of 3,000 cells per well in 96-well plates. The following day wells were incubated with sulforaphane, docetaxel, or a combination of the two drugs at varying concentrations for a period of 72 hours. Reduction in proliferation relative to control-treated cells was determined by the MTS assay (Promega) according to manufacturer's instruction. Reduction of tetrazolium compound MTS into a soluble formazan product with absorbance at 490 nm is directly proportional to number of viable cells in culture. Pharmacodynamic modeling was performed using WinNonlin (Pharsight) with a sigmoid inhibitory effect model which estimates baseline effect, maximum effect, EC50, and shape parameter Gamma. In the case of treatment with both SF and docetaxel, calculation of the combination indices were automated using Compusyn (ComboSyn Inc.) software where a fit of $r > 0.95$ was considered an accurate simulation of dose and effect.

Flow Cytometry Analysis. Cell lines were plated at a density of 500,000 cells in 10 cm plates and allowed to adhere overnight. Treatments with sulforaphane, docetaxel, or combination at various concentrations of both drugs were carried out for 72 hours. Following treatment adherent cells were collected, counted for determination of absolute cell numbers, and stained with CD44-APC (BD Biosciences), CD24-PE (BD Biosciences), and EpCAM-PE-CY7 (Biolegend) in HBSS with 2% FBS on ice for 45 min. The Aldefluor assay (STEMCELL Technologies) was carried out according to manufacturer's instruction. Incubation with ALDH substrate was performed for 45 min in a 37 °C water bath. For each replicate within a given treatment group, a DEAB

negative control was present to set a positive gate with a background positivity of 0.1%. After staining, cells were washed with 2% FBS in HBSS followed by addition of DAPI immediately before analysis to determine viability.

Determination of secreted cytokines. Cell lines were seeded at a density of 250,000 cells in a 6-well plate and allowed to adhere overnight. Treatment with docetaxel was performed in the presence or absence of SF for 8 hours. Afterward cells were washed with PBS and resuspended in cell culture medium with or without SF. After 72 hours media was collected, centrifuged, and 200 µl were subjected to an ELISA to determine secretion of human IL-6 and IL-8. Assays were performed using paired antibody kits (Duosets, R&D Systems, Minneapolis, MN) according to manufacturer's protocol with two exceptions: samples were incubated overnight at 4 °C, and the blocking/assay buffer was 0.2% casein in tris-buffered saline. Data was acquired with a BioTek Synergy HT plate reader and analyzed using Gen5 software (Winooski, VT).

Immunocytochemistry. SUM159 cells were seeded at a density of 20,000 cells per well in 4-well glass chambers slides (lab-tek) and allowed to adhere overnight. Sulforaphane was incubated at the indicated concentration for 30 min, followed by the addition of 50 ng/ml TNF-α for two hours. Treated cells were fixed using ice cold 1:1 methanol to acetonitrile followed by blocking with 3% bovine serum albumin. Primary incubation with anti-p65 NF-κB (Cell Signaling Technology) was carried out at 4 °C overnight, followed by incubation with Alexa Fluor 488-conjugated secondary antibody (Invitrogen) for two hours at room temperature. Fluorescent imaging was carried out with a Nikon Eclipse TE2000-S microscope and photos were acquired using MetaMorph 7.6.0.0.

Luciferase Reporter Assay. Lentiviral particles containing luciferase reporter construct driven by NF-κB (system biosciences) were obtained and transfected into SUM159 and MDA-MB-231 cell lines. Briefly, four copies of NF-κB TRE sequences "GGGACTTTCC" were inserted upstream of minimal essential CMV (mCMV) promoter which drives GFP-T2A-luciferase. Polyprotein is cleaved at the T2A site to give rise to GFP and Luciferase. Cell lines were plated at a density of 2500 cells per well in a clear bottom, white 96-well plate and treated with the indicated concentration of SF. Two hours following incubation with SF, the TNF-α concentration in media was brought to 50 ng/ml. After six hours Luciferase activity was measured according to manufacturer's instructions using oneGlo assay (promega) on a Bio-Tek Synergy 2 plate reader.

Mammosphere Formation Assay. SUM149 cells were plated at a density of 2,000 cells per well in an ultra-low attachment 6 well plate (Corning). Serum free medium consisted of MEBM base medium supplemented with 2% B27 (Invitrogen), 1% P/S (Invitrogen), 4 ug/ml gentamicin (Invitrogen), 5 ug/ml insulin (Sigma-aldrich), 20 ng/ml EGF (Sigma-aldrich), 20 ng/ml bFGF (Sigma-aldrich), 1 ug/ml hydrocortisone (Sigma-aldrich), and 1:25,000,000 β-ME (Sigma-aldrich). Drug treatment with sulforaphane, docetaxel, or the combination of the two was carried out for seven days. After drug treatment individual spheres were counted manually and representative images were acquired using a Nikon Eclipse TE2000-S microscope. Generation of secondary spheres was carried out by collection of primary spheres using a nylon 40 μm mesh filter, followed by collection of single cells from spheres by trypsinization in conjunction with manual dissociation by passage through a 25 gauge needle. A fixed number of live cells was then equally distributed into 96-well plates for each treatment group, and cultured for an additional

seven days in the absence of drug. Secondary sphere formation rate was manually determined by counting the number of cells plated and total number of spheres formed.

Advanced Tumor Model. All studies involving mice were conducted in accordance with a standard animal protocol approved by the University Committee on the Use and Care of Animals at the University of Michigan. Female five week old non-obese diabetic/severe combined immunodeficient (NOD/SCID) mice were obtained from Jackson Laboratory. Xenograft formation was generated by direct injection of 1.5 million SUM149 cells, suspended in 50 ul of 25% F-12 in matrigel, into the exposed no.4 inguinal mammary pad. Tumor detection was assessed by palpation and, once identified, measurement of tumor volume was carried out using digital calipers every five days. Sulforaphane (50 mg/kg daily), docetaxel (10 mg/kg once every seven days), or the combination of both were administered via I.P. injection beginning when tumor volume reached approximately 50 mm^3. When the combined sulforaphane and docetaxel treatment began to cause significant tumor regression mice were euthanized by CO_2 inhalation, tumors were isolated, and extreme limiting dilution analysis in secondary mice was performed.

Extreme Limiting Dilution analysis. Isolated primary tumors were mechanically dissociated using a gentleMACS octo tissue dissociator with C tubes (Miltenyi Biotec). In order to consistently obtain single cell suspensions a human tumor dissociation kit (Miltenyi Biotec) was used according to manufacturer's instruction for "tough tumors." Briefly, tumors were cut into 2-4 mm pieces and exposed to dissociation enzymes. Following incubation at 37 °C for 30 min on an orbital shaker, mechanical dissociation was carried out with the genteMACS and this process was repeated three times.

Dissociated cells were collected after passage through a 40 μm nylon mesh filter. Live human cells from xenografts were obtained by FACS on a SY3200 (Sony Biotechnology) flow cytometer after selection of DAPI- and H2KD- cells. Secondary female, five week old NOD/SCID mice were inoculated with 10,000, 1,000, or 100 cells from each treatment group as described above. Tumor formation rate in secondary mice was assessed by direct palpitation for seven weeks following cell implantation and used to assess BCSC frequency using the ELDA webtool (http://bioinf.wehi.edu.au/software/elda/).

References

1. Parise CA & Caggiano V (2014) Breast Cancer Survival Defined by the ER/PR/HER2 Subtypes and a Surrogate Classification according to Tumor Grade and Immunohistochemical Biomarkers. *Journal of Cancer Epidemiology* 2014:11.
2. Onitilo AA, Engel JM, Greenlee RT, & Mukesh BN (2009) Breast Cancer Subtypes Based on ER/PR and Her2 Expression: Comparison of Clinicopathologic Features and Survival. *Clinical Medicine & Research* 7(1-2):4-13.
3. Hudis CA & Gianni L (2011) Triple-Negative Breast Cancer: An Unmet Medical Need. *The Oncologist* 16(suppl 1):1-11.
4. Dent R, *et al.* (2007) Triple-Negative Breast Cancer: Clinical Features and Patterns of Recurrence. *Clinical Cancer Research* 13(15):4429-4434.
5. Carey LA, *et al.* (2007) The Triple Negative Paradox: Primary Tumor Chemosensitivity of Breast Cancer Subtypes. *Clinical Cancer Research* 13(8):2329-2334.
6. Liedtke C, *et al.* (2008) Response to Neoadjuvant Therapy and Long-Term Survival in Patients With Triple-Negative Breast Cancer. *Journal of Clinical Oncology* 26(8):1275-1281.
7. Huober J, *et al.* (2010) Effect of neoadjuvant anthracycline–taxane-based chemotherapy in different biological breast cancer phenotypes: overall results from the GeparTrio study. *Breast Cancer Res Treat* 124(1):133-140.
8. von Minckwitz G, *et al.* (2012) Definition and Impact of Pathologic Complete Response on Prognosis After Neoadjuvant Chemotherapy in Various Intrinsic Breast Cancer Subtypes. *Journal of Clinical Oncology* 30(15):1796-1804.
9. von Minckwitz G & Martin M (2012) Neoadjuvant treatments for triple-negative breast cancer (TNBC). *Annals of Oncology* 23(suppl 6):vi35-vi39.

10. Kassam F, *et al.* (2009) Survival Outcomes for Patients with Metastatic Triple-Negative Breast Cancer: Implications for Clinical Practice and Trial Design. *Clinical Breast Cancer* 9(1):29-33.
11. Carey LA (2011) Directed Therapy of Subtypes of Triple-Negative Breast Cancer. *The Oncologist* 16(suppl 1):71-78.
12. Lehmann BD, *et al.* (2011) Identification of human triple-negative breast cancer subtypes and preclinical models for selection of targeted therapies. *The Journal of Clinical Investigation* 121(7):2750-2767.
13. Penault-Llorca F & Viale G (2012) Pathological and molecular diagnosis of triple-negative breast cancer: a clinical perspective. *Annals of Oncology* 23(suppl 6):vi19-vi22.
14. Cascione L, *et al.* (2013) Integrated MicroRNA and mRNA Signatures Associated with Survival in Triple Negative Breast Cancer. *PLoS ONE* 8(2):e55910.
15. Li X, *et al.* (2008) Intrinsic Resistance of Tumorigenic Breast Cancer Cells to Chemotherapy. *Journal of the National Cancer Institute* 100(9):672-679.
16. Tanei T, *et al.* (2009) Association of Breast Cancer Stem Cells Identified by Aldehyde Dehydrogenase 1 Expression with Resistance to Sequential Paclitaxel and Epirubicin-Based Chemotherapy for Breast Cancers. *Clinical Cancer Research* 15(12):4234-4241.
17. Shafee N, *et al.* (2008) Cancer Stem Cells Contribute to Cisplatin Resistance in Brca1/p53–Mediated Mouse Mammary Tumors. *Cancer Research* 68(9):3243-3250.
18. Bonnet D & Dick JE (1997) Human acute myeloid leukemia is organized as a hierarchy that originates from a primitive hematopoietic cell. *Nat Med* 3(7):730-737.
19. Al-Hajj M, Wicha MS, Benito-Hernandez A, Morrison SJ, & Clarke MF (2003) Prospective identification of tumorigenic breast cancer cells. *Proceedings of the National Academy of Sciences* 100(7):3983-3988.
20. Singh SK, *et al.* (2003) Identification of a Cancer Stem Cell in Human Brain Tumors. *Cancer Research* 63(18):5821-5828.
21. O'Brien CA, Pollett A, Gallinger S, & Dick JE (2007) A human colon cancer cell capable of initiating tumour growth in immunodeficient mice. *Nature* 445(7123):106-110.
22. Schatton T, *et al.* (2008) Identification of cells initiating human melanomas. *Nature* 451(7176):345-349.
23. Ginestier C, *et al.* (2007) ALDH1 Is a Marker of Normal and Malignant Human Mammary Stem Cells and a Predictor of Poor Clinical Outcome. *Cell Stem Cell* 1(5):555-567.
24. Prince ME, *et al.* (2007) Identification of a subpopulation of cells with cancer stem cell properties in head and neck squamous cell carcinoma. *Proceedings of the National Academy of Sciences* 104(3):973-978.
25. Reya T, Morrison SJ, Clarke MF, & Weissman IL (2001) Stem cells, cancer, and cancer stem cells. *Nature* 414(6859):105-111.
26. Zhou B-BS, *et al.* (2009) Tumour-initiating cells: challenges and opportunities for anticancer drug discovery. *Nat Rev Drug Discov* 8(10):806-823.

27. Sakariassen PØ, Immervoll H, & Chekenya M (2007) Cancer Stem Cells as Mediators of Treatment Resistance in Brain Tumors: Status and Controversies. *Neoplasia (New York, N.Y.)* 9(11):882-892.
28. Charafe-Jauffret E, *et al.* (2009) Breast cancer cell lines contain functional cancer stem cells with metastatic capacity and a distinct molecular signature. *Cancer Research* 69(4):1302-1313.
29. Lamb R, *et al.* (2013) Wnt Pathway Activity in Breast Cancer Sub-Types and Stem-Like Cells. *PLoS ONE* 8(7):e67811.
30. Liu S, *et al.* (2006) Hedgehog Signaling and Bmi-1 Regulate Self-renewal of Normal and Malignant Human Mammary Stem Cells. *Cancer Research* 66(12):6063-6071.
31. Dontu G, *et al.* (2004) Role of Notch signaling in cell-fate determination of human mammary stem/progenitor cells. *Breast Cancer Research* 6(6):R605-R615.
32. Korkaya H, *et al.* (2009) Regulation of Mammary Stem/Progenitor Cells by PTEN/Akt/β-Catenin Signaling. *PLoS Biol* 7(6):e1000121.
33. Yamamoto M, *et al.* (2013) NF-κB non-cell-autonomously regulates cancer stem cell populations in the basal-like breast cancer subtype. *Nat Commun* 4.
34. Lee HE, *et al.* (2011) An increase in cancer stem cell population after primary systemic therapy is a poor prognostic factor in breast cancer. *Br J Cancer* 104(11):1730-1738.
35. Ginestier C, *et al.* (2010) CXCR1 blockade selectively targets human breast cancer stem cells in vitro and in xenografts. *The Journal of Clinical Investigation* 120(2):485-497.
36. Korkaya H, *et al.* (2012) Activation of an IL6 Inflammatory Loop Mediates Trastuzumab Resistance in HER2+ Breast Cancer by Expanding the Cancer Stem Cell Population. *Molecular Cell* 47(4):570-584.
37. Tsavaris N, Kosmas C, Vadiaka M, Kanelopoulos P, & Boulamatsis D (2002) Immune changes in patients with advanced breast cancer undergoing chemotherapy with taxanes. *Br J Cancer* 87(1):21-27.
38. Sansone P, *et al.* (2007) IL-6 triggers malignant features in mammospheres from human ductal breast carcinoma and normal mammary gland. *The Journal of Clinical Investigation* 117(12):3988-4002.
39. Libermann TA & Baltimore D (1990) Activation of interleukin-6 gene expression through the NF-kappa B transcription factor. *Molecular and Cellular Biology* 10(5):2327-2334.
40. Elliott CL, Allport VC, Loudon JAZ, Wu GD, & Bennett PR (2001) Nuclear factor-kappa B is essential for up-regulation of interleukin-8 expression in human amnion and cervical epithelial cells. *Molecular Human Reproduction* 7(8):787-790.
41. Mani SA, *et al.* (2008) The Epithelial-Mesenchymal Transition Generates Cells with Properties of Stem Cells. *Cell* 133(4):704-715.
42. Iliopoulos D, Hirsch HA, & Struhl K (2009) An Epigenetic Switch Involving NF-κB, Lin28, Let-7 MicroRNA, and IL6 Links Inflammation to Cell Transformation. *Cell* 139(4):693-706.

43. Li Y, *et al.* (2010) Sulforaphane, a Dietary Component of Broccoli/Broccoli Sprouts, Inhibits Breast Cancer Stem Cells. *Clinical cancer research : an official journal of the American Association for Cancer Research* 16(9):2580-2590.
44. Li Y, *et al.* (2012) Sulforaphane inhibits pancreatic cancer through disrupting Hsp90–p50Cdc37 complex and direct interactions with amino acids residues of Hsp90. *The Journal of Nutritional Biochemistry* 23(12):1617-1626.
45. Li Y, Zhang T, Schwartz SJ, & Sun D (2011) Sulforaphane Potentiates the Efficacy of 17-Allylamino 17-Demethoxygeldanamycin Against Pancreatic Cancer Through Enhanced Abrogation of Hsp90 Chaperone Function. *Nutrition and Cancer* 63(7):1151-1159.
46. Zhang Y, Talalay P, Cho CG, & Posner GH (1992) A major inducer of anticarcinogenic protective enzymes from broccoli: isolation and elucidation of structure. *Proceedings of the National Academy of Sciences* 89(6):2399-2403.
47. Conaway CC, *et al.* (2005) Phenethyl Isothiocyanate and Sulforaphane and their N-Acetylcysteine Conjugates Inhibit Malignant Progression of Lung Adenomas Induced by Tobacco Carcinogens in A/J Mice. *Cancer Research* 65(18):8548-8557.
48. Chung F-L, Conaway CC, Rao CV, & Reddy BS (2000) Chemoprevention of colonic aberrant crypt foci in Fischer rats by sulforaphane and phenethyl isothiocyanate. *Carcinogenesis* 21(12):2287-2291.
49. KANEMATSU S, *et al.* (2010) Autophagy Inhibition Enhances Sulforaphane-induced Apoptosis in Human Breast Cancer Cells. *Anticancer Research* 30(9):3381-3390.
50. Hollestelle A, *et al.* (2010) Distinct gene mutation profiles among luminal-type and basal-type breast cancer cell lines. *Breast Cancer Res Treat* 121(1):53-64.
51. Hutti JE, *et al.* (2012) Oncogenic PI3K Mutations Lead to NF-κB–Dependent Cytokine Expression following Growth Factor Deprivation. *Cancer Research* 72(13):3260-3269.
52. Guzman ML, *et al.* (2001) *Nuclear factor-κB is constitutively activated in primitive human acute myelogenous leukemia cells* pp 2301-2307.
53. Hinohara K, *et al.* (2012) ErbB receptor tyrosine kinase/NF-κB signaling controls mammosphere formation in human breast cancer. *Proceedings of the National Academy of Sciences* 109(17):6584-6589.
54. Hartman ZC, *et al.* (2013) Growth of Triple-Negative Breast Cancer Cells Relies upon Coordinate Autocrine Expression of the Proinflammatory Cytokines IL-6 and IL-8. *Cancer Research* 73(11):3470-3480.
55. Kim G, *et al.* (2015) SOCS3-mediated regulation of inflammatory cytokines in PTEN and p53 inactivated triple negative breast cancer model. *Oncogene* 34(6):671-680.
56. Chou T-C & Talalay P (1984) Quantitative analysis of dose-effect relationships: the combined effects of multiple drugs or enzyme inhibitors. *Advances in Enzyme Regulation* 22:27-55.
57. Chou T-C (2010) Drug Combination Studies and Their Synergy Quantification Using the Chou-Talalay Method. *Cancer Research* 70(2):440-446.
58. Dontu G, Al-Hajj M, Abdallah WM, Clarke MF, & Wicha MS (2003) Stem cells in normal breast development and breast cancer. *Cell Proliferation* 36:59-72.

59. Hu Y & Smyth GK (2009) ELDA: Extreme limiting dilution analysis for comparing depleted and enriched populations in stem cell and other assays. *Journal of Immunological Methods* 347(1–2):70-78.
60. Cardoso F, *et al.* (2012) Locally recurrent or metastatic breast cancer: ESMO Clinical Practice Guidelines for diagnosis, treatment and follow-up. *Annals of Oncology* 23(suppl 7):vii11-vii19.
61. André F & Zielinski CC (2012) Optimal strategies for the treatment of metastatic triple-negative breast cancer with currently approved agents. *Annals of Oncology* 23(suppl 6):vi46-vi51.
62. Gupta PB, *et al.* (2009) Identification of Selective Inhibitors of Cancer Stem Cells by High-Throughput Screening. *Cell* 138(4):645-659.
63. Hirsch HA, Iliopoulos D, Tsichlis PN, & Struhl K (2009) Metformin selectively targets cancer stem cells, and acts together with chemotherapy to block tumor growth and prolong remission. *Cancer Research* 69(19):7507-7511.
64. Hermann PC, *et al.* (2007) Distinct Populations of Cancer Stem Cells Determine Tumor Growth and Metastatic Activity in Human Pancreatic Cancer. *Cell Stem Cell* 1(3):313-323.
65. Conley SJ, *et al.* (2012) Antiangiogenic agents increase breast cancer stem cells via the generation of tumor hypoxia. *Proceedings of the National Academy of Sciences* 109(8):2784-2789.
66. Pawlik A, Wiczk A, Kaczyńska A, Antosiewicz J, & Herman-Antosiewicz A (2013) Sulforaphane inhibits growth of phenotypically different breast cancer cells. *Eur J Nutr* 52(8):1949-1958.
67. Gamet-Payrastre L, *et al.* (2000) Sulforaphane, a Naturally Occurring Isothiocyanate, Induces Cell Cycle Arrest and Apoptosis in HT29 Human Colon Cancer Cells. *Cancer Research* 60(5):1426-1433.
68. Suppipat K, Park CS, Shen Y, Zhu X, & Lacorazza HD (2012) Sulforaphane Induces Cell Cycle Arrest and Apoptosis in Acute Lymphoblastic Leukemia Cells. *PLoS ONE* 7(12):e51251.
69. Kallifatidis G, *et al.* (2011) Sulforaphane Increases Drug-mediated Cytotoxicity Toward Cancer Stem-like Cells of Pancreas and Prostate. *Mol Ther* 19(1):188-195.
70. Li S-H, Fu J, Watkins D, Srivastava R, & Shankar S (2013) Sulforaphane regulates self-renewal of pancreatic cancer stem cells through the modulation of Sonic hedgehog–GLI pathway. *Mol Cell Biochem* 373(1-2):217-227.
71. Juge N, Mithen RF, & Traka M (2007) Molecular basis for chemoprevention by sulforaphane: a comprehensive review. *Cell. Mol. Life Sci.* 64(9):1105-1127.
72. Hahm E-R & Singh SV (2010) Sulforaphane Inhibits Constitutive and Interleukin-6–Induced Activation of Signal Transducer and Activator of Transcription 3 in Prostate Cancer Cells. *Cancer Prevention Research* 3(4):484-494.
73. Kallifatidis G, *et al.* (2009) Sulforaphane targets pancreatic tumour-initiating cells by NF-κB-induced antiapoptotic signalling. *Gut* 58(7):949-963.

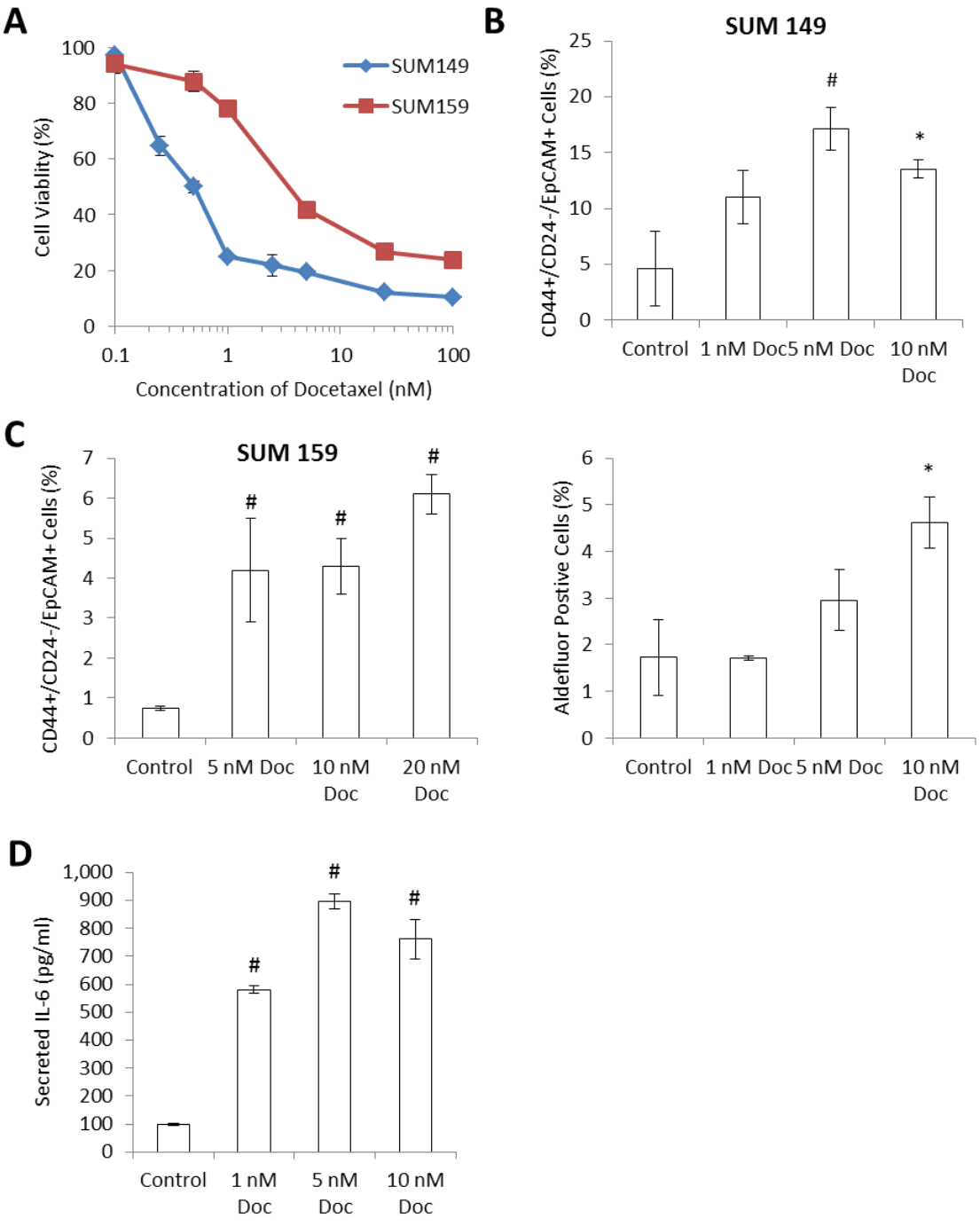

Figure 2.1 Docetaxel reduces bulk cell line viability while increasing IL-6 expression and breast cancer stem cells. (A) MTS proliferation assay performed in triple negative

breast cancer cell lines SUM149 and SUM159 in the presence of increasing concentrations of docetaxel (Doc) for 72 hours. N=6. (B) SUM149 cells, which exhibit distinct populations CD44+/CD24-/EpCAM+ and ALDH+ breast cancer stem cells, cultured in the presence of increasing concentrations of docetaxel for 72 hours followed by antibody staining (top) or Aldefluor assay (bottom) as determined by FACS analysis. N=3. (C) FACS analysis of SUM159 cells treated with docetaxel for 72 hours followed by staining of CD44, CD24, and EpCAM. N=3. (D) Concentration of secreted IL-6 protein in media from 64 hour culture of SUM149 cells after being exposed to docetaxel for eight hours as determined by enzyme-linked immunosorbent assay. N=3. Data presented as average value ± standard deviation. * $P<0.05$, # $P<0.01$.

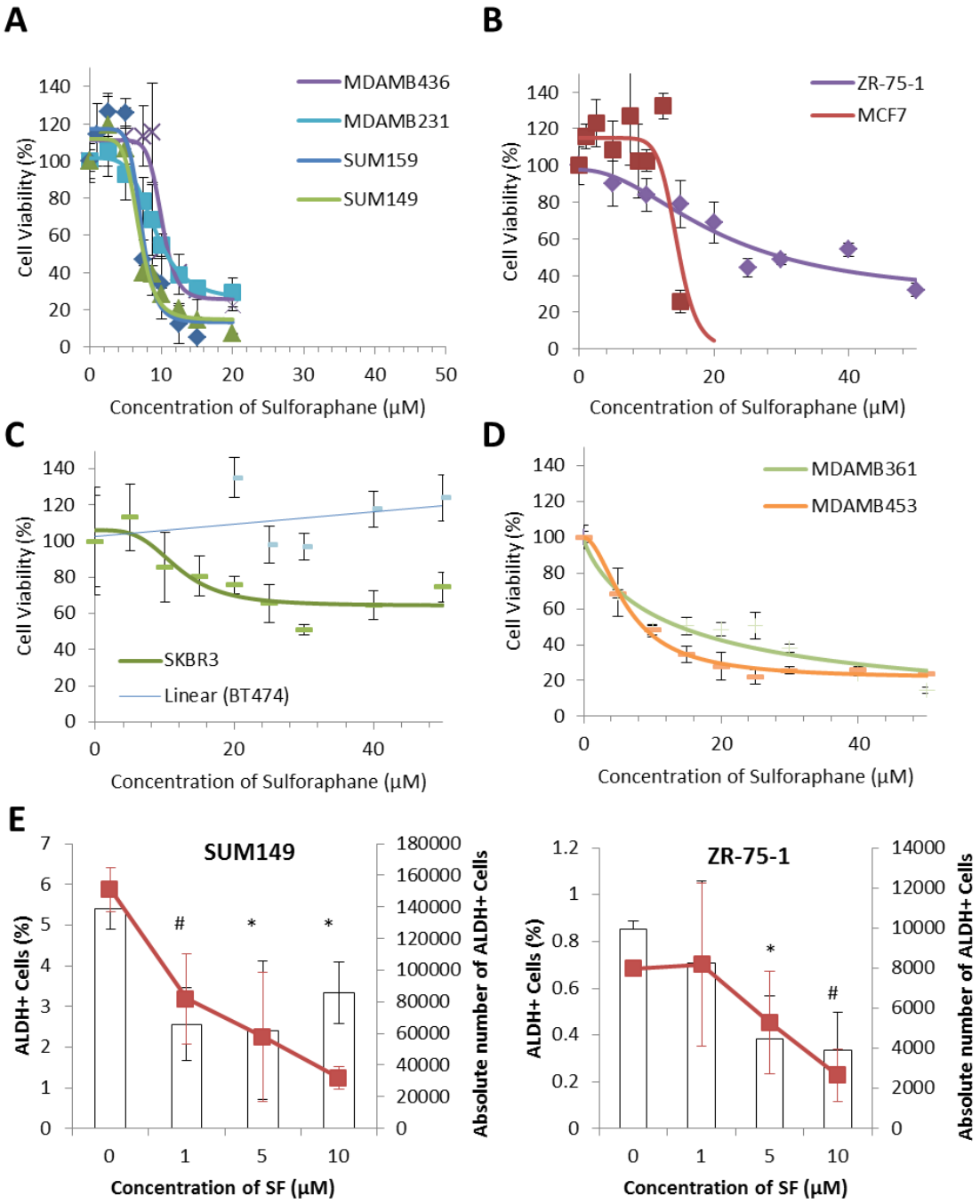

Figure 2.2 Sulforaphane preferentially inhibits triple negative breast cancers and ALDH+ breast cancer stem cells. MTS proliferation assay was carried out after incubating cell lines with increasing concentrations of sulforaphane (SF) for 72 hours. N=6 (A) Triple negative cell lines SUM149, SUM159, MDA-MB-231, and MDA-MB-436 exhibit the highest maximum effect values and lowest IC50s. (B) Luminal cell lines MCF7 and ZR-75-1, containing estrogen and progesterone receptors, exhibit higher variability in efficacy. (C) HER2 amplified SKBR3 and BT474 exhibit SF resistance (D) Luminal B MDA-MB-361 and MDA-MB-453, expressing HER2 and containing AKT

activating mutations, and are sensitive to SF. (E) FACS analysis of the Aldefluor assay following 72 hour incubation of SUM149 or ZR-75-1 cells exposed to increasing concentrations of SF. N=3. Data presented as average value ± standard deviation. * $P<0.05$, # $P<0.01$.

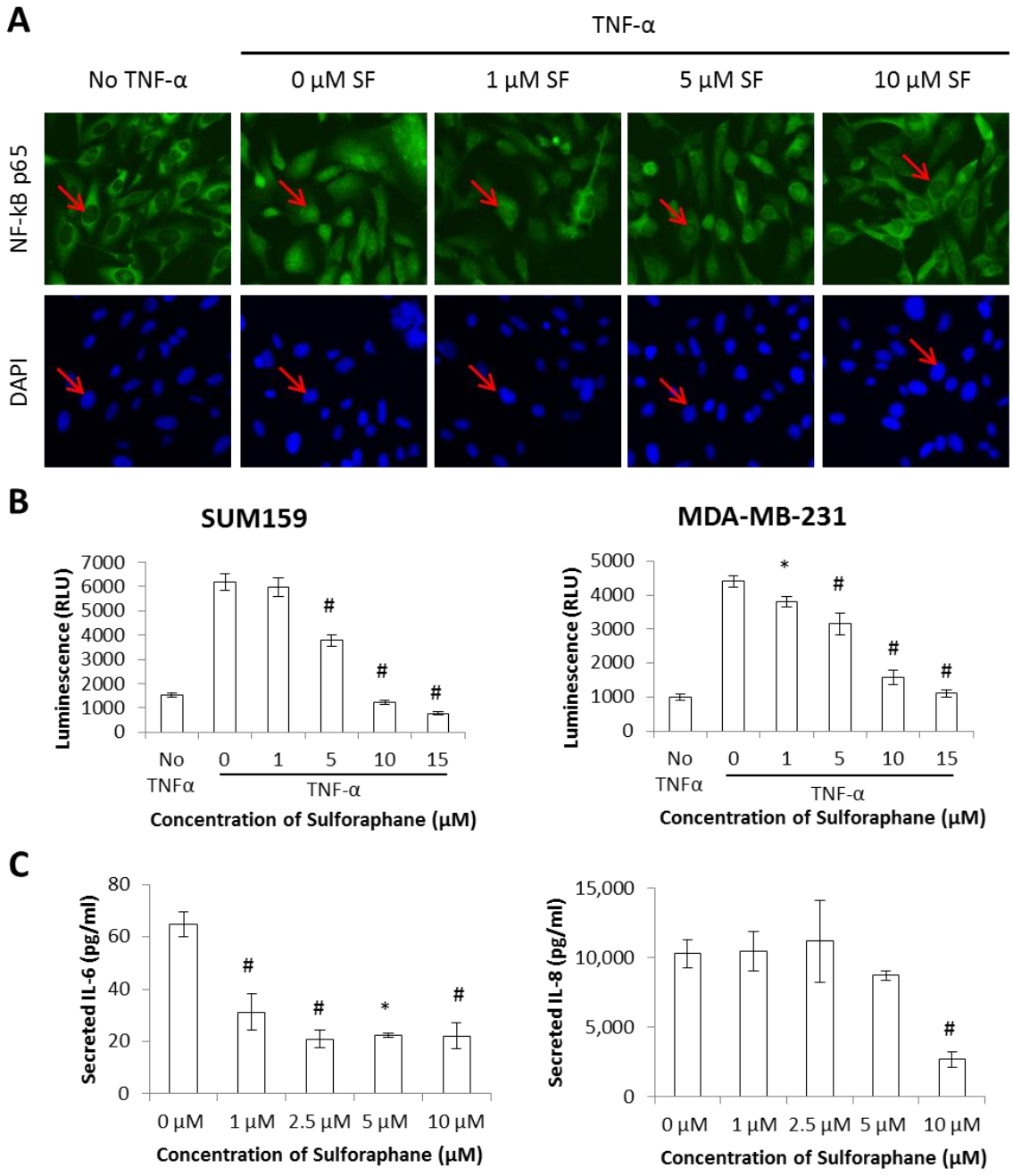

Figure 2.3 Sulforaphane inhibits NF-kB nuclear translocation and transcriptional activity in triple negative breast cancers. (A) Representative immunocytochemical staining of the SUM159 cell line for the p65 subunit of NF-kB after pre-incubation for 30 min with increasing concentrations of SF with and without the addition of 50 ng/ml TNF-α for 2 hours. Counter staining of nuclei was carried out with 1 μg/ml DAPI immediately before imaging (bottom). Red arrow indicates the cytoplasmic-nuclear boarder. Images obtained using a 40X objective. (B) TNBC cell lines SUM159 and MDA-MB-231 were transfected with a NF-kB-dependent luciferase reporter. Cell lines were treated with

increasing concentrations of SF for 2 hours followed by the addition of 50 ng/ml TNF-α; six hours later luminescence was measured. N=3. (C) Concentration of secreted IL-6 (left) and IL-8 (right) protein in media from 72 hour culture of SUM159 cells after being exposed to increasing concentrations of SF, as determined by enzyme-linked immunosorbent assay. N=3. Data presented as average value ± standard deviation. * $P<0.05$, # $P<0.01$.

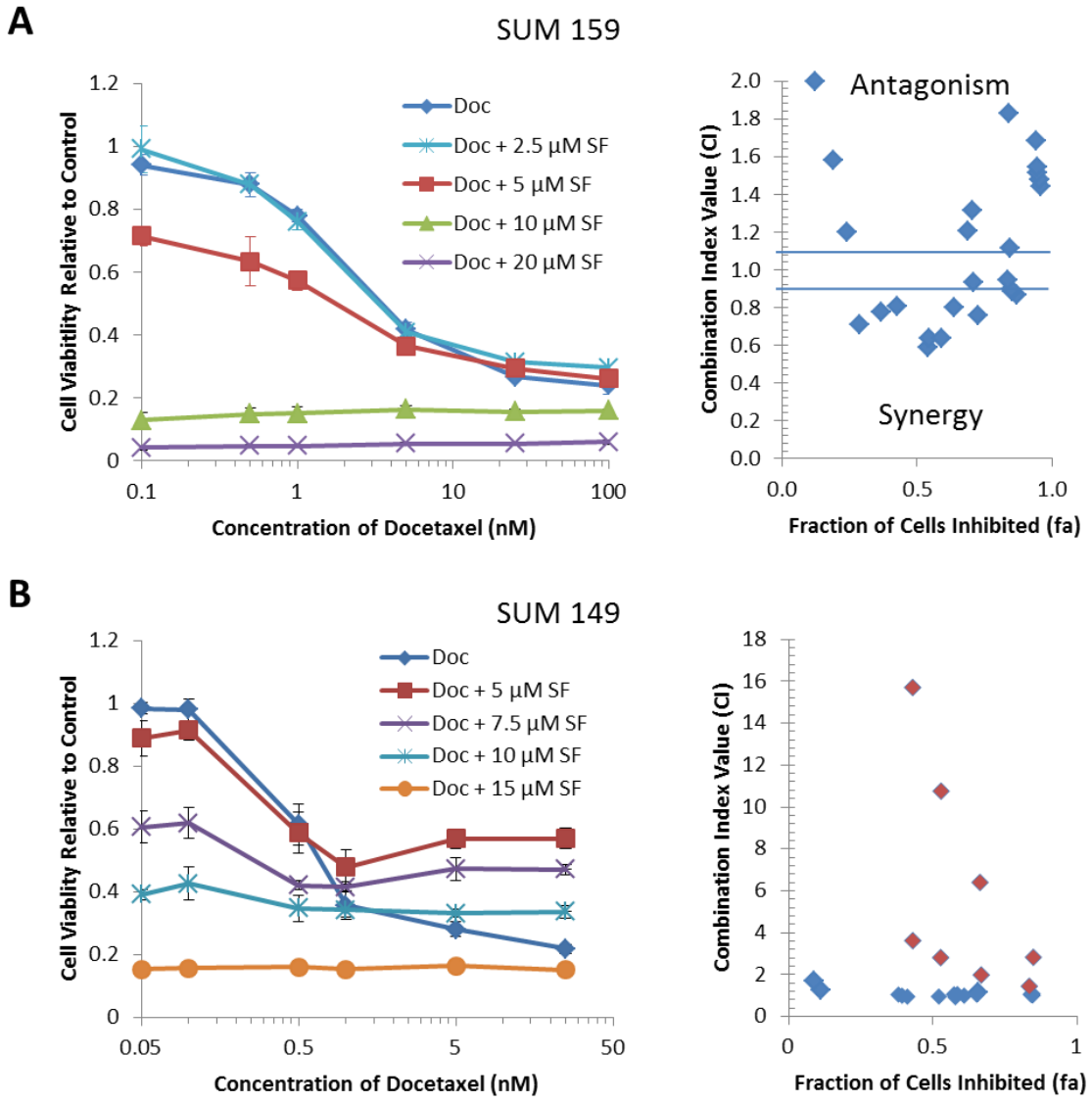

Figure 2.4 Combination of docetaxel and sulforaphane cooperate to inhibit bulk cell line proliferation at specific concentrations. MTS proliferation assay was performed in TNBC cell lines (A) SUM159 and (B) SUM149 cell viability following incubation with increasing concentrations of docetaxel alone or in combination with fixed concentrations of SF. N=4. Data presented as average value ± standard deviation. Calculations of combination index (CI) values versus fraction of cells inhibited (fa) were automated by inputting MTS results into Compusyn (Combosyn) software. Typical interpretations of CI values for an additive effect range from 0.9-1.1 (A, right, blue lines), while <0.9 suggests synergism and >1.1 indicates antagonism.

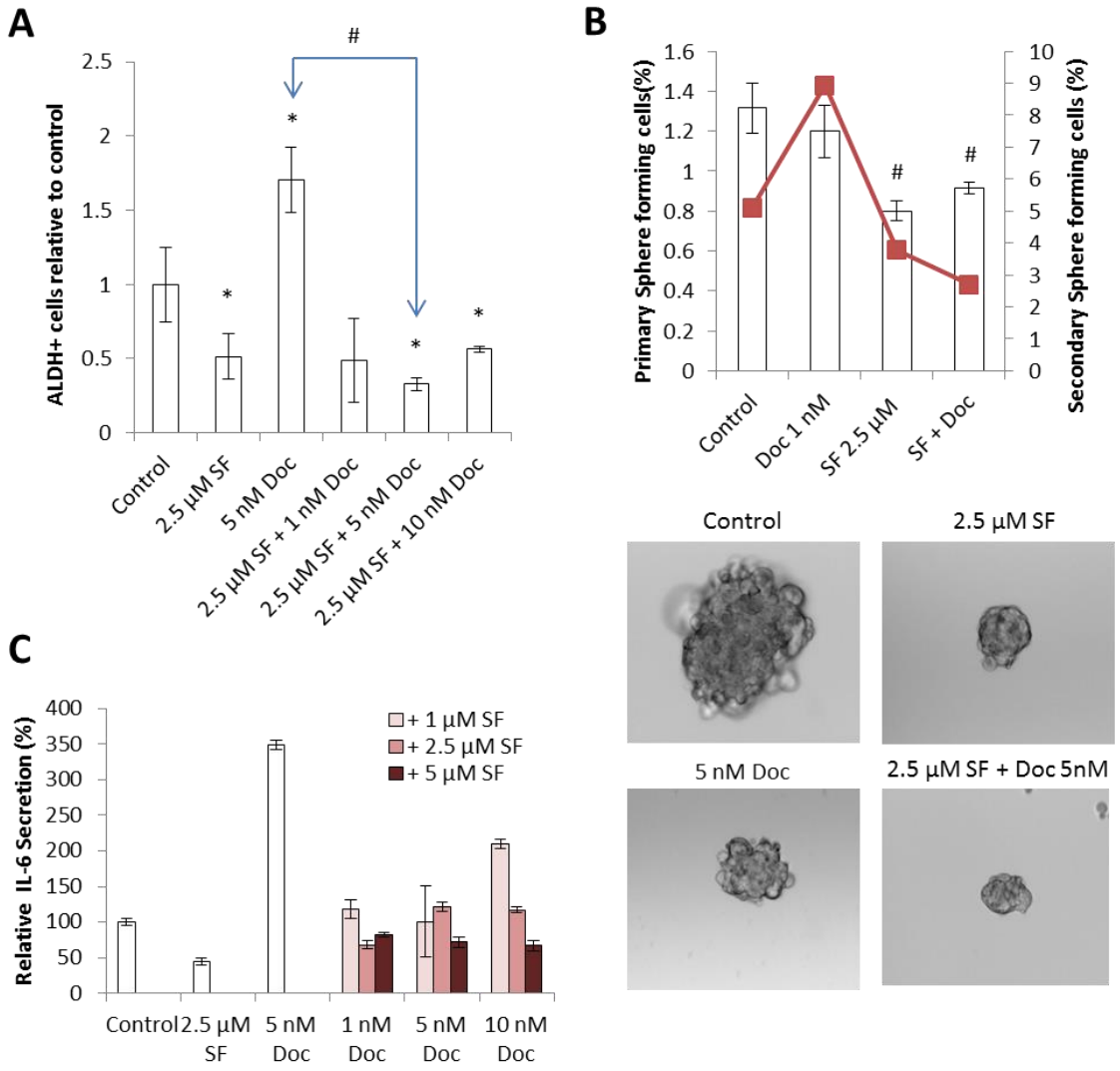

Figure 2.5 Sulforaphane prevents docetaxel-mediated IL-6 production and reduces BCSCs during combination treatment. (A) FACS analysis of the Aldefluor assay following 72 hour incubation of SUM149 cells exposed to increasing sulforaphane (SF) and docetaxel (Doc) alone or in combination. N=3. (B) Percentage of cells from bulk SUM149 cell line which are capable of forming mammospheres when treated with SF and Doc alone or in combination. Bars represent primary sphere formation and lines represent secondary generation which was not exposed to further drug treatment after passage. N=3. A representative image of a sphere for each treatment group included below where and a 40X objective was used for image acquisition. (C) SUM149 cells were treated for eight hours in the presence of SF and Doc alone or in increasing combination of both drugs. Cells were washed and media replaced with SF supplemented medium where indicated for an additional 64 hours before measurement of secreted IL-6. N=3. Data presented as average value ± standard deviation. * $P<0.05$, # $P<0.01$.

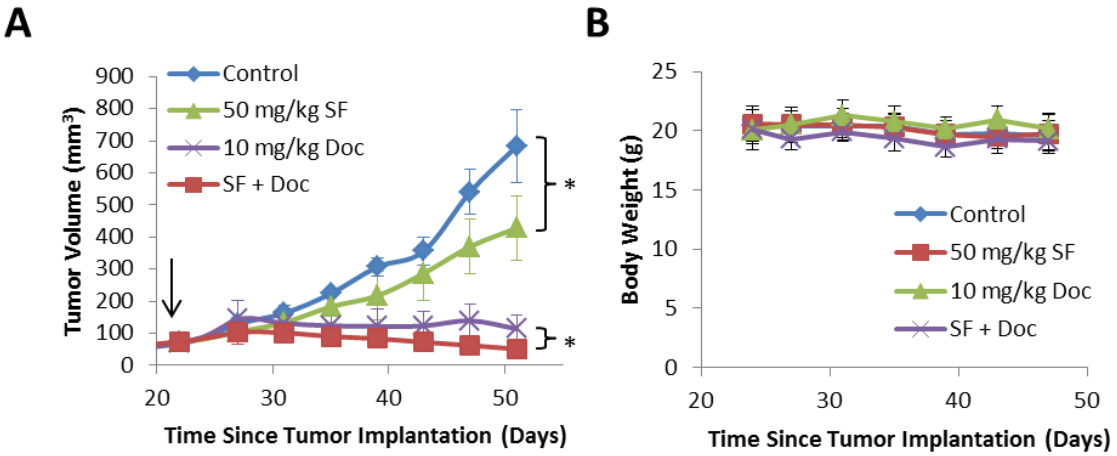

C

Group	Limiting Dilutions (Tumors/Implantations) 10,000	1,000	100	CSC Frequency (1 in /...)
Control	5/6	4/4	4/6	1514
SF	5/6	3/6	1/6	3181
Doc	6/6	5/6	3/4	330
SF + Doc	4/6	2/6	3/6	4245

Pairwise Difference		P-Value
Control	Doc	0.0071
Control	SF	0.163
Control	SF + Doc	0.0424
Doc	SF	0.000183
Doc	SF + Doc	1.70E-05
SF	SF + Doc	0.593

Figure 2.6 Docetaxel and sulforaphane cooperate to eliminate both bulk tumor volume and BCSCs in vivo. (a) NOD/SCID mice bearing SUM149 xenografts with an average tumor volume of 50 mm^3 were randomized into treatment groups which received daily 0.9% saline (Control), daily 50 mg/kg sulforaphane (SF), weekly 10 mg/kg docetaxel (Doc), or daily 50 mg/kg SF in combination with weekly 10 mg/kg Doc as a cassette dose. Each drug was administered via I.P. injection. Arrow denotes the beginning of treatment in primary mice. N=5. * $p \leq 0.05$ in final tumor volume comparisons. (B) Body weight of mice receiving each treatment regimen over the course of administration. N=5. (C) Primary xenografts were removed, dissociated, and serially reimplanted into secondary mice allowing for calculation of tumor initiating CSC frequency by extreme limiting dilution analysis (ELDA). The total number of tumors formed, the number of tumors implanted for each treatment group, and the dilutions of cells implanted used to calculate CSC frequency is shown (left). Estimates of CSC frequency and the p-value associated with pairwise differences (right) was automated using the ELDA web resource.

Chapter 3

Trastuzumab resistance induces EMT and transforms HER2^{+}PTEN^{-} to a triple negative breast cancer that is susceptible to inhibition by sulforaphane

Abstract

Although the development of trastuzumab has made significant advances for HER2+ breast cancer treatment, the majority of patients develop trastuzumab resistance, in which 40% patients have loss of PTEN function. However the consequence of continued use of trastuzumab in these patients predisposed to drug resistance is unknown. We demonstrate that trastuzumab resistance by long term treatment (LTT) in HER2+ breast cancer cells with PTEN inactivation (BT474 PTEN-LTT) induces characteristics of the epithelial-mesenchymal transition (EMT), and transforms HER2+PTEN- breast cancer to triple negative phenotype. In addition, these cells undergo a signaling shift from HER2/AKT dependency to activation of IL-6/STAT3/NF-κB positive feedback loop. Inhibition of IL-6/NF-κB loop by sulforaphane (SF) suppresses IL-6 production, NF-κB translocation, and transcriptional activity. The disruption of IL-6/NF-κB loop by sulforaphane leads to preferential inhibition of trastuzumab-resistant BT474 PTEN-LTT cells, while it showed minimal efficacy in trastuzumab-sensitive BT474. In advanced treatment xenograft models, SF inhibited tumor growth in mice bearing trastuzumab-resistant BT474 PTEN-LTT tumors to the same extent as cytotoxic chemotherapy. Importantly, SF reduced the frequency of breast cancer stem cells by 5.4-fold as shown by re-implantation assays. In

contrast, trastuzumab treatment increased the cancer stem cells population by 4.6-fold. This data suggest that continued use of trastuzumab in HER2+ tumors with PTEN inactivation may induce EMT, increase breast CSCs, and result in a subtype switch generating a TNBC through the IL-6/NF-κB signaling loop. Sulforaphane mediated inhibition of the IL-6/NF-κB signaling loop may provide a novel treatment strategy for trastuzumab-resistant breast cancers with PTEN deletion.

Introduction

The development of anti-HER2 targeted therapy (trastuzumab) has significantly improved the survival of HER2+ breast cancer patients. However, initial response rates in women with HER2 overexpressing metastatic disease treated with single agent trastuzumab range from only 11.6-34 % (1, 2). Further, the majority of patients given trastuzumab treatment will develop drug resistance within one to two years (3, 4). Therefore, it is necessary to identify potential mechanisms of trastuzumab resistance and develop alternative therapeutics for trasutumab-resistant HER2+ breast cancers.

Previous studies have revealed compensatory signaling mechanisms responsible for the drug resistance of HER2+ breast cancer, including: inactivation of PTEN tumor suppressor; antigen masking on HER2 epitope by MUC4; enhanced signaling through other ERBB family receptors; cross-talk of HER2 with IGF-1R; and mutational activation of downstream signaling through PI3-K/AKT pathway (5-9). Inactivation of the PTEN tumor suppressor, found in ~40% of patients with HER2 overexpression, has been demonstrated to induce drug resistance in tumor xenografts and correlate with trastuzumab resistance in patients (10). In addition, inactivation of PTEN has been

shown to be a crucial factor inducing epithelial to mesenchymal transition (EMT) in breast, colon, nasopharyngeal, and prostate cancers (11-14). Furthermore, Recent evidence suggests that EMT may activate diverse alternative survival pathways or actually transform the molecular subtype of the malignancy in castration/enzalutamide resistant prostate cancer, RAF inhibitor resistant melanoma, and EGFR inhibitor resistant lung cancer (15-18).

Korkaya et.al. previously reported that drug resistance in HER2 overexpressing cell lines with PTEN deletion by long term culture with trastuzumab (LTT) induces characteristics of the EMT and expands the breast cancer stem cell (BCSC) population (19). This induction of EMT and expansion of cancer stem cells is proposed to occur through activation of an IL-6/NF-κB positive feedback loop. Interestingly, several studies have demonstrated that inflammatory cytokines such as IL-6 are upregulated in triple negative breast cancers (TNBC) and correlated with poor patient prognosis (20-23).

In this study, we report that trastuzumab resistance in PTEN-deficient HER2+ breast cancer results in the epithelial to mesenchymal transition (EMT), as evident by reduced expression of epithelial markers and increased mesenchymal makers. Following EMT, trastuzumab resistant PTEN-deficient breast cancer cells exhibit a reduction in HER2, estrogen, and progesterone protein expression while increasing proliferation, thus adapting a more aggressive TNBC phenotype. Furthermore, trastuzumab resistant cells exhibited a dramatic increase in IL-6/NF-κB positive feedback loop and expanded the BCSC population. Inhibition of IL-6/NF-κB loop by the natural product sulforaphane selectively eliminated both BCSCs and inhibits bulk PTEN-deficient trastuzumab-resistant breast cancer proliferation. These results suggest that following induction of

EMT by trastuzumab, and consequent molecular subtype switching, inhibition of the IL-6/NF-κB positive feedback loop by SF may offer a novel treatment option for trastuzumab resistant breast cancers with PTEN deletion.

Results

Trastuzumab resistance in breast cancer cells with PTEN deletion induces characteristics of the epithelial to mesenchymal transition (EMT)

In HER2 amplified breast cancer cell line BT474, lentiviral vector containing shPTEN was used to knockdown PTEN as reported previously (19). This cell line (BT474 PTEN-) was cultured long-term with trastuzumab (LTT, >3 weeks) to induce stable trastuzumab resistance (BT474 PTEN- LTT). In order to establish morphological and phenotypic properties of trastuzumab-sensitive and resistant cell lines, we analyzed these cells utilizing microscopy and flow cytometry. Bright field microscopy reveals each sequential step in the generation of trastuzumab resistance results in adaption of a more mesenchymal like phenotype (Fig. 3.1A). In addition, there was a dramatic increase in expression of basal like markers CD44+ CD24- in trastuzumab resistant BT474 PTEN-LTT cells (69.1%) as well as PTEN deleted cells (9.5%) compared to parental BT474 which lacks this population (Fig. 3.1B).

To further characterize the parental and trastuzumab resistant cell lines, real time PCR analysis of EMT related genes was performed. While parental BT474 exhibit high expression of both E-cadherin and EpCAM, these epithelial markers are at undetectable levels in the BT474 PTEN- LTT cell line (Fig. 3.1C). Conversely, the expression of mesenchymal cell markers N-cadherin and vimentin are increased by 16 and 266-fold

respectively (Fig. 3.1D). This data confirms the generation of trastuzumab resistance by PTEN knockdown and long term trastuzumab treatment induces characteristics of the EMT.

Induction of EMT associated with trastuzumab-resistance is concurrent with the transition to a triple negative like breast cancer.

In order to explore the potential changes in diverse signaling pathways which may be differentially regulated following the induction of EMT by trastuzumab we utilized RNA sequencing. Strikingly, the expression of classical breast cancer subtype markers ER and PR were reduced to near undetectable levels while HER2 was reduced 64-fold and Ki-67 mRNA was increased 4-fold (Fig 3.2A). These results were confirmed at the protein level in each cell line (Fig 3.2B). When grown in an orthotopic mouse xenograft model BT474 cells exhibit strong HER2 staining, intermediate Ki-67, low PR, and no ER as determined by immunohistochemistry. In contrast, BT474 PTEN- LTT xenografts *in vivo* exhibit a higher Ki-67 expression and low to undetectable levels of HER2, PR and ER (Fig 3.2C). ERBB family members are characterized by their homo and hetero dimerization upon ligand binding and capable of activation of PI3K and downstream AKT signaling nodes. Consistent with a reduction in HER2 following induction of trastuzumab resistance, RNA sequencing revealed a 23% reduction in AKT1 mRNA (Fig 3.2D). Similarly, relative quantitation of AKT1 protein expression was reduced 2.25-fold, as observed by enzyme-linked immunosorbent assay (ELISA), in BT474 PTEN-LTT cells when compared to the parental cell line (Fig 3.2E).

Induction of trastuzumab-resistance is concurrent with a transition to IL-6/STAT3/NF-κB signaling.

The observation that classical breast cancer subtype markers are down regulated suggests another signal transduction pathway may play a critical role in proliferation of BT474 PTEN- LTT cells. Recent evidence from several groups suggest that triple negative breast cancers exhibit a preferential expression of inflammatory cytokines such as IL-6 and IL-8 (23, 24). Consistent with previous studies (19), real time PCR demonstrated >50-fold up regulation of IL-6 and IL-8 mRNA following the generation of trastuzumab resistance (Fig. 3.3A). A quantitative ELISA showed that IL-6 and IL-8 secreted into cell culture media after 72 hr exhibited a 15 and 17-fold enhancement respectively when compared to parental cell line (BT474) (Fig. 3.3B).

Iliopoulos and colleagues propose that IL-6 activation of STAT3, through binding to its receptors IL6R and complex formation with GP130, elicits NF-κB mediated IL-6 production, thus generating a positive feedback loop capable of transforming immortalized breast cell line MCF10A (25). In later work this group and others identified that microRNA regulation of PTEN and CYLD is a critical link in this "epigenetic switch", and that IL-6 production in PTEN deficient cells is capable of inducing EMT (26). RNA sequencing results demonstrate that expression of IL-6 co-receptor GP130, and downstream signaling node STAT3 were increased 22 fold and 54% respectively in BT474 PTEN- LTT cells (Fig 3.3C). Enhanced production of GP130 mRNA was consistent with the stepwise increase in protein as the parental cell line BT474 was subjected to PTEN deletion and long term culture with trastuzumab (Fig. 3.3D, vimentin increase is displayed as indicator of the EMT). Further, increased

production of IL-6 and GP130 was accompanied by an 86.7% increase in p-STAT3 as determined by ELISA (Fig 3.3E). Since STAT3 has also been shown to activate NF-κB to promote IL-6 production (26), a luciferase reporter driven by the NF-κB transcriptional response element (TRE) was employed and demonstrated that BT474 PTEN- LTT cells exhibit 17.5 -fold higher NF-κB activity relative to parental BT474 (Fig. 3.3F). Together these results suggest that trastuzumab resistance in PTEN-deficient HER2+ breast cancer results in EMT, mediated by IL-6/NF-κB positive feedback loop, to transforms PTEN-deficient HER2+ breast cancer to a triple negative phenotype (Fig 3.3G).

Sulforaphane inhibits IL-6/NF-κB signaling loop in breast cancer cell lines.

Functional activation of canonical NF-κB signaling requires phosphorylation of IκB and subsequent nuclear translocation of NF-κB subunits from the cytoplasm followed by DNA binding and initiation of transcription (27). The ability of sulforaphane (SF) to inhibit nuclear translocation of p65 as assessed by western blot has been previously demonstrated in human prostate cancer cell line PC-3 and breast cancer cell line MCF-7 (28, 29). We sought to examine the effect of SF on NF-κB nuclear translocation in trastuzumab-resistant breast cancer cells with PTEN deletion. Under typical culture conditions p65 resides primarily in the cytoplasm of BT474 PTEN- LTT cells. Following the addition of tumor necrosis factor alpha (TNF-α) in the absence of SF, the NF-κB p65 subunit translocated to the nucleus, as evident by the disappearance of a clearly defined nuclear border (Fig. 3.4A, two left panels). However, stimulation of cells with TNF-α in the presence of increasing concentration of SF blocked p65 NF-κB nuclear translocation

in a dose dependent manner, with inhibition occurring in some cells at concentrations as low as 1 μM (Fig 3.4A, right panels).

In order to elucidate whether the inhibition of NF-κB intracellular translocation by SF also reduces its transcriptional activity, we employed the NF-κB luciferase reporter assay. Following stimulation of BT474 or BT474 PTEN- LLT cell lines with TNF-α, luciferase activity increases 4.14 and 2.70-fold (Fig. 3.4B). The enhanced reporter activity is substantially reduced by 61% in a dose dependent manner by SF treatment in both BT474 and BT474 PTEN- LTT. To assess the ability of SF to further regulate endogenous NF-κB targets, we employed real time PCR and ELISA to monitor the mRNA and protein levels of IL-6. We found sulforaphane reduced both mRNA level and secretion of IL-6 by more than 70% in both BT474 and BT474 PTEN- LTT cell lines (Fig. 3.4*C* and D). Together, these findings provide evidence that sulforaphane (SF) is able to disrupt IL-6/NF-κB signaling across breast cancer cell lines.

Sulforaphane selectively inhibits trastuzumab-resistant breast cancer cells with PTEN deletion in vitro.

The significant up-regulation of IL-6/STAT3/NF-κB in BT474 PTEN- LTT cells relative to parental BT474, along with the inhibition of this pathway by SF, suggests that it may exhibit preferential efficacy in the trastuzumab resistant cell line. Thus, we utilized the MTS proliferation assay to compare sensitivity of BT474, BT474 PTEN-, and BT474 PTEN- LTT cells to SF (Fig. 3.5A). SF exhibited a poor reduction in proliferation of BT474 at concentrations as high as 50 μM over 72 hours. Strikingly, deletion of PTEN resulted in a sensitization of the cell line to SF with 50% reduction in proliferation

established at 29.06 μM. BT474 PTEN$^-$ LTT cells further displayed a marked increase in their sensitivity to SF with IC50 reduced to 8.96 μM, demonstrating a strong link between IL-6/STAT3/NF-κB signaling and SF sensitivity in trastuzumab-resistant breast cancer cells with PTEN deletion.

Previous reports from our laboratory have identified the efficacy of SF in basal/claudin-low SUM159 which exhibited an IC50 of approximately 10 μM (30), and is significantly different when compared to that of HER2 amplified BT474. To identify if the presence of HER2 is responsible for reduced efficacy of SF, we overexpressed this receptor in SUM159. Indeed, overexpression of HER2 in SUM159 cells resulted in a near doubling of IC50 from 7.63 to 13.22 μM (Fig. 3.5B). Furthermore, shRNA knockdown of PTEN in SUM159 HER2+ cells, restored sensitivity of these cells to sulforaphane. Taken together, these results suggest that SF preferentially suppresses proliferation in cell lines which primarily rely on IL-6/NF-κB for their survival, whereas strong activation of HER2/AKT signaling may predict resistance to SF (Fig. 3.5C).

Sulforaphane preferentially reduces breast cancer stem cells (CSC) and bulk tumor volume in trastuzumab-resistant xenograft models.

To assess the ability of sulforaphane (SF) to inhibit tumor growth compared to conventional therapy (docetaxel and trastuzumab) we implanted BT474 PTEN- LTT and BT474 cells into NOD/SCID mice and began treatment after the tumor volume reached 40 mm^3. Docetaxel and trastuzumab were administered via IP injection once weekly while sulforaphane (SF) was administered daily. In BT474 PTEN- LTT xenograft bearing mice, 10 doses of SF significantly reduced tumor volume by 51.8% (Fig. 3.6A).

Daily SF treatment ultimately resulted in a 61.0% reduction in tumor volume relative to saline control, an effect that is comparable to that of docetaxel (60.1%) which serves as a positive control for bulk tumor volume reduction. As expected, treatment of mice with weekly IP injections of trastuzumab resulted in no statistically significant change in tumor volume. Conversely, in BT474 xenografts SF was only able to produce a significant reduction in tumor volume (47.4%) after 30 doses (Fig 3.6B). Histological staining of primary xenografts using haematoxylin and eosin reveal significantly larger areas of necrosis with BT474 PTEN- LTT cells treated with SF in comparison with SF treated BT474 or control xenografts (Fig 3.6C).

We further confirmed that SF preferentially reduced CSCs (Fig. 3.6D and E) in BT474 PTEN- LTT versus parental BT474 tumors using secondary reimplantation assay with extreme limiting dilution analysis (ELDA)(31). When control tumor volumes reached protocol specific endpoint xenografts were dissociated into a single cell suspension FACS sorted for the use in secondary reimplantation assays. Nine weeks post-reimplantation of vehicle treated tumors from mice bearing BT474 PTEN- LTT xenografts demonstrated a tumor initiating frequency of 1/522 cells (Fig. 3.6D). In contrast, residual tumors from sulforaphane (SF) treated mice showed significantly lower tumor initiating frequency (1/2807 cells) when implanted into secondary mouse fat pads. BT474 PTEN- LTT xenografts treated with trastuzumab had a significant increase in frequency of tumor initiating cells (1/112 cells $p=0.015$ vs. 1/522 cells in control group). The tumors from docetaxel treated mice showed a modest increase of tumor initiating frequency relative to control, consistent with previous reports (32). Secondary implantation from BT474 xenografts treated with SF demonstrated only a modest

decrease in tumor initiating cell frequency, with 1/1245 cells in SF treated group vs.1/558 cells in control group p=0.247 (Fig. 3.6E).

In order to simulate if SF treatment would be beneficial as adjuvant therapy in patients following surgical resection of tumors, and inhibit breast CSC tumor initiation, we utilized an early treatment xenograft model. Two days following inoculation of BT474 PTEN- LTT cells, animals were randomized and treated with 10 mg/kg SF, 50 mg/kg SF, or saline vehicle. Daily dosing was continued until control tumors reached a volume of 100 mm^3 at which point treatment was stopped and tumor monitoring was continued. Over the course of treatment 50 mg/kg SF prevented 66.7% of tumors from forming in mice implanted with BT474 PTEN- LTT, an effect persistent 30 days after discontinuation of treatment (Fig. 3.6F). Furthermore, administration of 10 mg/kg reduced tumor formation 31.25%, revealing a dose dependent therapeutic effect. In addition, SF treatment inhibited BT474 PTEN-LTT tumor volume by 68.7% and 87.3% at doses 10 and 50 mg/kg respectively (Fig. 3.6G).

Discussion

The contribution of the tumor suppressor PTEN to efficacy of trastuzumab in HER2 amplified breast cancer patients has been previously reported in the literature. Inactivation of PTEN is associated with reduced function of trastuzumab in BT474 and SKBR3 cell lines in vitro and correlates with poor response to trastuzumab in patients (10, 33). However the translation of these findings to clinical application of trastuzumab to patients has yet to be fully realized, where HER2 amplified patients regardless of PTEN status are usually treated with trastuzumab in combination with surgery,

radiotherapy, and conventional chemotherapies depending upon expression of other hormone receptors, tumor size, lymph node status, and the presence of distant metastasis. Since it is unknown what the potential clinical consequences of continued use of trastuzumab as a therapy in HER+ PTEN deficient patients we sought to explore this using genetic manipulation and drug conditioning in the breast cancer cell line BT474.

Consistent with a previous report we demonstrate that long term culture with trastuzumab in BT474 containing reduced PTEN function (shPTEN) induces morphological and transcriptional changes characteristic of the epithelial to mesenchymal transition in a stepwise manner (19). These results suggest deletion of PTEN may be critical for priming the cells for further transformation. Iliopoulos et. al. have demonstrated that microRNA targeting of PTEN is a critical step in triggering transformation of the immortalized MCF-10A cell line by IL-6 (25, 26). More recently, transformation of MCF-10A by PTEN and p53 knockdown has been shown to generate a triple negative type breast cancer cell line (24).

Upon further characterization of BT474 PTEN- LTT cells, we identified that expression of classical breast cancer cell markers ER, PR, and HER2 were all significantly reduced at mRNA and protein level both *in vitro* and *in vivo*, while expression of proliferation marker Ki-67 was increased. This stably resistant cell also exhibited a reduced mRNA and protein level of downstream signaling node AKT1 which can be regulated by multiple ERBB family members. This is consistent with previous reports demonstrating that culture with trastuzumab significantly down regulates HER2 protein in the HER2+ MDA-MB-453, which contains mutations in both PIK3CA and PTEN (34-36). Multiple studies have utilized BT474 in xenograft model, treated with trastuzumab, which provide

insight into the molecular mechanisms associated with acquired trastuzumab resistance (37, 38). In vivo, these studies report trastuzumab treatment does not cause a significant down regulation of HER2 and resistant cell lines remain dependent on ERBB family signaling. However, our data showed that continued use of trastuzumab in HER2+ breast cancer with PTEN inactivation induces EMT and in the conversion to a triple negative molecular subtype. Taken together with our results these studies may suggest that the generation of acquired and *de novo* trastuzumab resistance exhibit two distinct molecular mechanisms, with patients exhibiting PTEN deletion at high risk for the observed molecular subtype switching.

Following the generation of trastuzumab resistance in HER2+ breast cancer cells with PTEN deletion, the mRNA and protein level of inflammatory cytokines IL-6 and IL-8 were dramatically unregulated. Indeed we postulate that IL-6 is the main driver of the EMT induction process. Constitutive expression of IL-6 in MCF-7 results in a dramatic reduction in E-cadherin while up regulating mesenchymal markers N-cadherin, vimentin, and twist (39). Similarly, IL-6 stimulation of CD44-CD24+ breast cancer patient derived cells has been demonstrated to reduce E-cadherin expression and generate a CD44+CD24- population. Further, the induction of EMT in Ras-transformed mammary epithelial cells has also been shown to rely on NF-κB signaling (40), which has previously been shown to be activated through the IL-6/STAT3/NF-κB positive feedback loop (13, 17, 25). Consistent with these reports we find that with the reduction of HER2/AKT signaling there is a significant increase in IL-6, GP130, level of p-STAT3, and activity of the NF-κB transcription factor.

In previous reports sulforaphane (SF) has been demonstrated to inhibit NF-κB transcriptional activity by preventing p65 DNA binding activity in pancreatic and breast cancer cell lines (41, 42). Additionally, in prostate cancer cell lines SF reduced NF-κB nuclear translocation and transcriptional activity (43). Further, SF's activity in pancreatic CSCs has been attributed to inhibition of the NF-κB transcription factor (41, 44). In this report, we demonstrate that SF is capable of disrupting NF-κB p65 translocation, transcriptional activity, and inhibiting endogenous target IL-6 at mRNA and secreted protein level across breast cancer cell lines. While SF did not inhibit proliferation of parental BT474 it inhibited the growth of BT474 with PTEN deletion and long term culture with trastuzumab both *in vitro* and in mouse xenograft model. Additionally, the inhibitory effect of SF on both tumor volume and tumor initiation in secondary mice was preferentially observed in trastuzumab-resistant BT474 PTEN- LTT relative to BT474 xenografts. Of note, the reduction of bulk tumor volume by SF in trastuzumab-resistant xenografts, at the indicated dosing regimen, was comparable to that of conventional chemotherapy while the additional ability to reduce tumor initiating cell frequency was observed.

These data suggest that continued use of trasuzumab in drug-resistant HER2+ breast cancer with PTEN deletion may pose potential challenges for therapeutics of HER2+ breast cancers via induction of EMT, expansion of BCSC populations, and by switching the molecular subtype to triple negative. Further, adjuvant SF treatment may provide a novel strategy towards targeting both bulk tumor volume and breast cancer stem cells in trastuzumab-resistant breast cancers with PTEN deletion in patients by disrupting the IL-

6/NF-κB. Further clinical investigation may be warranted to explore the role of this phenomenon in breast cancer patients with different status of PTEN and HER2.

Materials and Methods

Cell Culture and Reagents. Cell lines and culture conditions can be obtained in SI Material and Methods. Sulforaphane was obtained from Quality Phytochemicals LLC (New Jersey, USA) and diluted in DMSO (< 0.1%) for *in vitro* studies or 0.9% saline *in vivo*. Docetaxel (Hospira) and Trastuzumab (Herceptin, Genentech) were obtained through the University of Michigan Cancer Center Pharmacy.

Quantification of mRNA. Total RNA from cell lines was extracted using RNeasy mini kit (Qiagen) according to manufacturer's protocol. Purified total RNA was further prepared for RNA-sequencing using TruSeq RNA sample preparation kit (Illumina) followed by 50 cycle, single end reads carried out using the HiSeq 2000 sequencing system (Illumina). RNA expression analysis was performed by normalization using reads per kilobase per million reads (RPKM) method. RNA purified for real time PCR analysis was converted to cDNA using the M-MLV RT (Promega) and subjected to real time PCR analysis using TaqMan universal PCR master mix (Roche) and indicated primers using ABI PRISM 7900GT sequencing detection system (Applied Biosystems).

Luciferase Reporter Assay. Lentiviral particles containing luciferase reporter construct driven by NF-κB (System Biosciences) were obtained and transfected into BT474 and BT474 PTEN- LTT cells. Two hours following incubation with SF, TNF-α concentration in media was brought to 50 ng/ml. After 6 hr Luciferase activity was

measured according to manufacturer's instructions with oneGlo reagent (promega) on Synergy 2 plate reader (BioTek).

Protein Expression Analysis. After culture for 72 hours media or cells were collected and subjected to ELISA for Human IL-6, IL-8, AKT, and p-STAT3. Assays were performed using antibody kits for AKT and p-STAT3 (Cell Signaling Technology) or IL-6 and IL-8 (Duosets, R&D Systems) according to manufacturer's protocol. Data was acquired with a BioTek Synergy plate reader and analyzed using Gen5 software. Antibodies for western blot (HER2, PR α/β, ER α, PTEN, GP130, Vimentin, β-actin, and secondary antibodies) were obtained from Cell Signaling Technology.

Flow Cytometry and Immunostaining. Flow cytometry analysis of cell lines in vitro was performed using anti-CD44-APC, anti-CD24-FITC, and corresponding isotype antibodies (BD Biosciences) on a SY3200 (Sony Biotechnology) flow cytometer. Immunofluorescent staining of p65 NF-κB (Cell Signaling Technology) in BT474 PTEN-LTT cell line was performed in 4-well glass chambers slides (lab-tek) following pretreatment with SF for 2 hours and 30 min and 50 ng/ml TNF-α for 2 hours. Cells were fixed and permeabilized with methanol/acetone followed by blocking with 3% BSA. Nuclear staining was identified with 1 μg/ml DAPI and imaging was carried out with a Nikon Eclipse TE2000-S microscope and MetaMorph 7.6.0.0 (Molecular Devices).

MTS Cell Proliferation Assay. Cell lines were plated at a density of 3,000 cells per well in 96-well plates and allowed to adhere overnight. Following 72 hour incubation with SF proliferation was determined by MTS assay according to manufacturer's instruction. Absorbance at 490 nm was measured using Synergy 2 plate reader.

Pharmacodynamic modeling was performed using a nonlinear, variable slope model in GraphPad Prism (GraphPad Software).

Mouse Xenograft Models. Female 5 week old non-obese diabetic/severe combined immunodeficient (NOD/SCID) mice were obtained from Jackson Laboratory. Xenograft formation in advanced treatment model was generated by direct injection of BT474 or BT474 PTEN- LTT cells (1,000,000), suspended in matrigel (BD Biosciences), into the exposed no.4 inguinal mammary pad. Trastuzumab (10 mg/kg once every 7 days), sulforaphane (50 mg/kg daily), and docetaxel (10 mg/kg once every 7 days) were administered via I.P. injection beginning when tumor volume reached approximately 40 mm^3 or the day after surgery for adjuvant treatment model. When control tumors reached approximately 500 mm^3 mice were euthanized with CO2 inhalation and tumors resected.

Secondary Reimplantation Assay. Isolated primary tumors were mechanically and enzymatically dissociated using gentleMACS Octo Dissociator and tumor dissociation kit (Miltenyi Biotec) according to manufacturer's instructions. Human tumor cells with DsRed label were then isolated using fluorescent activated cell sorting on a SY3200 (Sony Biotechnology) flow cytometer. Secondary mice were inoculated with 10,000, 5,000, or 1,000 cells for BT474 xenografts and 5,000, 1,000, or 200 cells for BT474 PTEN- LTT xenografts as described above. Tumor formation rate in secondary mice was assessed 9 weeks following implanting cells by direct palpitation.

References

1. Baselga J, *et al.* (1996) Phase II study of weekly intravenous recombinant humanized anti-p185HER2 monoclonal antibody in patients with HER2/neu-

overexpressing metastatic breast cancer. *Journal of Clinical Oncology* 14(3):737-744.
2. Vogel CL, *et al.* (2002) Efficacy and Safety of Trastuzumab as a Single Agent in First-Line Treatment of HER2-Overexpressing Metastatic Breast Cancer. *Journal of Clinical Oncology* 20(3):719-726.
3. Slamon DJ, *et al.* (2001) Use of Chemotherapy plus a Monoclonal Antibody against HER2 for Metastatic Breast Cancer That Overexpresses HER2. *New England Journal of Medicine* 344(11):783-792.
4. Nahta R & Esteva FJ (2007) Trastuzumab: triumphs and tribulations. *Oncogene* 26(25):3637-3643.
5. Nagy P, *et al.* (2005) Decreased Accessibility and Lack of Activation of ErbB2 in JIMT-1, a Herceptin-Resistant, MUC4-Expressing Breast Cancer Cell Line. *Cancer Research* 65(2):473-482.
6. Agus DB, *et al.* (2002) Targeting ligand-activated ErbB2 signaling inhibits breast and prostate tumor growth. *Cancer Cell* 2(2):127-137.
7. Konecny GE, *et al.* (2006) Activity of the Dual Kinase Inhibitor Lapatinib (GW572016) against HER-2-Overexpressing and Trastuzumab-Treated Breast Cancer Cells. *Cancer Research* 66(3):1630-1639.
8. Nahta R, Yuan LXH, Zhang B, Kobayashi R, & Esteva FJ (2005) Insulin-like Growth Factor-I Receptor/Human Epidermal Growth Factor Receptor 2 Heterodimerization Contributes to Trastuzumab Resistance of Breast Cancer Cells. *Cancer Research* 65(23):11118-11128.
9. Kondapaka SB, Singh SS, Dasmahapatra GP, Sausville EA, & Roy KK (2003) Perifosine, a novel alkylphospholipid, inhibits protein kinase B activation. *Mol Cancer Ther* 2(11):1093-1103.
10. Nagata Y, *et al.* (2004) PTEN activation contributes to tumor inhibition by trastuzumab, and loss of PTEN predicts trastuzumab resistance in patients. *Cancer Cell* 6(2):117-127.
11. Mulholland DJ, *et al.* (2012) Pten Loss and RAS/MAPK Activation Cooperate to Promote EMT and Metastasis Initiated from Prostate Cancer Stem/Progenitor Cells. *Cancer Research* 72(7):1878-1889.
12. BOWEN KA, *et al.* (2009) PTEN Loss Induces Epithelial—Mesenchymal Transition in Human Colon Cancer Cells. *Anticancer Research* 29(11):4439-4449.
13. Song L-B, *et al.* (2009) The polycomb group protein Bmi-1 represses the tumor suppressor PTEN and induces epithelial-mesenchymal transition in human nasopharyngeal epithelial cells. *The Journal of Clinical Investigation* 119(12):3626-3636.
14. Wang H, *et al.* (2014) Trail Resistance Induces Epithelial-Mesenchymal Transition and Enhances Invasiveness by Suppressing PTEN via miR-221 in Breast Cancer. *PLoS ONE* 9(6):e99067.
15. Sawyers CL (2014) Overcoming Cancer Drug Resistance. *Proceedings of the 105th Annual Meeting of the American Association for Cancer Research*, (Philadelphia (PA): AACR).
16. Zhang Z, *et al.* (2012) Activation of the AXL kinase causes resistance to EGFR-targeted therapy in lung cancer. *Nat Genet* 44(8):852-860.

17. Van Allen EM, *et al.* (2014) The Genetic Landscape of Clinical Resistance to RAF Inhibition in Metastatic Melanoma. *Cancer Discovery* 4(1):94-109.
18. Sequist LV, *et al.* (2011) Genotypic and Histological Evolution of Lung Cancers Acquiring Resistance to EGFR Inhibitors. *Science Translational Medicine* 3(75):75ra26.
19. Korkaya H, *et al.* (2012) Activation of an IL6 Inflammatory Loop Mediates Trastuzumab Resistance in HER2+ Breast Cancer by Expanding the Cancer Stem Cell Population. *Molecular Cell* 47(4):570-584.
20. Salgado R, *et al.* (2003) Circulating interleukin-6 predicts survival in patients with metastatic breast cancer. *International Journal of Cancer* 103(5):642-646.
21. Bachelot T, *et al.* (2003) Prognostic value of serum levels of interleukin 6 and of serum and plasma levels of vascular endothelial growth factor in hormone-refractory metastatic breast cancer patients. *Br J Cancer* 88(11):1721-1726.
22. Sheridan C, *et al.* (2006) CD44+/CD24- breast cancer cells exhibit enhanced invasive properties: an early step necessary for metastasis. *Breast Cancer Research* 8(5):R59.
23. Hartman ZC, *et al.* (2013) Growth of Triple-Negative Breast Cancer Cells Relies upon Coordinate Autocrine Expression of the Proinflammatory Cytokines IL-6 and IL-8. *Cancer Research* 73(11):3470-3480.
24. Kim G, *et al.* (2014) SOCS3-mediated regulation of inflammatory cytokines in PTEN and p53 inactivated triple negative breast cancer model. *Oncogene*.
25. Iliopoulos D, Hirsch HA, & Struhl K (2009) An Epigenetic Switch Involving NF-κB, Lin28, Let-7 MicroRNA, and IL6 Links Inflammation to Cell Transformation. *Cell* 139(4):693-706.
26. Iliopoulos D, Jaeger SA, Hirsch HA, Bulyk ML, & Struhl K (2010) STAT3 Activation of miR-21 and miR-181b-1 via PTEN and CYLD Are Part of the Epigenetic Switch Linking Inflammation to Cancer. *Molecular Cell* 39(4):493-506.
27. Perkins ND (2012) The diverse and complex roles of NF-κB subunits in cancer. *Nat Rev Cancer* 12(2):121-132.
28. Xu C, Shen G, Chen C, Gelinas C, & Kong A-NT (2005) Suppression of NF-kB and NF-kB-regulated gene expression by sulforaphane and PEITC through IkBa, IKK pathway in human prostate cancer PC-3 cells. *Oncogene* 24(28):4486-4495.
29. Young-Rae Lee E-MN, Ji-Hey Han, Jeong-Mi Kim, Bo-Mi Hwang, Byeong-Soo Kim, Sung-Ho Lee, Sung Hoo Jung, Hyun Jo Youn, Eun Yong Chung, & Jong-Suk Kim (2013) Sulforaphane controls TPA-induced MMP-9 expression through the NF-κB signaling pathway, but not AP-1, in MCF-7 breast cancer cells. *BMB reports* 46(4):201-206.
30. Li Y, *et al.* (2010) Sulforaphane, a Dietary Component of Broccoli/Broccoli Sprouts, Inhibits Breast Cancer Stem Cells. *Clinical Cancer Research* 16(9):2580-2590.
31. Hu Y & Smyth GK (2009) ELDA: Extreme limiting dilution analysis for comparing depleted and enriched populations in stem cell and other assays. *Journal of Immunological Methods* 347(1–2):70-78.

32. Ginestier C, *et al.* (2010) CXCR1 blockade selectively targets human breast cancer stem cells in vitro and in xenografts. *The Journal of Clinical Investigation* 120(2):485-497.
33. Berns K, *et al.* (2007) A Functional Genetic Approach Identifies the PI3K Pathway as a Major Determinant of Trastuzumab Resistance in Breast Cancer. *Cancer Cell* 12(4):395-402.
34. Cuello M, *et al.* (2001) Down-Regulation of the erbB-2 Receptor by Trastuzumab (Herceptin) Enhances Tumor Necrosis Factor-related Apoptosis-inducing Ligand-mediated Apoptosis in Breast and Ovarian Cancer Cell Lines that Overexpress erbB-2. *Cancer Research* 61(12):4892-4900.
35. Narayan M, *et al.* (2009) Trastuzumab-Induced HER Reprogramming in "Resistant" Breast Carcinoma Cells. *Cancer Research* 69(6):2191-2194.
36. Hollestelle A, *et al.* (2010) Distinct gene mutation profiles among luminal-type and basal-type breast cancer cell lines. *Breast Cancer Res Treat* 121(1):53-64.
37. Ritter CA, *et al.* (2007) Human Breast Cancer Cells Selected for Resistance to Trastuzumab In vivo Overexpress Epidermal Growth Factor Receptor and ErbB Ligands and Remain Dependent on the ErbB Receptor Network. *Clinical Cancer Research* 13(16):4909-4919.
38. Moulder SL, *et al.* (2001) Epidermal Growth Factor Receptor (HER1) Tyrosine Kinase Inhibitor ZD1839 (Iressa) Inhibits HER2/neu (erbB2)-overexpressing Breast Cancer Cells in Vitro and in Vivo. *Cancer Research* 61(24):8887-8895.
39. Sullivan NJ, *et al.* (2009) Interleukin-6 induces an epithelial-mesenchymal transition phenotype in human breast cancer cells. *Oncogene* 28(33):2940-2947.
40. Huber MA, *et al.* (2004) NF-κB is essential for epithelial-mesenchymal transition and metastasis in a model of breast cancer progression. *The Journal of Clinical Investigation* 114(4):569-581.
41. Kallifatidis G, *et al.* (2009) Sulforaphane targets pancreatic tumour-initiating cells by NF-κB-induced antiapoptotic signalling. *Gut* 58(7):949-963.
42. Young-Rae Lee E-MN J-HH, Jeong-Mi Kim, Bo-Mi Hwang, Byeong-Soo Kim, Sung-Ho Lee, Sung Hoo Jung, Hyun Jo Youn, Eun Yong Chung, & Jong-Suk Kim (2013) Sulforaphane controls TPA-induced MMP-9 expression through the NF-κB signaling pathway, but not AP-1, in MCF-7 breast cancer cells. *BMB reports* 46:201-206.
43. Xu C, Shen G, Chen C, Gelinas C, & Kong A-NT (2005) Suppression of NF-κB and NF-κB-regulated gene expression by sulforaphane and PEITC through IκBα, IKK pathway in human prostate cancer PC-3 cells. *Oncogene* 24(28):4486-4495.
44. Rausch V, *et al.* (2010) Synergistic Activity of Sorafenib and Sulforaphane Abolishes Pancreatic Cancer Stem Cell Characteristics. *Cancer Research* 70(12):5004-5013.

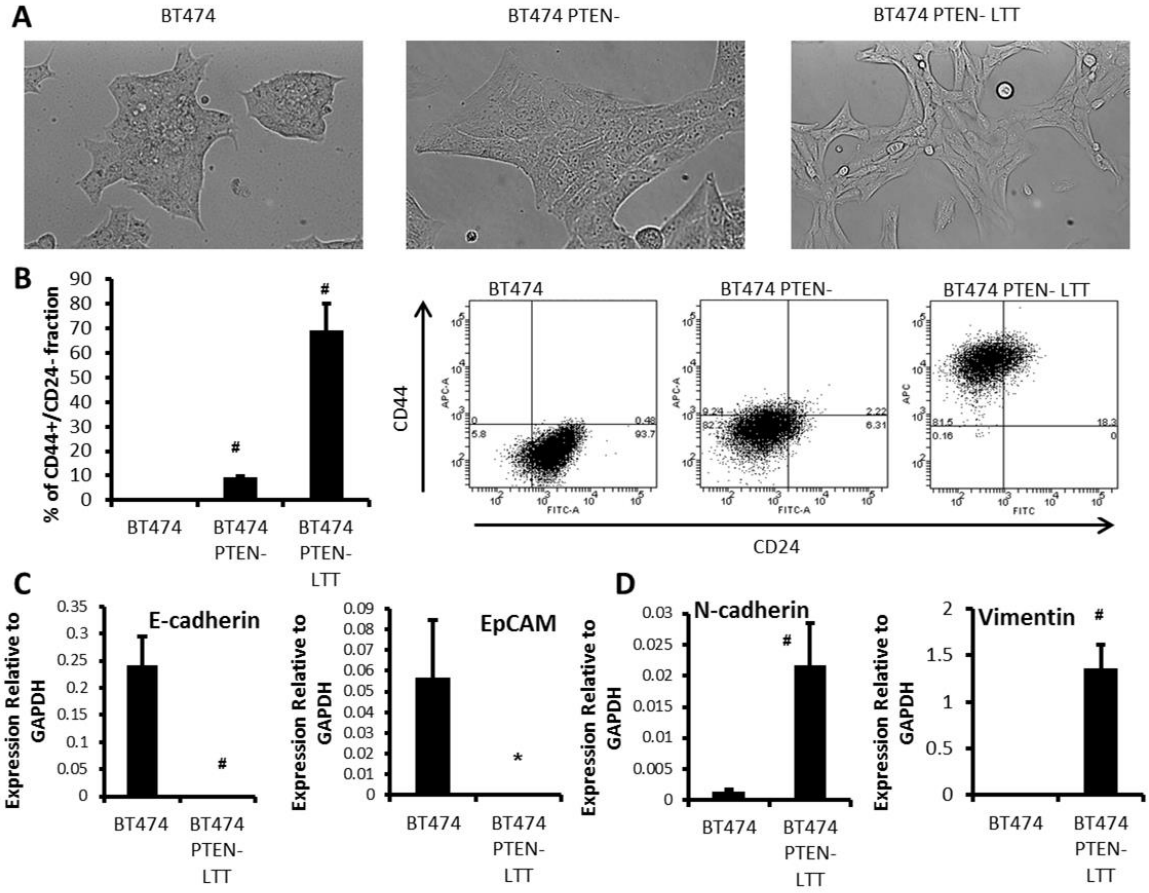

Figure 3.1 Trastuzumab-resistant BT474 with PTEN deletion exhibits mesenchymal phenotype and increases cancer stem cells. (A) Representative bright field microscopy images of BT474, BT474 shPTEN, and BT474 shPTEN with long term treatment of trastuzumab (LTT). Original images obtained with 20X objective. (B) Left, percent of cells expressing basal breast cancer markers CD44+/CD24- in cell lines as assessed by flow cytometry. N=3. Right, representative CD44 and CD24 flow cytometry analysis of each. (C) Real time PCR quantification of epithelial cell makers E-cadherin and EpCAM normalized to expression of GAPDH. (D) Real time PCR analysis of mesenchymal cell markers N-cadherin and Vimentin, expressed relative to GAPDH. N=4, Data shown as average ± SD. # $p \leq 0.01$.

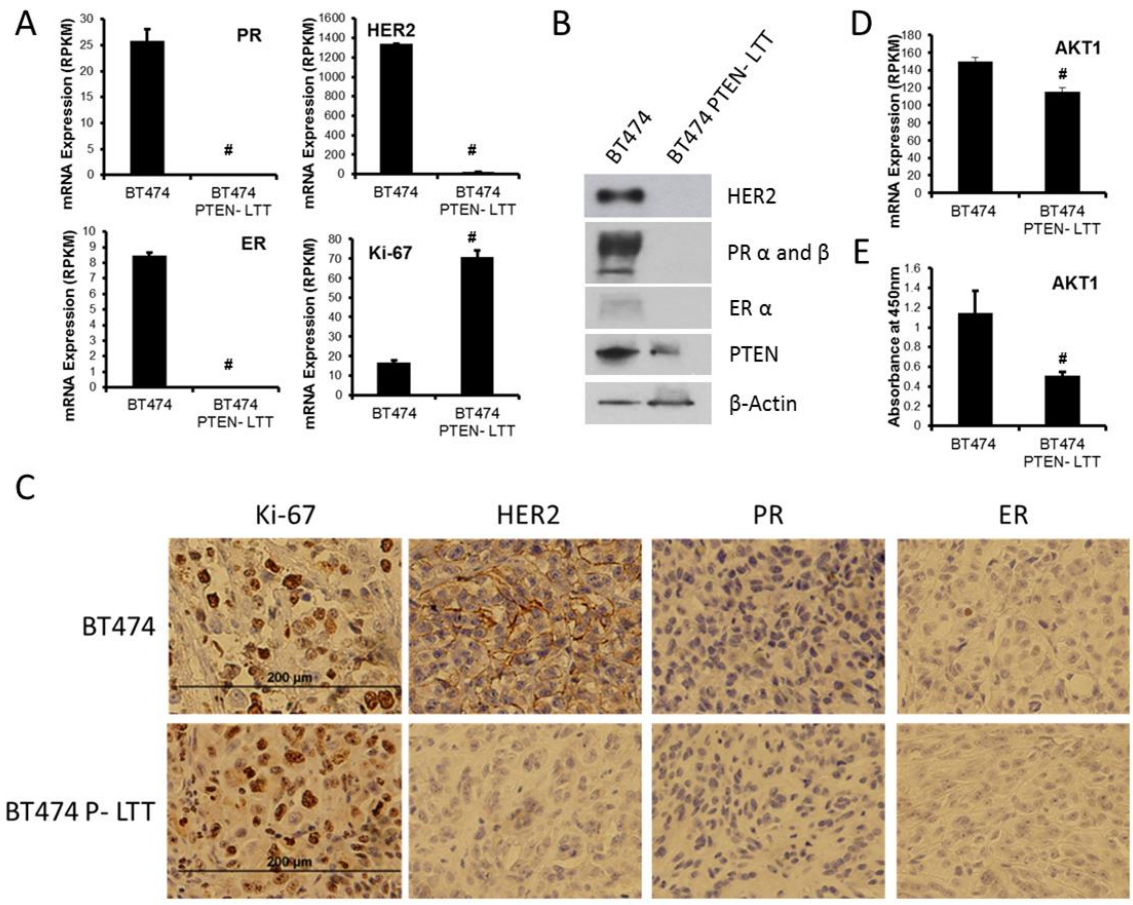

Figure 3.2 Induction of EMT associated with trastuzumab-resistance is concurrent with the transition to a triple negative like breast cancer. (A) Normalized mRNA expression (reads/kilobase/million reads) of breast cancer subtype markers ER, PR, HER2, and Ki-67 determined by RNA sequencing in Parental BT474 and BT474 PTEN-LTT cell lines N=4.(B) Western blot representing breast cancer subtype markers ER, PR, HER2 and PTEN with β-actin as loading control. (C) Immunohistological staining of breast cancer subtype markers in primary BT474 and BT474 PTEN- LTT xenografts when tumors reached 500 mm^3. (D) mRNA expression of HER2 signal transducer AKT1 as determined by RNA sequencing. (E) Normalized protein expression of AKT1 in cell lines by ELISA assay. N=3. Data shown as average ± SD. # $p \leq 0.01$.

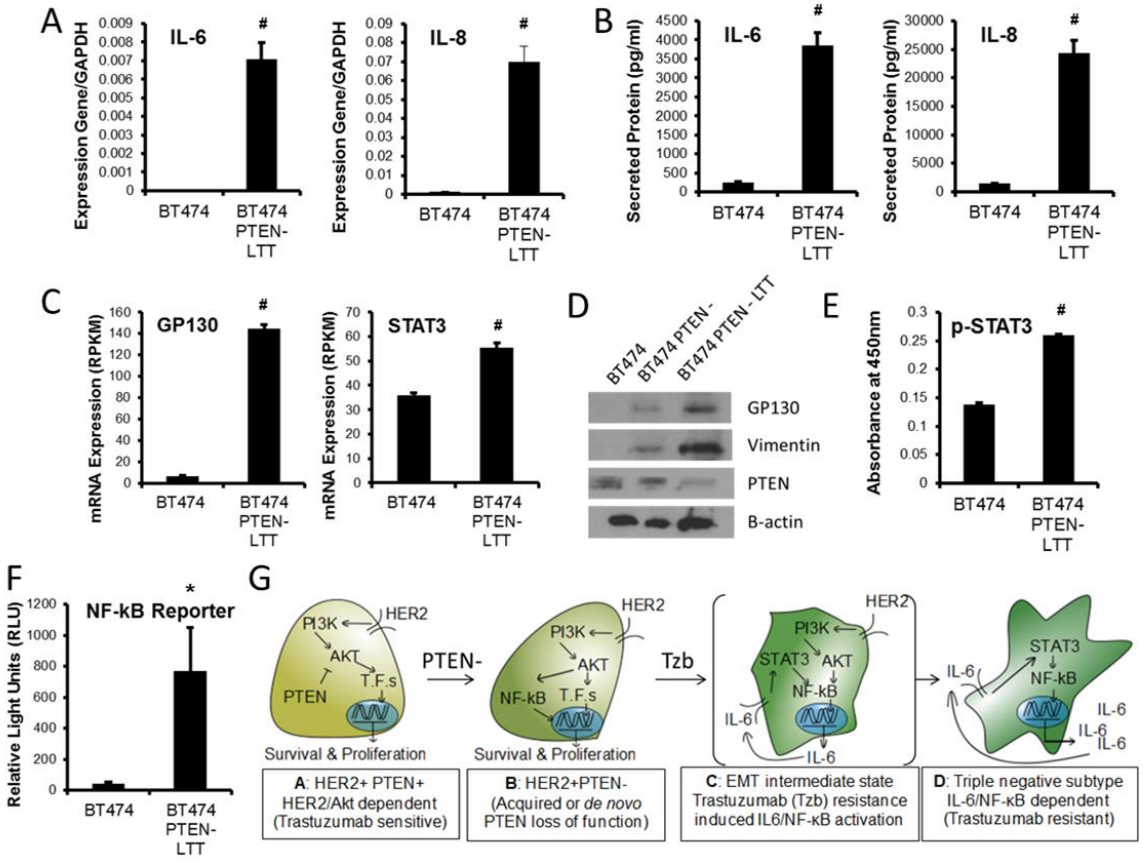

Figure 3.3 Induction of trastuzumab-resistance is concurrent with a transition to IL-6/STAT3/NF-κB signaling. (A) mRNA expression of endogenous inflammatory cytokines IL-6 and IL-8 normalized to GAPDH as identified by real time PCR. N=4 (B) Protein expression in pg/ml of IL-6 and IL-8 secreted into culture media, measured using quantitative enzyme-linked immunosorbent assay (ELISA). N=3 (C) Normalized mRNA expression (reads/kilobase/million reads) of IL-6 signal transducer GP130 (left) and downstream signaling node STAT3 (right) by RNA-sequencing. N=4 (D) Western blot analysis of protein expression for GP130, mesenchymal cell marker vimentin, and PTEN tumor suppressor in BT474, BT474 PTEN-, and BT474 PTEN- LTT cell lines. (E) ELISA relative quantitation of active STAT3, phosphorylated at Tyr705. N=3 (F) Luciferase activity of cell lines following infection of with retroviral vector inducing NF-κB driven expression of luciferase. N=3. (G) Model of trastuzumab resistance in PTEN deficient cells, T.F.s = other transcription factors. Data shown as average ± SD. * $p \leq 0.05$. # $p \leq 0.01$.

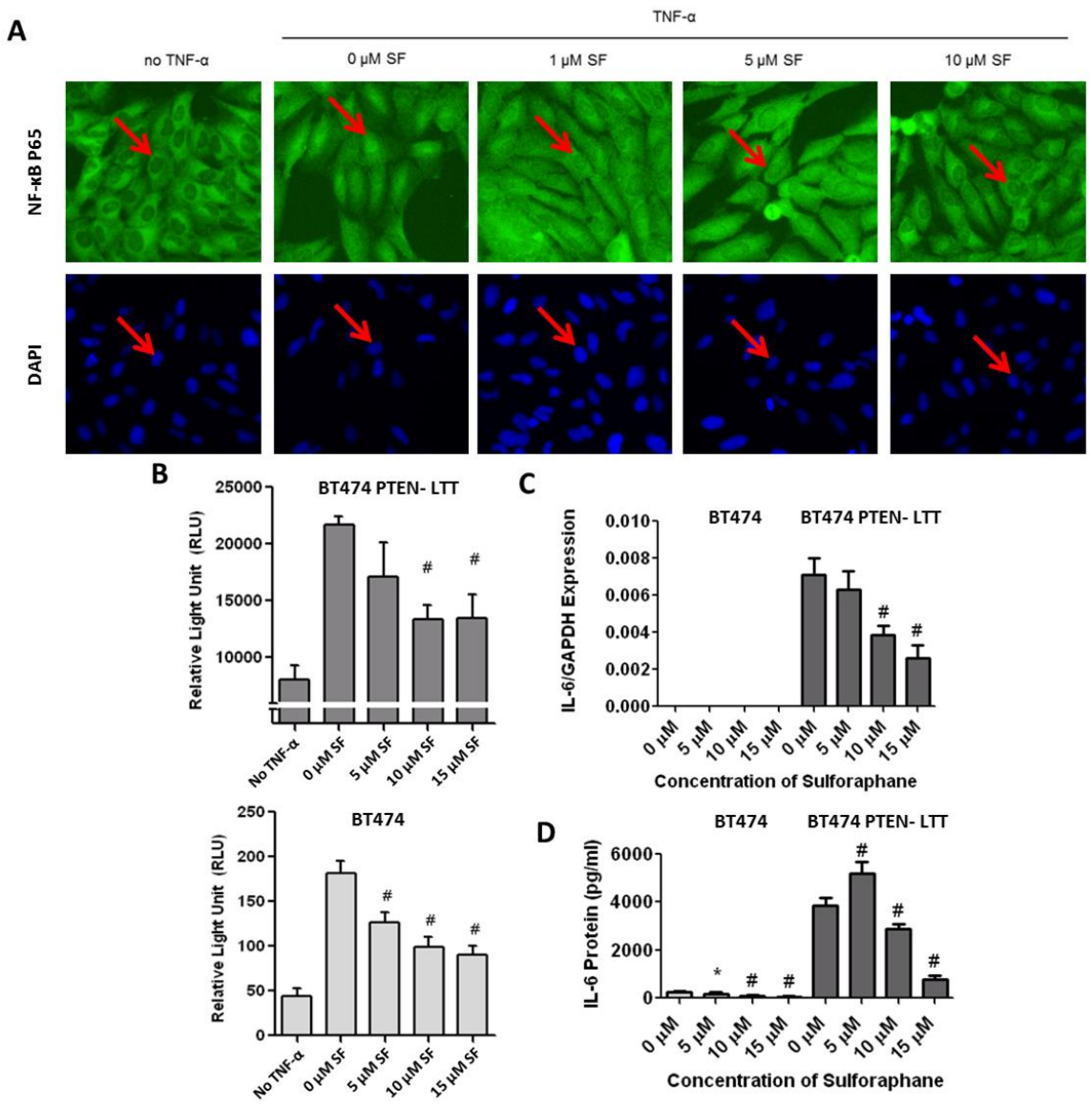

Figure 3.4 Sulforaphane inhibits IL-6/NF-κB signaling loop in breast cancer cell lines. (A) Immunofluorescent staining of NF-κB p65 subunit and DAPI in fixed BT474 PTEN- LTT cells exhibits primarily cytoplasmic staining (left). Translocation of p65 from cytoplasm to nucleus, induced using 50 ng/ml TNF-α, is prevented by pretreatment with SF in a dose dependent manner (right three panels). Red arrows indicate boarder between cytoplasm and nucleus of a representative cell. Original images were obtained using a 20X microscope objective. (B) BT474 PTEN- LTT and BT474 cell lines were transfected with NF-κB luciferase reporter. Luciferase reporter activity was obtained in the absence or presence of 50 ng/ml TNF-α in combination with increasing concentrations of SF. (C) mRNA expression of endogenous inflammatory cytokine IL-6 normalized to GAPDH as identified by real time PCR in the presence of increasing concentration of SF. (D) Quantitative ELISA identifying protein level endogenous NF-

κB target protein IL-6 when cell lines are incubated with increasing concentrations of SF for 72 hr. (B-D) N=3. Data are shown as averages ± SD. *$p \leq 0.05$. # $p \leq 0.01$.

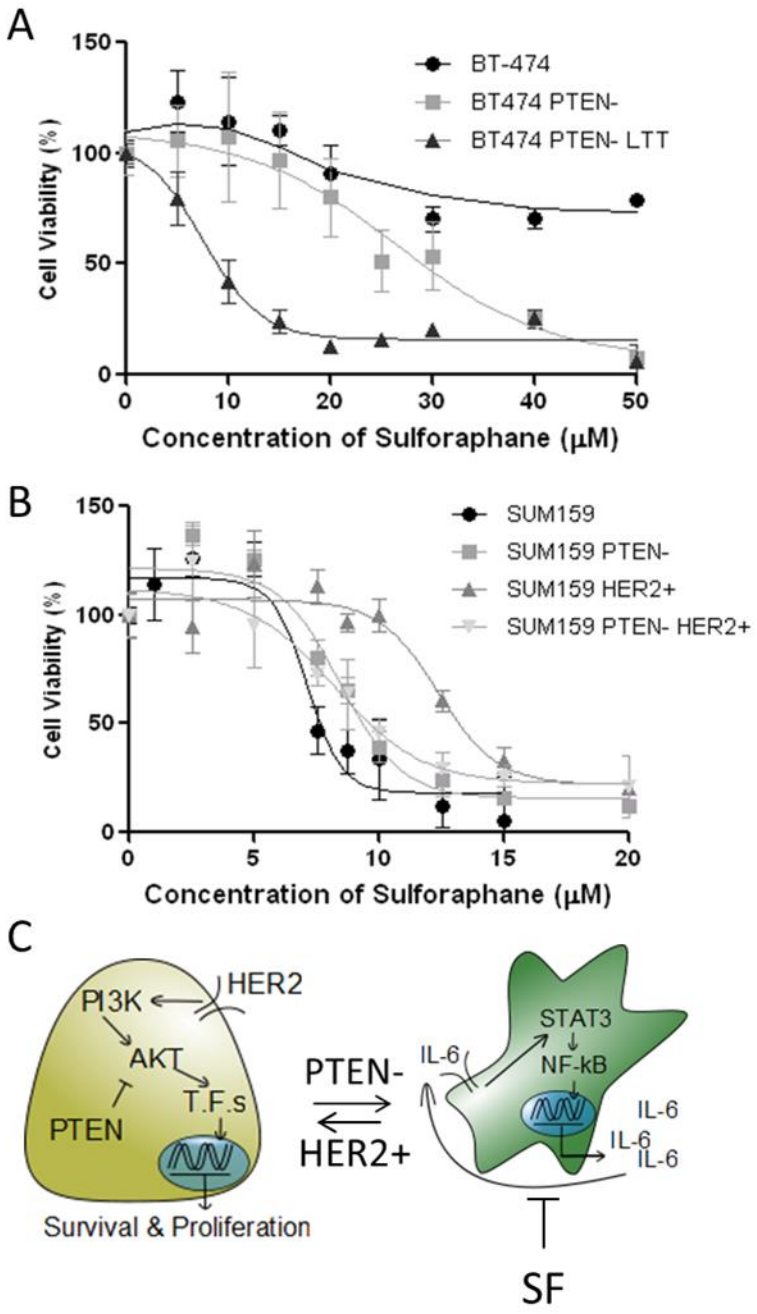

Figure 3.5 Sulforaphane (SF) selectively inhibits trastuzumab-resistant breast cancer cells with PTEN deletion in vitro. MTS proliferation assay (Promega) was carried out after incubating cell lines with increasing concentration of SF for 72 hours. (A) PTEN knock down and long term trastuzumab (LTT) culture with HER2 amplified BT474 sensitizes the cell line to SF. (B) MTS assay performed in triple negative SUM159, SUM 159 with shPTEN, SUM159 with HER2 over expression, and SUM159 shPTEN with HER2 overexpression. (C) Model of SF efficacy demonstrating cell lines with HER2 amplification in the absence of PTEN deletion are likely to be insensitive to

SF treatment whereas deletion of PTEN is likely to enhance efficacy. (A and B) N= 6. Data are shown as averages ± SD.

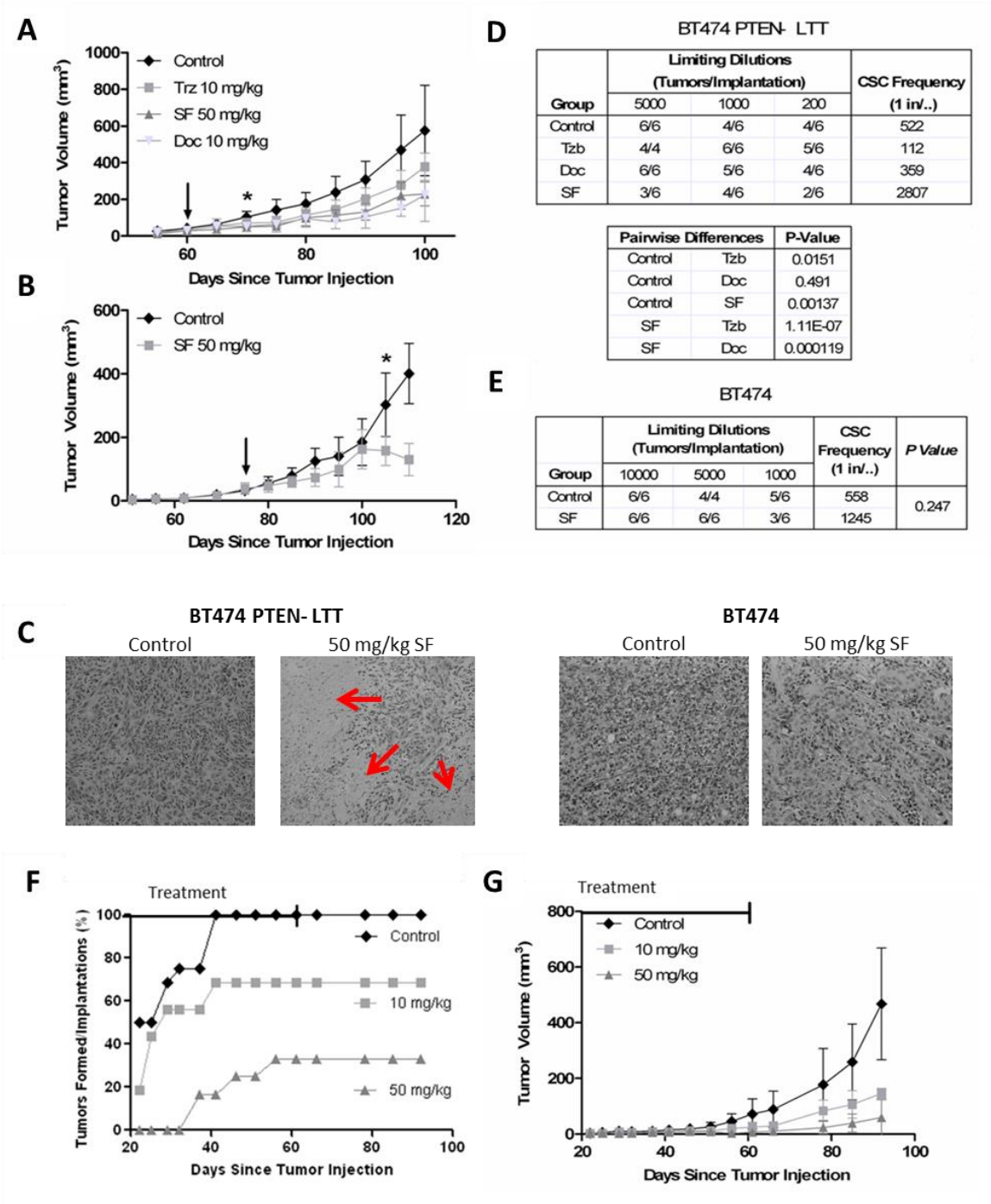

Figure 3.6 Sulforaphane (SF) reduces the breast cancer stem cells (CSC) population and bulk tumor volume in trastuzumab-resistant advanced xenograft model. (A) NOD/SCID mice bearing 40 mm^3 BT474 PTEN- LTT xengrafts were randomized into treatment groups, 50 mg/kg SF and 10 mg/kg Doc were sufficient to significantly reduce bulk tumor volume within 10 days. Trastuzumab treatment produced no significant reduction in tumor volume for BT474 PTEN- LTT xenografts over the course of the experiment. * $p \leq 0.05$. (B) Tumor volume of mice bearing primary BT474 xenografts,

30 doses of SF were required to significantly reduce tumor volume. Arrow denotes the beginning of treatment in primary mice. * $p \leq 0.05$. (A and B) Tumor volume represented SD of N=6 mice. (C) Representative H&E staining of primary BT47 and BT474 PTEN- LTT tumors. SF treatment in BT474 PTEN- LTT xenografts generated intratumoral regions of necrosis (red arrows) whereas this was not observed in BT474 xenografts. Primary xenografts were removed, dissociated, and serially reimplanted into secondary mice to determine the tumor initiating CSC frequency by extreme limiting dilution analysis of primary (D) BT474 PTEN- LTT and (E) BT474 xenografts. (F) Tumor formation rate of mice injected with 50,000 BT474 PTEN- LTT cells followed 2 days later by daily SF treatment. Control N=16, 10 mg/kg N=16, 50 mg/kg N=12. (F) Average volume of BT474 PTEN- LTT xenografts that formed with adjuvant treatment. Control N=16, 10 mg/kg N=9, 50 mg/kg N=4.

Chapter 4

MEOX1 as a Novel Cancer Stem Cell Target for Treatment of Trastuzumab-Resistant HER2^{+} Breast Cancers

Abstract

The development of resistance to trastuzumab in HER2+ breast cancer patients represents a significant clinical challenge. Accumulating evidence suggests that inactivation of the tumor suppressor PTEN may predispose HER2+ patients to the development of resistance to trastuzumab therapy. Knockdown of PTEN and long term culture with trastuzumab (LTT) has been demonstrated to induce the epithelial to mesenchymal transition (EMT) and expand the breast cancer stem cell (CSC) population. In this study we apply RNA sequencing to identify novel targets which can be exploited for the development of therapeutics for PTEN deficient patients following the generation of trastuzumab resistance. Gene expression analysis reveals 3901 differentially expressed genes between trastuzumab sensitive BT474 and trastuzumab resistant BT474 shPTEN LTT cell lines. Using the natural product sulforaphane which exhibits preferential efficacy in BT474 shPTEN LTT cells, in conjunction with differentially expressed genes following trastuzumab resistance, we identify a set of 44 candidate genes for the treatment of trastuzumab resistant patients. Of these genes siRNA to MEOX1 reveal it to be a critical factor for bulk cell line proliferation and regulation of breast cancer stem cells. In addition, MEOX1 expression was enriched in TNBC patient tissues and

inversely correlated with PTEN expression. These studies demonstrate MEOX1 is a novel target for drug development which may provide clinical benefit to breast cancer patient with poor clinical prognosis.

Introduction

Accumulating evidence has shown that many tumors, including breast cancer, are initiated from and maintained by a small population of cancer stem cells (CSCs)(1). Current cancer treatment strategies may reduce tumor bulk but in some cases fail to eradicate cancer stem cells (CSCs), leading to chemotherapy and radiotherapy resistance(2). Therefore, targeting CSCs provides a novel therapeutic strategy for cancer treatment to improve cancer patients outcome.

$HER2^{+}$ breast cancers typically respond well to trastuzumab treatment, particularly in early stage diseases. However, in metastatic HER2+ breast cancers the majority of patients will either demonstrate de novo trastuzumab resistance or acquired trastuzumab resistance after one to two year of treatment(3-5). Previous studies have shown that approximately 40% of $HER2^{+}$ breast cancers have reduced expression of the PTEN tumor suppressor (6, 7). Reduced PTEN activity mediates trastuzumab resistance via activation of the downstream signaling molecule AKT, bypassing the requirement for HER2 activation. Additionally, inactivation of PTEN in HER2 overexpressing cell lines results in activation of cross-talk between AKT and NF-kB signaling nodes(8). We and others have demonstrated trastuzumab treatment in HER2+ PTEN inactivated cell lines generates the epithelial to mesenchymal transition (EMT), expands breast CSCs, and establishes a positive feedback loop between IL-6/STAT3/NF-kB (9). The resistance

generated in these PTEN deficient cancers is stable even without trastuzumab treatment for greater than 1 month, and is thought to be maintained by the IL-6/NF-kB positive feedback. However, the induction of EMT and expansion of breast CSCs may activate diverse signaling pathways which are functionally relevant with respect to proliferation and self –renewal but have yet to be exploited as drug targets in trastuzumab resistant breast cancers(10, 11).

Sulforaphane (SF), a natural compound derived from broccoli sprouts, has shown to be effective at abrogating CSCs in breast, pancreatic, and prostate cancers. Previously, we have shown that SF was able to decrease the ALDH+ cell population in TNBC cell lines and suppress secondary tumor formation in vivo (12). Similarly in prostate and pancreatic cancer cell lines SF reduces CSC function in vitro and in vivo as evident by reduced tumorsphere formation, colony formation, and secondary tumor formation in mice(13-15). In addition, our reports and those of others demonstrate the efficacy of SF as both a single agent therapeutic and in combination with other therapies to effectively eliminate both bulk cells and CSCs (15, 16). However, due to the staggering number of proposed mechanisms of action attributed to SF's efficacy, including those by our laboratory, it remains a possibility that SF may have a context dependent inhibition on certain signaling pathways. Regardless of proposed mechanisms, the efficacy of SF in breast CSCs and specific subtypes of breast cancer make it a valuable small molecule probe which can be utilized to interrogate pathways that may be critical to inhibition of CSCs across cancer types. However in order to determine which of the many pathways SF may regulate, and which is responsible for its selective efficacy in trastuzumab resistant breast cancers, a more global approach to gene expression analysis is needed.

HOX genes, encoding homeodomain-containing master regulators of embryonic development, play key roles in stem cell proliferation and differentiation(17). Further, reports have shown that HOX genes can be re-expressed in cancerous cells following transformation and have been associated with cancer progression(18). MEOX1, a homeobox transcription factor, is well-established as one of the key transcriptional regulators during embryonic development by interacting with multiple signaling pathways (19, 20). In cancer, MEOX1 has been shown to participate in PBX1 transcriptional activity, potentially mediating PBX1-related growth signaling (21). However, the potential role of MEOX1 in regulating self-renewal of CSCs and proliferation of bulk tumor cells in trastuzumab resistant cell lines has yet to be explored.

In this report, we study the differences in global gene expression profiles between trastuzumab sensitive BT474 and resistant BT474 shPTEN with long term trastuzumab culture (>3 weeks, BT474 PTEN- LTT) by RNA sequencing (RNA-seq). Conversion of the BT474 cell lines to trastuzumab resistant BT474 PTEN- LTT resulted in a cell line which was capable of enhanced mammosphere formation and metastasis. Further, this conversion was associated with increased expression of EMT-like breast CSC markers and reduced expression of MET-like breast CSC markers. Using the natural product SF, which preferentially inhibits trastuzumab resistant BT474 PTEN- LTT cells and the breast CSCs within them, we identify novel gene targets capable of the same. Characterization of genes upregulated in BT474 PTEN- LTT cells and downregulated by SF in dose dependent manner identified MEOX1 as a novel potential drug target for the treatment of trastuzumab resistant PTEN- breast cancers. Using siRNA knockdown, we confirm that MEOX1 is functionally capable of regulating bulk cell proliferation,

mammosphere formation, and colony formation in soft agar. Interestingly, in an additional cell line MDA-MB-453 MEOX1 expression was significantly correlated with that of ALDH1A1. Immunohistochemical (IHC) staining of a breast cancer tissue microarray (TMA) revealed MEOX1 is expressed at high levels in TNBCs from patients and is significantly correlated with PTEN deletion. Our findings suggest that MEOX1 is a novel regulator of both breast CSCs and proliferation of bulk tumor cells in trastuzumab resistant breast cancers and potentially a subset of TNBCs.

Results

Trastuzumab resistance dramatically alters signal transduction in PTEN- breast cancer cells

In order to reveal the potential genes involved in trastuzumab resistance and the EMT phenotype observed in BT474 PTEN- LTT cells an RNA-seq approach was used to compare all mRNA transcripts in BT474 and BT474 PTEN- LTT cell lines. Data analysis was performed based on the random variance model (RVM) algorithm (p-value < 0.05, FDR < 0.05) and genes which exhibit great than 2-fold change as evident by RNA-seq. This revealed 3901 genes which were differentially regulated between the two cell lines, including 2023 up-regulated genes and 1878 down-regulated genes following the generation of trastuzumab resistance (Fig. 4.1A, left). Gene ontology (GO) enrichment analysis was then employed to categorize the attributes associated with differentially regulated genes. GO analysis revealed that BT474 PTEN- LTT cells overexpress genes that are significantly associated with 3 functions; focal adhesion, extracellular matrix and receptor interactions, and pathway in cancer progression. While largely general in scope,

pathways in cancer progression includes Cytokine/NF-kB, HIF-1α, and WNT signaling pathways among others. Conversely, down-regulated genes were enriched for pathways which primarily promote metabolic activity (Fig. 4.1A, right).

Previously, we have identified that trastuzumab resistance induces EMT and that BT474 PTEN- LTT cells adapt a TNBC phenotype. In order to validate these results gene set enrichment analysis (GSEA) was performed on the differentially regulated gene set between BT474 and BT474 PTEN- LTT cells and enrichment scores (ES) and their associated p-values obtained (Fig. 4.1B). GSEA reveals that the trastuzumab resistant BT474 derivative exhibits similar gene expression to cells which have transitioned to a mesenchymal cell type (ES=0.81, p-value<0.01). Similarly, the genes which were down regulated after the generation of trastuzumab resistance were enriched in a data set encompassing genes which are lower in basal breast cancer cell lines when compared to luminal (ES=0.76, p-value<0.01). Together, these results independently confirm our previous observation that the generation of trastuzumab resistance in PTEN- BT474 cells results in EMT and the conversion to a TNBC subtype.

In order to validate the reports of Korkaya et.al that expansion of breast CSCs follows the generation of trastuzumab resistance, mammosphere formation assay was performed and resulted in BT474 PTEN- LTT cells exhibiting 2.4-fold higher sphere formation potential (Fig. 4.1C) (9). In further in vivo studies, these cells were capable of producing macro-metastasis in lymph nodes whereas parental BT474 xenografts are not (Fig. 4.1D). It is expected that an increase in the CSC population could be observed by alterations in gene expression of common breast CSC markers at the mRNA level. While the expression of CD44 was increased 20.4-fold and CD24 was reduced 6.7-fold as expected, expression of

ALDH1A1 and ALDH1A3 were dramatically reduced 682-fold and 9.6-fold respectively (Fig 4.1E). These ALDH enzymes are thought to be the isoforms largely responsible for activity of the Aldefluor assay. This data suggests that not only have BT474 PTEN- LTT cells adapted a TNBC phenotype, but the CSCs within them have transitioned from an MET like state to an EMT like state.

Generation of trastuzumab resistance in BT474 with PTEN deletion is unlikely to occur through traditional mechanisms

Due to the importance of trastuzumab resistance numerous studies have identified potential drug resistance mechanism in HER2+ breast cancer (22-25). First, the epitope to which trastuzumab binds may be removed by shedding of the extracellular HER2 domain or masked by additional proteins thereby preventing access to the binding site. Further, activation of other ERBB family members and their corresponding ligands provide an additional mechanism by which downstream PI3K and AKT can be activated even in the presence of HER2 inhibition. Likewise, activation of additional signaling molecules by HER2, such as IGF-1R can lead to a diverse variety of additional downstream signaling nodes. In order to evaluate if these changes are likely responsible for our observed phenotype change we sought to look at the expression of proteins responsible for the proposed mechanisms above via RNA-seq. In addition to the observed reduction in HER2 noted earlier, expression of ERBB receptor family members HER3 and HER4 were reduced 80 and 25-fold respectively (Fig 4.2A). While EGFR was significantly upregulated 6.4-fold the expression of its ligand EGF was reduced 12.8-fold, as well as, the major ligands associated with the HER3 and HER4 (BTC and HRG).

Further, MUC4 which has previously been associated with antigen masking was reduced 6.6-fold in the BT474 PTEN- LTT cells and IGF-1R exhibited only a modest increase of 27.6% in expression (Fig 4.2B). Due to the down regulation of most ERBB family receptors, their ligands, MUC4, and only modest changes in IGF-1R, taken together with the importance of additional pathways, it is reasonable to assume that classical trastuzumab resistance mechanisms are unlikely to account for the resistance observed in PTEN deficient BT474.

Sulforaphane preferentially regulates MEOX1 mRNA in trastuzumab resistant breast cancers.

The dramatic alterations in signal transduction following PTEN knockdown and LTT make identifying novel regulators of trastuzumab resistance difficult. However, SF elicits a therapeutic response only in trastuzumab resistant cells in vitro (Fig 4.3A). By coupling the treatment of SF with analysis of differentially expressed genes in BT474 and BT474 PTEN- LTT cells it may be possible to narrow down which targets are responsible for regulating proliferation and CSCs within these cell lines. To this end both parental and BT474 PTEN- LTT cells were treated with increasing concentrations of SF (2 and 10 μM) to identify dose dependent changes in gene expression. In addition, both cell lines were treated with a dose of SF capable of inhibiting bulk cell line proliferation specifically within the BT474 PTEN- LTT cells at 8 and 24 hours to identify time dependent gene expression changes.

With increasing SF concentration and duration of treatment in both cell lines RNA-seq of total isolated mRNA was performed (Fig 4.3B). A Venn diagram illustrating the number

of genes down regulated >2-fold in the trastuzumab resistant cell line under different treatment conditions reveals that only 110 gene candidates exhibit both time and dose dependent inhibition by SF (Fig 4.3C). Of these 110 genes only 44 are upregulated >2-fold in BT474 PTEN- LTT cells relative to the parental cell line (Fig 4.3D). Functional GSEA reveals that only one functional group is enriched within these 44 genes, Homeobox transcription factors (Fig 4.3E). Among these genes MEOX1 displays the highest mRNA expression in BT474 PTEN- LTT cells and its expression was nearly undetectable in BT474 cells (2989-fold upregulated). Thus it was identified as the top candidate gene for further analysis.

Sulforaphane reduces MEOX1 protein expression in vitro and in vivo.

In order to evaluate if the reduction of MEOX1 mRNA led to a reduction in protein expression immunofluorescent staining of MEOX1 was performed. Under typical culture conditions for BT474 PTEN- LTT cells in vitro MEOX1 resides primarily within the nucleus, as evident by overlap between MEOX1 (Green) and DAPI (Blue) staining (Fig 4.4A). The addition of 10 μM SF for 24 hours led to a reduction in both overall intensity and number of MEOX1 nuclear foci, suggesting SF reduces MEOX1 protein expression in vitro. In order to validate if SF was capable of reducing MEOX1 expression in vivo and advanced treatment orthotopic mouse xenograft model was employed using the BT474 PTEN- LTT cell line. Daily treatment of mice with 50 mg/kg SF significantly reduced the tumor mass when primary treatment ended (Fig 4.4B, left), and as previously identified SF reduced the frequency of CSCs within these tumors based on secondary reimplantation with extreme limiting dilution analysis (ELDA)(Fig 4.4B, right). A

section of primary tumor was harvested before ELDA and immunohistochemical (IHC) staining of MEOX1 was performed (Fig 4.4C). IHC demonstrates that the use of SF in BT474 PTEN- LTT xenografts reduces MEOX1 expression at the protein level in vivo (Fig 4.4C, left), whereas parental BT474 tumors express no MEOX1 protein (Fig 4.4C, right). Taken together, these results suggest that SF reduces MEOX1 expression at the mRNA and protein level both in vitro and in vivo.

MEOX1 functionally regulates bulk cell line proliferation and BCSCs in vitro.

To elucidate the function of MEOX1 in the trastuzumab resistant BT474 PTEN- LTT cell line its expression was reduced by siRNA knockdown, which reduced mRNA expression by more than 90% (Fig 4.5A). The number of BT474 PTEN- LTT cells incubated with lipofectamine (vehicle), or lipofectamine and a non-targeted siRNA control (NT-control) increased 4-fold over the course of 72 hours (Fig 4.5B). However, MEOX1 siRNA (siMEOX1) completely inhibited proliferation over the same time period as evident by the MTS assay. To further evaluate the efficacy of MEOX1 knockdown on in vitro tumorigenicity the colony formation assay in soft agar was performed. Over 14 days the number of colonies from siMEOX treatment was reduced 86.7% relative to control treated BT474 PTEN- LTT cells (Fig 4.5C). The role of MEOX1 in BCSC self-renewal was also determined using the mammospheres formation assay. Over the course of 7 days siMEOX treatment led to a 60.5% reduction in the number of mammospheres formed and the size of the average sphere was reduced by 90% (Fig 4.5D). Taken together, these results suggest that MEOX1 is capable of regulating both CSCs and bulk cell line proliferation in trastuzumab resistant, PTEN deficient, breast cancers.

While the role of MEOX1 in regulating both cell line proliferation and CSCs was identified in trastuzumab resistant BT474 PTEN- LTT cells it is possible that, like SF, it may demonstrate utility in other cell lines. The MDA-MB-453 cell line expresses HER2 protein and contains mutations in PI3K and PTEN. In this context it represents a cell line which may be predisposed to resistance against trastuzumab. Further, previous work by Charafe-Jauffret et. al. have demonstrated that Aldefluor positive cells within this cell line accurately reflect CSCs (26). Therefore we thought to determine if MEOX1 protein expression in this cell line correlates with ALDH1A1 expression. Confocal microscopy of immunofluorescently labeled MDA-MB-453 cells reveals co-expression of MEOX1 and ALDH1A1, albeit at different intracellular locations (Fig 4.5C, left). Quantification of fluorescent intensity for each individual channel identifies a linear correlation between protein expression (Spearman rho=0.797, $p<0.01$) (Fig 4.5C, right). This suggests that MEOX1 may also play a role within CSCs in additional breast cancers.

MEOX1 is significantly associated with TNBC and PTEN inactivation.

MEOX1 demonstrated a critical functional role with respect to regulation of CSCs and proliferation of bulk cells in the BT474 PTEN- LTT cell line. In addition, its presence in ALDH1A1 high cells in MDA-MB-453 suggested that MEOX1 expression may also be present in additional subtypes of breast cancer. To expand the scope of our investigation MEOX1 staining was performed in a small TMA which contained paired normal cancer adjacent tissues and breast cancers from 75 different patients encompassing all major breast cancer subtypes. Interestingly, no normal adjacent tissues or benign fibroadenomas exhibited MEOX1 expression (Fig 4.6A). IHC staining revealed that

MEOX1+ cells can be found in 9.5% of tumor tissue from patients (Fig 4.6B, 7 out of 75). Of these seven patients five tumor samples were from TNBCs and grading ranged from ductal carcinoma in situ to node positive invasive carcinomas.

In vitro MEOX1 expression can be identified in BT474 PTEN- LTT and MDA-MB-453 cells, both of which contain reduced function of the PTEN tumor suppressor. With this in mind we sought to determine if MEOX1 protein expression was inversely correlated with PTEN expression in patients. TMA IHC staining (Fig 4.6C) demonstrated an inverse correlation between MEOX1 and PTEN (Spearman rho=-0.186, $p<0.05$). Taken together with in vitro data, these results suggest that development of novel therapeutics which target MEOX1 may demonstrate clinical utility in patients predisposed to trastuzumab resistance via PTEN inactivation, those already resistant, and potentially a subset of TNBC patients.

Discussion

Cancer is currently estimated to be the leading cause of death worldwide and breast cancer is the 2nd leading cause of cancer related deaths among women in the United States (27). Identification of different breast cancer subtypes has led to significant advances in targeted therapy (28). For HER2+ breast cancers several targeted therapies are currently in use with the front line therapy being trastuzumab. While this antibody has proven extremely useful for early stage HER2+ breast cancer patients the majority of late stage (metastatic) patients demonstrate de novo resistance or will develop acquired resistance within 1 to 2 years (3-5). Several mechanisms have been associated with the generation of trastuzumab resistance including antigen masking, activation of non-

canonical HER2 binding partners, or activation of downstream signaling nodes which bypass the requirement for HER2.

Accumulating evidence suggests that the induction of EMT and expansion of CSCs may be critical to the generation of trastuzumab resistance. For instance, JIMT-1 cells that exhibit de novo trastuzumab resistance express relatively high levels of EMT markers SLUG and SNAIL and are primarily CD44+/CD24-, whereas trastuzumab sensitive SKBR3 cells are primarily CD24+ and lack expression of EMT markers (29). In another report associated with acquired resistance, 3 month culture of SKBR3 cells with trastuzumab generated drug resistance and resulted in expression of EMT inducer TGF-β and downstream target ZEB1 (30). Further, Lesniak et al. demonstrated rare colonies within the SKBR3 cell line had spontaneously undergone EMT to generated drug resistance and the cells derived from these colonies were primarily CD44+/CD24- with lower HER2 expression (31). Numerous studies also have indicated that inactivation of PTEN genes may contribute to trastuzumab resistance. In line with these studies our work, and that by Korkaya et. al., have established that induction of trastuzumab resistance by longer term trastuzumab culture in PTEN deficient cells rapidly induces EMT and expands CSCs (9). While initially attributed to the activation of the IL-6/STAT3/NF-kB positive feedback loop it is possible that additional signaling pathways may be critical to maintaining the observed phenotype.

To further characterize pathways which may play a critical role in the trastuzumab resistance observed we surveyed the transcriptional landscape in parental BT474 and BT474 PTEN- LTT cell lines using RNA-Seq. These experiments identified 3901 differentially-expressed genes between the trastuzumab sensitive and resistant cell lines.

Utilizing bioinformatics analysis differentially expressed genes were categorized into 36 canonical pathways. From them, most up-regulated genes were significantly enriched for 3 pathways including focal adhesion, ECM-receptor interaction and pathway in cancer progression. These pathways in cancer progression included cytokine/NF-kB, HIF-1α, and WNT signaling, all of which are known to play a role in regulating breast CSCs(32-35). Conversely, following the generation of trastuzumab resistance expression of most ERBB receptors, their ligands, and genes classically associated with trastuzumab resistance either decreased or didn't exhibit major changes in expression. These results also confirm our previous observations that BT474 PTEN- LTT cells have adopted a TNBC subtype by undergoing the EMT. Interestingly, we observed that expression of mRNA for breast cancer stem cell markers CD44+/CD24- was increased whereas ALDH1A1 and ALDH1A3 were dramatically decreased.

Recently, Liu et. al. have identified that BCSCs exist in two distinct states: the MET state marked by the Aldefluor assay (proliferative with hypoxic niche) and the EMT state marked by CD44+/CD24- cell surface markers (quiescent with invasive characteristics) (36). However, the relative percentage of CSCs in the MET and EMT states may vary among cell lines (26, 36, 37). We hypothesize that HER2+ breast cancers have shifted the equilibrium of CSCs primarily toward the MET like state, as evident by high percentages of ALDH+ cells (26) which giving rise to epithelial or luminal like cell markers and little to no CD44+/CD24- cells. This is supported by the observation that ALDH+ BCSCs rely on HER2 signaling for self-renewal (38). Conversely, in claudin-low (triple negative) breast cancers the equilibrium is shifted primarily toward the EMT state giving rise to mesenchymal differentiated TNBCs in which greater than 90% of

cells with the cell line are CD44+/CD24- (37). Based on our previously mentioned data, and literature, we postulate that PTEN inactivation in HER2+ breast cancers expands the EMT-like CSC state. With both EMT and MET CSCs present the addition of trastuzumab shifts the equilibrium toward EMT state, by eliminating HER2 expressing cells, which upon differentiation create a mesenchymal triple negative cell line (Fig 4.7).

Due to the dramatic alterations in gene expression between trastuzumab sensitive and resistant cell lines, and the numerous reported mechanisms of SF action, a knowledge based approach to determining critical pathways affected is difficult. In order to take an unbiased approach toward identifying what genes are specifically inhibited to the largest extent by SF in the trastuzumab resistant cells we developed a treatment based filtering scheme to narrow our search. Noting the relative sensitivity of both BT474 and BT474 PTEN- LTT cell lines to SF we chose to focus on genes which were decreased in both a dose and time dependent manner by SF and were upregulated following trastuzumab resistance. This filtering scheme allowed us to narrow our search to only 44 genes, which upon functional classification identified 4 homeobox transcription factors as potential targets. Among them MEOX1 displaying the highest expression and fold-change difference between parental and trastuzumab resistant cell lines and was therefore selected as the top candidate gene for further study.

The MEOX1 (previously MOX1) homeobox transcriptional factor represents a critical mediator of normal somite formation in a developing embryo, a process which requires both the EMT and MET process (39-42). In patients, homozygous truncation mutations in the MEOX1 gene cause an autosomal-recessive form of Klippel-Feil Syndrome, a disease characterized by fusion of cervical vertebrae (43, 44). Recent evidence in zebra fish

demonstrates MEOX1+ cells regulate normal hematopoietic stem cell formation in a cytokine dependent manner (45). Further, MEOX1 has been shown to mediate Hedgehog signaling by regulating Gli1/2 expression in cardiomyogenesis(46). While the role of MEOX-1 in cancer has largely been unexplored, one study by Thiaville et. al. suggests that this transcription factor partially mediates PBX1 signaling in ovarian cancers (21). PBX1 has been shown to be a downstream target of NOTCH signaling in breast cancer, and NOTCH itself is a known regulator of ALDH+ CSCs (47, 48).

Validation of SF mediated MEOX1 suppression identified by RNA-seq was confirmed at the protein level in vitro via immunofluorescence and in an orthotopic mouse xenograft model in vivo. To elucidate the functional of MEOX1, with respect to trastuzumab resistance, expression was reduced by siRNA knockdown in the BT474 PTEN- LTT cell line. Knockdown of MEOX1 significantly reduced bulk cell line proliferation, mammosphere formation, and colony formation in soft agar. These results indicate that MEOX1 plays a critical role both in regulating bulk cell line and the CSC within them. To further identify if MEOX1 may regulate CSCs in other HER2 expressing cell lines with PTEN inactivation its expression was associated with that of ALDH1A1 in MDA-MB-453 cells. Indeed, MEOX1 and ALDH1A1 exhibited a positive correlation in this cell line, suggesting that it may be capable of regulating CSCs in patients predisposed to trastuzumab resistance because of PTEN inactivation. However, further studies are likely need to address this question.

In order to survey the expression of MEOX1 in a broader patient population TMA staining of paired normal adjacent tissue and tumor samples was carried out. Expression of MEOX1 was not identified in normal adult tissues or benign fibroadenomas.

However, MEOX1 expression was enriched in TNBC tissues at various stages of progression. Using gene expression analysis of TNBC patient tissues Lehmann et. al. have demonstrated that TNBCs can be classified into six major subtypes (49). Interestingly, the mesenchymal stem-like subtype of TNBC they identified was characterized by the expression of HOX genes such as MEOX1. This may suggest that the TNBCs identified to express MEOX1 in our TMA were of that TNBC subtype. Further, MEOX1 was inversely correlated with PTEN expression in patients. These results are not surprising because in this context the discovery of MEOX1 took place in the BT474 PTEN- LTT cell line, which following generation of trastuzumab resistance via PTEN reduction ultimately became a TNBC. In summary, we have identified MEOX1 as a novel drug target capable of regulating both bulk cell line proliferation and CSCs in trastuzumab resistant, PTEN deficient, breast cancers. Taken together with our preliminary TMA data these results suggest MEOX1 may represent a novel drug target for the treatment of late stage HER2+ and a subset of TNBC patients.

Methods

Cell Lines and Reagents. BT474 was cultured in DMEM supplemented with 10% fetal bovine serum and 1% antibiotic-antimycotic under a 5% CO2 environment. BT474-PTEN- LTT cells, which were induced by shRNA knockdown of PTEN and long term treatment of trastuzumab, were maintained in the same media as the parental cell line. Sulforaphane was obtained from LKT Laboratories. Polyclonal antibodies against MEOX1 were purchased from Abcam (ab75895) and mouse anti-ALDH1A1 antibody was obtained from BD biosciences (611194).

RNA-seq data analysis. Total RNA was extracted using RNeasy Mini kit (Qiagen) and mRNA library was prepare for RNA-seq (poly A selection based) using Illumina TruSeq technology (Illumina). The generated libraries were sequenced on Illumina Hi-Seq 2000 with 50 cycle single ended reads. RNA-Seq reads were aligned to annotated RefSeq(50) transcripts using Bowtie(51). Overall >80% of reads mapped to RefSeq transcripts and >95% were uniquely mapped. Only uniquely mapped reads were used for further analysis. Gene expression was expressed as reads/kilobase/million mapped reads (RPKM) (52) and differences in gene expression were estimated using rSeq(53). Gene set enrichment analysis was performed using the GSEA Java desktop software application (Broad Institute) (54, 55). Finally, gene functional classification was performed using the DAVID Bioinformatics Resources v6.7 (56, 57).

Knockdown by siRNA. Small interfering RNAs for gene MEOX1 was purchased from Qiagen (validated FlexiTube si RNA, SI00630266). siRNA amount varied by assay and was optimized relative to volume of total amount of media and transfection reagent used. Transfection of BT474 PTEN- LTT cells was carried out using Lipofectamine® RNAiMAX vehicle according to the manufacturer's instruction following optimization. As a negative control, a non-targeting sequence siRNA was utilized (Qiagen, catalog number 1027281). Knockdown at mRNA level was confirmed by isolating total RNA (RNeasy Mini kit, Quigen), converting to cDNA (QuantiTect Rev. Transcription Kit, Qiagen), and performing real-time quantitative RT-PCR in triplicate. Real-time PCR was carried out on an ABI PRISM 7900HT sequence detection system with 96-well block module and automation accessory (Applied Biosystems).

MTS Cell Proliferation Assay. Cell lines were seeded at a density of 3,000 cells per well in 96-well plates and allowed to adhere overnight. Cells were then incubated with SF in increasing concentrations for a period of 48 hours. Proliferation was determined by MTS assay according to manufacturer's instruction by measuring the absorbance at 490 nm on a Synergy 2 plate reader (Biotek).

Advanced Tumor Model. All the mice in this study were conducted in accordance with a standard animal protocol approved by the University Committee on the Use and Care of Animals at the University of Michigan. 5 week old female non-obese diabetic/severe combined immunodeficient (NOD/SCID) mice were obtained from Jackson Laboratory. BT474 or BT474 PTEN- LTT cells (500,000) mixed with Matrigel (BD Biosciences) were injected to the mammary fat pads of NOD/SCID mice. Tumors were measured by caliper and the volume was calculated using V = 1/2 (width2 × length). When tumor volume reached approximately 40 mm3, the mice were randomly separated into two groups, once receiving daily i.p. injected with 0.9% saline solution and the other receiving 50 mg/kg sulforaphane daily. Final tumor mass was measured on an analytical balance.

Secondary Reimplantation. Isolated primary tumors were mechanically dissociated by mincing with scalpels and suspended in Media 199 (invitrogen). Single cell suspensions were generated by incubation with collagenase and hyaluronidase (Stem Cell Technologies) at 37oC for 45 min and passage through a 40 μm nylon mesh filter. Human tumor cells with DsRed label were then isolated using fluorescent activated cell sorting on a SY3200 (Sony Biotechnology) flow cytometer. Secondary female, 5 week old, NOD/SCID mice were inoculated with 5,000, 1,000, or 200 cells for BT474 PTEN-

LTT xenografts as described above. Tumor formation rate in secondary mice was assessed 8 weeks following implanting cells by direct palpitation and used to assess cancer stem cell frequency by extreme limiting dilution analysis (58).

Colony Formation Assay. Colony formation was carried out in six-well plates layered with 1.5 mL of 0.5% agar (Difco Agar Noble) in Dulbecco's modified Eagle's medium supplemented with 10% fetal bovine serum and 1% penicillin-streptomycin. Subsequently, 1000 cells mixed with 0.35% agar and allowed to set in each well of the six-well plates in order to form the upper gel. After 2 weeks, pictures of colonies were taken using a digital camera after staining with 0.005% blue violet. Each treatment was performed in triplicate.

Immunofluorescence. Cells were seated in glass chambers slides and allowed to adhere overnight. After rinsing with PBS, cells were fixed in PBS containing 4% paraformaldehyde for 30 minutes and permeabilized with 0.1% Triton X-100 (Roche Diagnostics) for 10 minutes at 4°C. Cells were then incubated with MEOX1 (1:200) primary antibodies, followed by FITC-conjugated anti-rabbit IgG (1:300) secondary antibodies. Samples were then mounted onto slides and visualized using confocal microscopy (Leica Microsystems). Data shown represents the max intensity image.

Mammosphere formation assay. Mammosphere culture was done as previously described in a serum-free mammary epithelium basal medium (Lonza, Inc.) supplemented with B27 (Invitrogen), 1% antibiotic-antimycotic, 5 μg/mL insulin, 1 μg/mL hydrocortisone, 4 μg/mL gentamicin, 20 ng/mL EGF (Sigma-Aldrich), 20 ng/mL basic fibroblast growth factor (Sigma-Aldrich), and 1:25,000,000 β-mercaptoethanol

(Sigma-Aldrich)(59). Single cells prepared from mechanical and enzymatic dissociation were plated in six-well ultralow attachment plates (Corning) at a density of 500 cells/ml. After 7 days of culture, the number of mammospheres was counted on a Nikon Eclipse TE2000-S microscope and the photos were acquired with MetaMorph 7.6.0.0.

Immunohistochemistry and Tissue Microarray Assay. Immunohistochemical analysis was performed on isolated tumors from mouse xenografts and patients tissues on a tissue micro array (TMA) obtained from US Biomax (BR1503b). Standard avidin-biotin complex peroxidase immunohistochemical staining (Histostain-*Plus*, Invitrogen) was performed according to manufacturer's instruction. Briefly, after removal of paraffin in xylene and rehydration in graded alcohols, heated antigen retrieval was performed in citrate buffer (10 mmol/L pH 6.0) by waterbath heating for 30 min. Endogenous peroxidase activity was prevent by incubation in 0.3% hydrogen peroxide for 10 min. Nonspecific binding was blocked by incubation in 10% normal animal serum for 10 min. Sections were incubated at 4 °C for 24 h with each antibody. Correlation of MEOX1 and PTEN protein expression levels were initially scored by intensity and the percentage of immunoreactive cells. Tissues with no staining were rated as 0, with faint staining or moderate to strong staining in <25% of cells as 1, with moderate staining or strong staining in 25% to 50% of cells as 2, and with strong staining in >50% of cells as 3. Breast cancer tissues that registered levels 0 and 1 were defined as negative for expression, whereas samples at levels 2 or 3 were defined as positive.

Reference

1. Al-Hajj M, Wicha MS, Benito-Hernandez A, Morrison SJ, & Clarke MF (2003) Prospective identification of tumorigenic breast cancer cells. *Proc Natl Acad Sci U S A* 100(7):3983-3988.
2. Tanei T, *et al.* (2009) Association of Breast Cancer Stem Cells Identified by Aldehyde Dehydrogenase 1 Expression with Resistance to Sequential Paclitaxel and Epirubicin-Based Chemotherapy for Breast Cancers. *Clinical Cancer Research* 15(12):4234-4241.
3. Gajria D & Chandarlapaty S (2011) HER2-amplified breast cancer: mechanisms of trastuzumab resistance and novel targeted therapies. *Expert Rev Anticancer Ther* 11(2):263-275.
4. Bartsch R, Wenzel C, & Steger GG (2007) Trastuzumab in the management of early and advanced stage breast cancer. *Biologics : Targets & Therapy* 1(1):19-31.
5. Vogel CL, *et al.* (2002) Efficacy and Safety of Trastuzumab as a Single Agent in First-Line Treatment of HER2-Overexpressing Metastatic Breast Cancer. *Journal of Clinical Oncology* 20(3):719-726.
6. Bailey TA, *et al.* (2011) Mechanisms of Trastuzumab resistance in ErbB2-driven breast cancer and newer opportunities to overcome therapy resistance. *J Carcinog* 10:28.
7. Nagata Y, *et al.* (2004) PTEN activation contributes to tumor inhibition by trastuzumab, and loss of PTEN predicts trastuzumab resistance in patients. *Cancer Cell* 6(2):117-127.
8. Pianetti S, Arsura M, Romieu-Mourez R, Coffey RJ, & Sonenshein GE (2001) Her-2/neu overexpression induces NF-nB via a PI3-kinase/Akt pathway involving calpain-mediated degradation of InB-a that can be inhibited by the tumor suppressor PTEN. *Oncogene* 20:1287-1299.
9. Korkaya H, *et al.* (2012) Activation of an IL6 inflammatory loop mediates trastuzumab resistance in HER2+ breast cancer by expanding the cancer stem cell population. *Mol Cell* 47(4):570-584.
10. Zhang Z, *et al.* (2012) Activation of the AXL kinase causes resistance to EGFR-targeted therapy in lung cancer. *Nature genetics* 44(8):852-860.
11. Sequist LV, *et al.* (2011) Genotypic and histological evolution of lung cancers acquiring resistance to EGFR inhibitors. *Science translational medicine* 3(75):75ra26-75ra26.
12. Li Y, *et al.* (2010) Sulforaphane, a dietary component of broccoli/broccoli sprouts, inhibits breast cancer stem cells. *Clin Cancer Res* 16(9):2580-2590.
13. Xu C, Shen G, Chen C, Gelinas C, & Kong A-NT (2005) Suppression of NF-kB and NF-kB-regulated gene expression by sulforaphane and PEITC through IkBa, IKK pathway in human prostate cancer PC-3 cells. *Oncogene* 24(28):4486-4495.
14. Kallifatidis G, *et al.* (2009) Sulforaphane targets pancreatic tumour-initiating cells by NF-κB-induced antiapoptotic signalling. *Gut* 58(7):949-963.
15. Rausch V, *et al.* (2010) Synergistic Activity of Sorafenib and Sulforaphane Abolishes Pancreatic Cancer Stem Cell Characteristics. *Cancer Research* 70(12):5004-5013.

16. Kallifatidis G, *et al.* (2011) Sulforaphane Increases Drug-mediated Cytotoxicity Toward Cancer Stem-like Cells of Pancreas and Prostate. *Mol Ther* 19(1):188-195.
17. Leucht P, *et al.* (2008) Embryonic origin and Hox status determine progenitor cell fate during adult bone regeneration. *Development* 135(17):2845-2854.
18. Abate-Shen C (2002) Deregulated homeobox gene expression in cancer: cause or consequence? *Nat Rev Cancer* 2(10):777-785.
19. Gianakopoulos PJ & Skerjanc IS (2005) Hedgehog Signaling Induces Cardiomyogenesis in P19 Cells. *Journal of Biological Chemistry* 280(22):21022-21028.
20. Mankoo BS, *et al.* (2003) The concerted action of Meox homeobox genes is required upstream of genetic pathways essential for the formation, patterning and differentiation of somites. *Development* 130(19):4655-4664.
21. Thiaville MM, *et al.* (2012) Identification of PBX1 target genes in cancer cells by global mapping of PBX1 binding sites. *PLoS One* 7(5):e36054.
22. Nagy P, *et al.* (2005) Decreased accessibility and lack of activation of ErbB2 in JIMT-1, a herceptin-resistant, MUC4-expressing breast cancer cell line. *Cancer Research* 65(2):473-482.
23. Agus DB, *et al.* (2002) Targeting ligand-activated ErbB2 signaling inhibits breast and prostate tumor growth. *Cancer Cell* 2(2):127-137.
24. Nahta R, Yuan LX, Zhang B, Kobayashi R, & Esteva FJ (2005) Insulin-like growth factor-I receptor/human epidermal growth factor receptor 2 heterodimerization contributes to trastuzumab resistance of breast cancer cells. *Cancer Research* 65(23):11118-11128.
25. Kondapaka SB, Singh SS, Dasmahapatra GP, Sausville EA, & Roy KK (2003) Perifosine, a novel alkylphospholipid, inhibits protein kinase B activation. *Molecular Cancer Therapeutics* 2(11):1093-1103.
26. Charafe-Jauffret E, *et al.* (2009) Breast cancer cell lines contain functional cancer stem cells with metastatic capacity and a distinct molecular signature. *Cancer Research* 69(4):1302-1313.
27. Siegel R, Ma J, Zou Z, & Jemal A (2014) Cancer statistics, 2014. *CA: a cancer journal for clinicians* 64(1):9-29.
28. Sørlie T, *et al.* (2001) Gene expression patterns of breast carcinomas distinguish tumor subclasses with clinical implications. *Proceedings of the National Academy of Sciences* 98(19):10869-10874.
29. Oliveras-Ferraros C, *et al.* (2012) Epithelial-to-mesenchymal transition (EMT) confers primary resistance to trastuzumab (Herceptin). *Cell Cycle* 11(21):4020-4032.
30. Bai WD, *et al.* (2014) MiR-200c suppresses TGF-β signaling and counteracts trastuzumab resistance and metastasis by targeting ZNF217 and ZEB1 in breast cancer. *International Journal of Cancer* 135(6):1356-1368.
31. Lesniak D, *et al.* (2013) Spontaneous epithelial-mesenchymal transition and resistance to HER-2-targeted therapies in HER-2-positive luminal breast cancer. *PLoS One* 8(8):e71987.
32. Kim G, *et al.* (2014) SOCS3-mediated regulation of inflammatory cytokines in PTEN and p53 inactivated triple negative breast cancer model. *Oncogene*.

33. Liu M, *et al.* (2010) The canonical NF-κB pathway governs mammary tumorigenesis in transgenic mice and tumor stem cell expansion. *Cancer Research* 70(24):10464-10473.
34. Conley SJ, *et al.* (2012) Antiangiogenic agents increase breast cancer stem cells via the generation of tumor hypoxia. *Proceedings of the National Academy of Sciences* 109(8):2784-2789.
35. Turashvili G, Bouchal J, Burkadze G, & Kolar Z (2005) Wnt signaling pathway in mammary gland development and carcinogenesis. *Pathobiology: journal of immunopathology, molecular and cellular biology* 73(5):213-223.
36. Liu S, *et al.* (2014) Breast cancer stem cells transition between epithelial and mesenchymal states reflective of their normal counterparts. *Stem cell reports* 2(1):78-91.
37. Fillmore CM & Kuperwasser C (2008) Human breast cancer cell lines contain stem-like cells that self-renew, give rise to phenotypically diverse progeny and survive chemotherapy. *Breast cancer res* 10(2):R25.
38. Korkaya H, Paulson A, Iovino F, & Wicha MS (2008) HER2 regulates the mammary stem/progenitor cell population driving tumorigenesis and invasion. *Oncogene* 27(47):6120-6130.
39. Kirilenko P, *et al.* (2011) Transient activation of meox1 is an early component of the gene regulatory network downstream of hoxa2. *Molecular and cellular biology* 31(6):1301-1308.
40. Jukkola T, *et al.* (2005) Meox1Cre: a mouse line expressing Cre recombinase in somitic mesoderm. *Genesis* 43(3):148-153.
41. Petropoulos H, Gianakopoulos PJ, Ridgeway AG, & Skerjanc IS (2004) Disruption of Meox or Gli activity ablates skeletal myogenesis in P19 cells. *Journal of Biological Chemistry* 279(23):23874-23881.
42. Umeda K, *et al.* (2012) Human chondrogenic paraxial mesoderm, directed specification and prospective isolation from pluripotent stem cells. *Scientific reports* 2.
43. Bayrakli F, *et al.* (2013) Mutation in MEOX1 gene causes a recessive Klippel-Feil syndrome subtype. *BMC genetics* 14(1):95.
44. Mohamed JY, *et al.* (2013) Mutations in MEOX1, encoding mesenchyme homeobox 1, cause Klippel-Feil anomaly. *The American Journal of Human Genetics* 92(1):157-161.
45. Nguyen PD, *et al.* (2014) Haematopoietic stem cell induction by somite-derived endothelial cells controlled by meox1. *Nature* 512(7514):314-318.
46. Candia AF, *et al.* (1992) Mox-1 and Mox-2 define a novel homeobox gene subfamily and are differentially expressed during early mesodermal patterning in mouse embryos. *Development* 116(4):1123-1136.
47. Magnani L, *et al.* (2013) Genome-wide reprogramming of the chromatin landscape underlies endocrine therapy resistance in breast cancer. *Proceedings of the National Academy of Sciences*:201219992.
48. Zhao D, *et al.* (2014) NOTCH-induced aldehyde dehydrogenase 1A1 deacetylation promotes breast cancer stem cells. *The Journal of Clinical Investigation* 124(124 (12)):5453-5465.

49. Lehmann BD, *et al.* (2011) Identification of human triple-negative breast cancer subtypes and preclinical models for selection of targeted therapies. *The Journal of Clinical Investigation* 121(7):2750-2767.
50. Pruitt KD, Tatusova T, Brown GR, & Maglott DR (2012) NCBI Reference Sequences (RefSeq): current status, new features and genome annotation policy. *Nucleic Acids Research* 40(D1):D130-D135.
51. Langmead B, Trapnell C, Pop M, & Salzberg S (2009) Ultrafast and memory-efficient alignment of short DNA sequences to the human genome. *Genome Biology* 10(3):R25.
52. Mortazavi A, Williams BA, McCue K, Schaeffer L, & Wold B (2008) Mapping and quantifying mammalian transcriptomes by RNA-Seq. *Nat Meth* 5(7):621-628.
53. Jiang H & Wong WH (2009) Statistical inferences for isoform expression in RNA-Seq. *Bioinformatics* 25(8):1026-1032.
54. Subramanian A, *et al.* (2005) Gene set enrichment analysis: A knowledge-based approach for interpreting genome-wide expression profiles. *Proceedings of the National Academy of Sciences* 102(43):15545-15550.
55. Mootha VK, *et al.* (2003) PGC-1[alpha]-responsive genes involved in oxidative phosphorylation are coordinately downregulated in human diabetes. *Nat Genet* 34(3):267-273.
56. Huang DW, Sherman BT, & Lempicki RA (2008) Systematic and integrative analysis of large gene lists using DAVID bioinformatics resources. *Nat. Protocols* 4(1):44-57.
57. Huang DW, Sherman BT, & Lempicki RA (2009) Bioinformatics enrichment tools: paths toward the comprehensive functional analysis of large gene lists. *Nucleic Acids Research* 37(1):1-13.
58. Hu Y & Smyth GK (2009) ELDA: Extreme limiting dilution analysis for comparing depleted and enriched populations in stem cell and other assays. *Journal of Immunological Methods* 347(1–2):70-78.
59. Ginestier C, *et al.* (ALDH1 Is a Marker of Normal and Malignant Human Mammary Stem Cells and a Predictor of Poor Clinical Outcome. *Cell Stem Cell* 1(5):555-567.

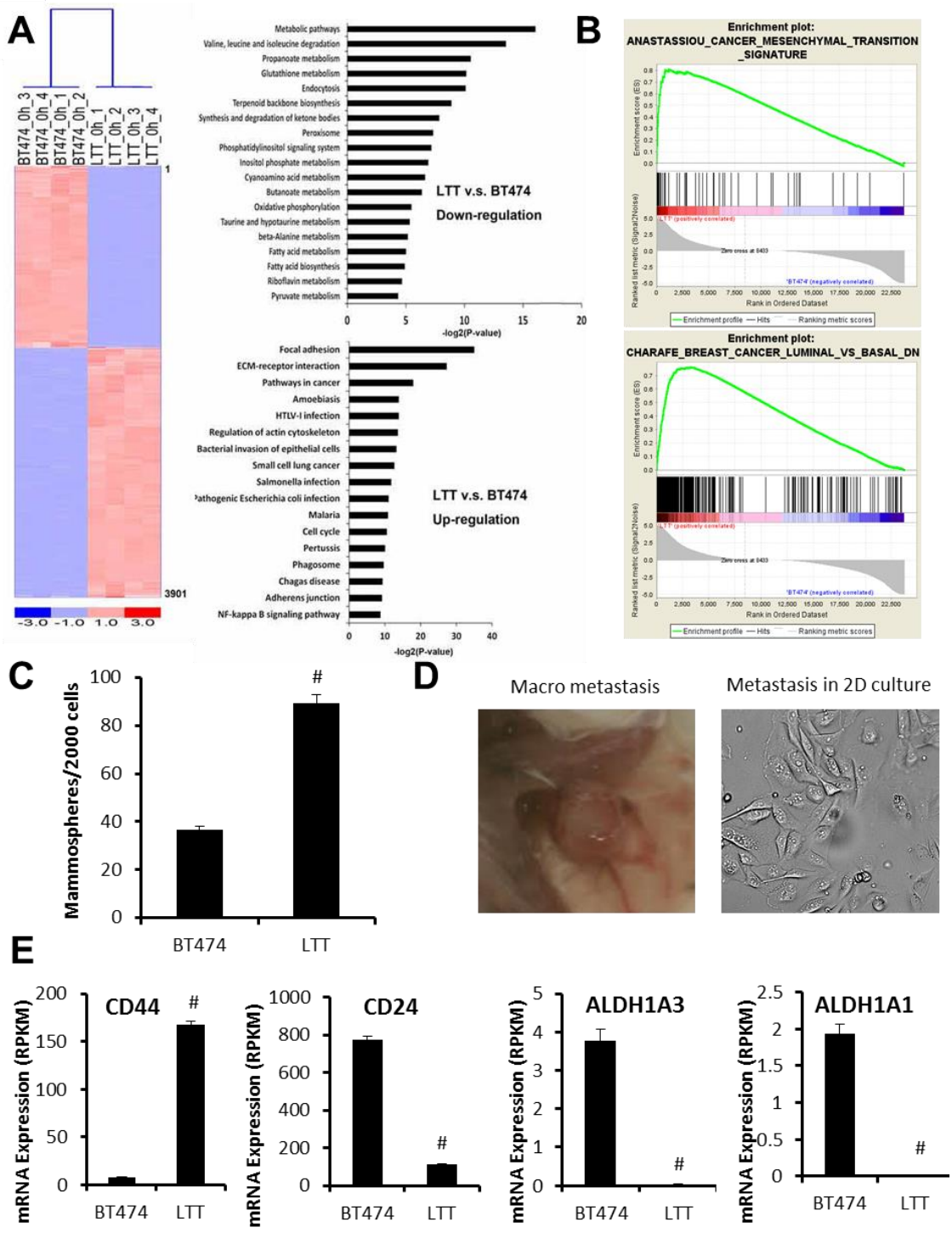

Figure 4.1 Trastuzumab resistance activates diverse signaling pathways and alters BCSC marker expression. A) Left, heat map representation of the differentially expressed genes between BT474 and BT474 PTEN- LTT cell lines, gene expression is shown with pseudocolor scale (−3 to 3) with red denoting high gene expression levels. Right, the top ranking gene ontology attributes enriched in upregulated and down

regulated genes with associated p values. B) Gene set enrichment analysis identifying enrichment of upregulated genes in BT474 PTEN- LTT cells (Top) and those downregulated (Bottom) pertaining to EMT and molecular subtype. C) Mammosphere formation rates of parental BT474 and BT474 PTEN- LTT cell lines. D) Representative image of macrometastasis that forms in 1 in 5 mice BT474 PTEN- LTT xenograft bearing mice before primary tumors reach 500 mm^3. E) RNA expression of common BCSC markers determined by RNA-seq expressed as reads/kilobase/million mapped reads (RPKM). N=4. Data shown as average ± SD. # $p \leq 0.01$.

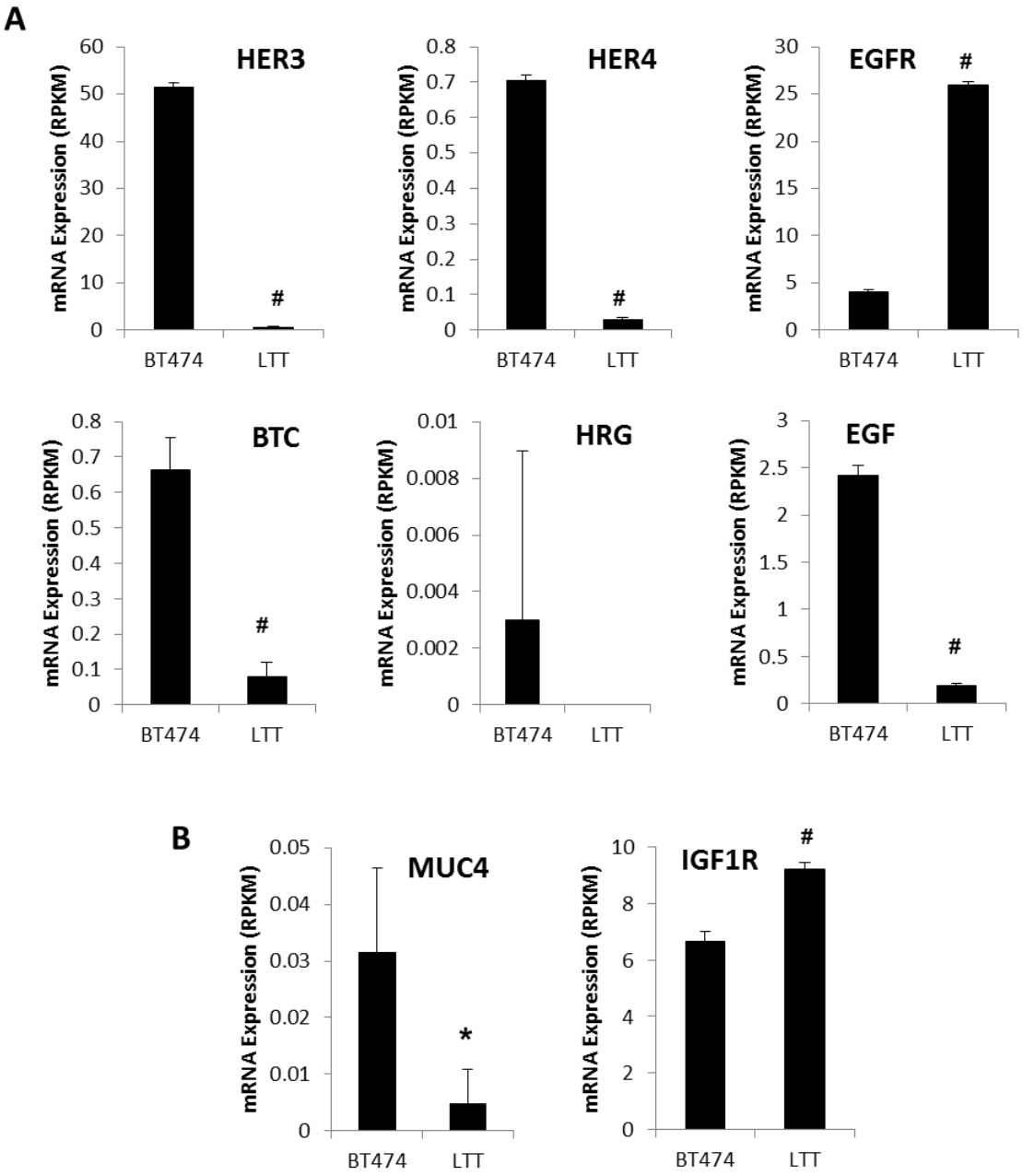

Figure 4.2 Generation of trastuzumab resistance from BT474 with PTEN deletion reduces ERBB family receptors and ligands with modest change in classical mechanisms associated with resistance. Normalized mRNA expression (reads/kilobase/million reads) of (A) ERBB family members HER3, HER4, and EGFR with corresponding major ligands and (B) genes previously associated with antigen masking on HER2 and resistance induced signaling crosstalk, MUC4 and IGF1R respectively. N=4. Data shown as average ± SD. * $p \leq 0.05$, # $p \leq 0.01$

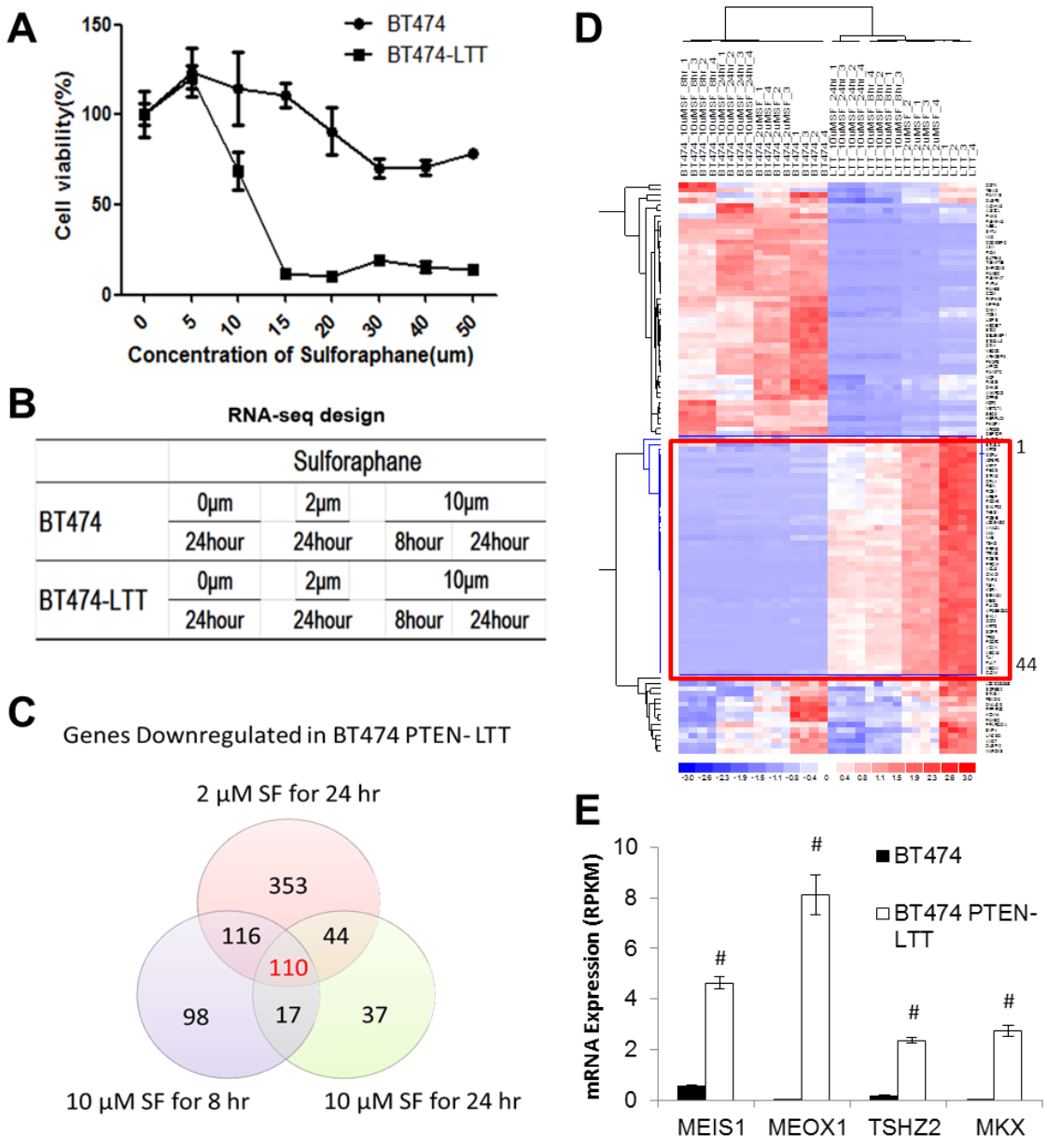

Figure 4.3 Sulforaphane preferentially inhibits Homeobox transcription factors in trastuzumab resistant cells. A) Cell viability of BT474 and BT474 PTEN- LTT cell lines following 72 hour treatment with SF as determined by the MTS assay. N=6. B) Schematic of treatment groups for RNA-sequencing to identify both time (10 μM SF 8 hours v.s. 10 μM SF 24 hours) and dose (2 μM SF 24 hours v.s. 10 μM SF for 24 hours). N=4. C) Venn diagram illustrating number of genes reduced 2-fold in BT474 PTEN- LTT cells following each treatment. D) Heat map illustrating expression changes in BT474 and BT474 PTEN- LTT cells of the 110 genes which are inhibited in a dose and time dependent manner by 2-fold after SF treatment. Red box highlights the 44 genes which were also upregulated in the BT474 PTEN- LTT cell line. E) mRNA expression level of the 4 homeobox transcription factors which were functionally enriched from the

44 gene set. N=4. Data shown as average ± SD. # $p \leq 0.01$ from t test between BT474 and BT474 PTEN- LTT.

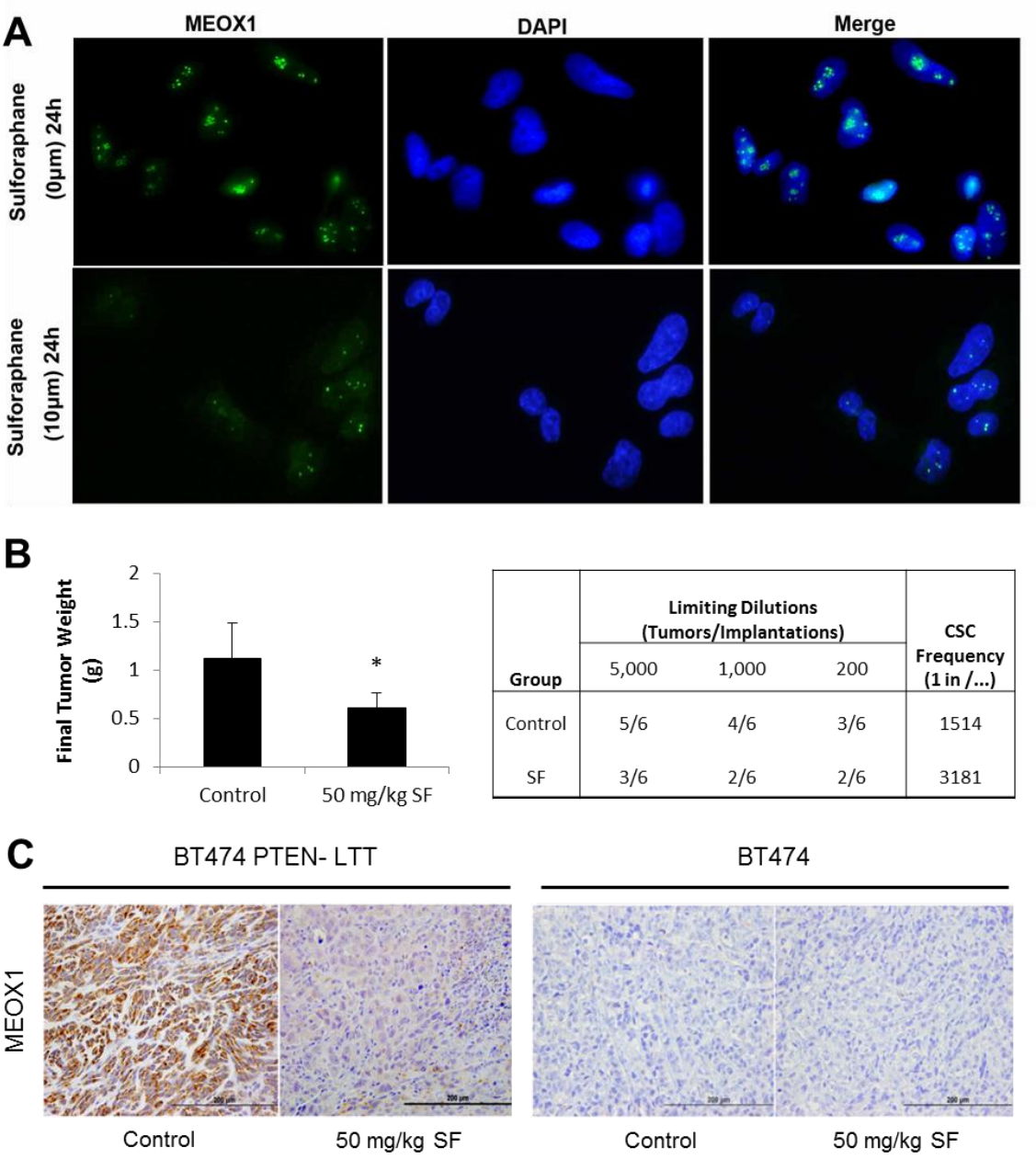

Figure 4.4 Sulforaphane inhibits MEOX1 protein expression in vitro and in vivo. A) Representative Immunofluorescent imaging of fixed BT474 PTEN- LTT cells following 24 hours in the presence of absence of SF. MEOX1 (green) resides primarily within the nucleus as evident by overlap with DAPI (Blue) staining. Images obtained originally with 40X objective. B) Left, final tumor of orthotopic mouse xenografts treated with daily I.P. administration of 0.9% saline or 50 mg/kg SF. N=5. Data shown as average ± SD. * $p \leq 0.05$. Right, tumor formation rates in secondary untreated mice 8 weeks following implantation of residual cells from primary tumors. C) Representative IHC staining of MEOX1 from control or SF treated primary xenografts counter stained with hematoxylin and eosin.

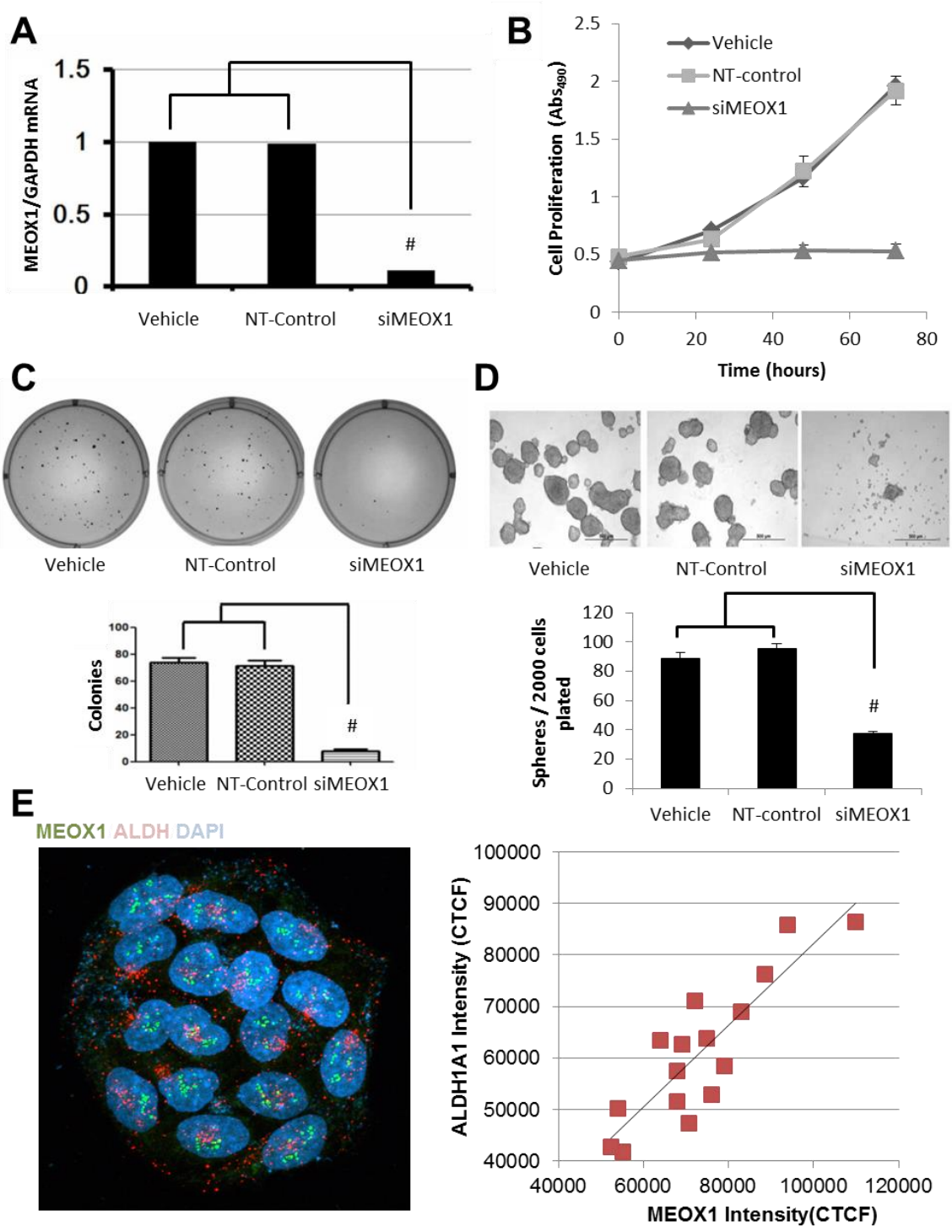

Figure 4.5 MEOX1 regulates bulk cell line proliferation and BCSCs in cell lines with reduced PTEN activity in vitro. A) Real time PCR analysis of MEOX1 mRNA expression relative to GAPDH in BT474 PTEN- LTT cells treated with transfection reagent (Vehicle), non-targeted siRNA control (NT-control), or siRNA for MEOX1 (siMEOX1). N=3. B) Proliferation of BT474 PTEN- LTT cells in the presence of

vehicle, NT-control, or siMEOX1 over the course of 42 hours as determined by MTS proliferation assay. N=3. C) Top, representative images of colonies formed after 14 days from BT474 PTEN- LTT cells treated with vehicle, NT-control, or siMEOX1for 24 hours. Bottom, quantification of number of colonies formed after 14 days of culture in soft agar. N=3. D) Top, representative images of mammospheres formed after 7 days from BT474 PTEN- LTT cells treated with vehicle, NT-control, or siMEOX1for 24 hours. Bottom, quantification of number of mammospheres formed after 7 days of culture in serum free non-adherent conditions. N=3. Data shown as average ± SD. * $p \leq 0.05$, # $p \leq 0.01$. E) Left, representative maximum intensity confocal microscopy image of MDA-MB-453 cell line stained for MEOX1 (Green), ALDH1A1 (Red), and DAPI (Blue). Right, corrected total cell fluorescence (CTCF) of MEOX1 and ALDH1A1 for each individual MDA-MB-453 shown. N=16. Spearman rho = 0.797, $p<0.01$.

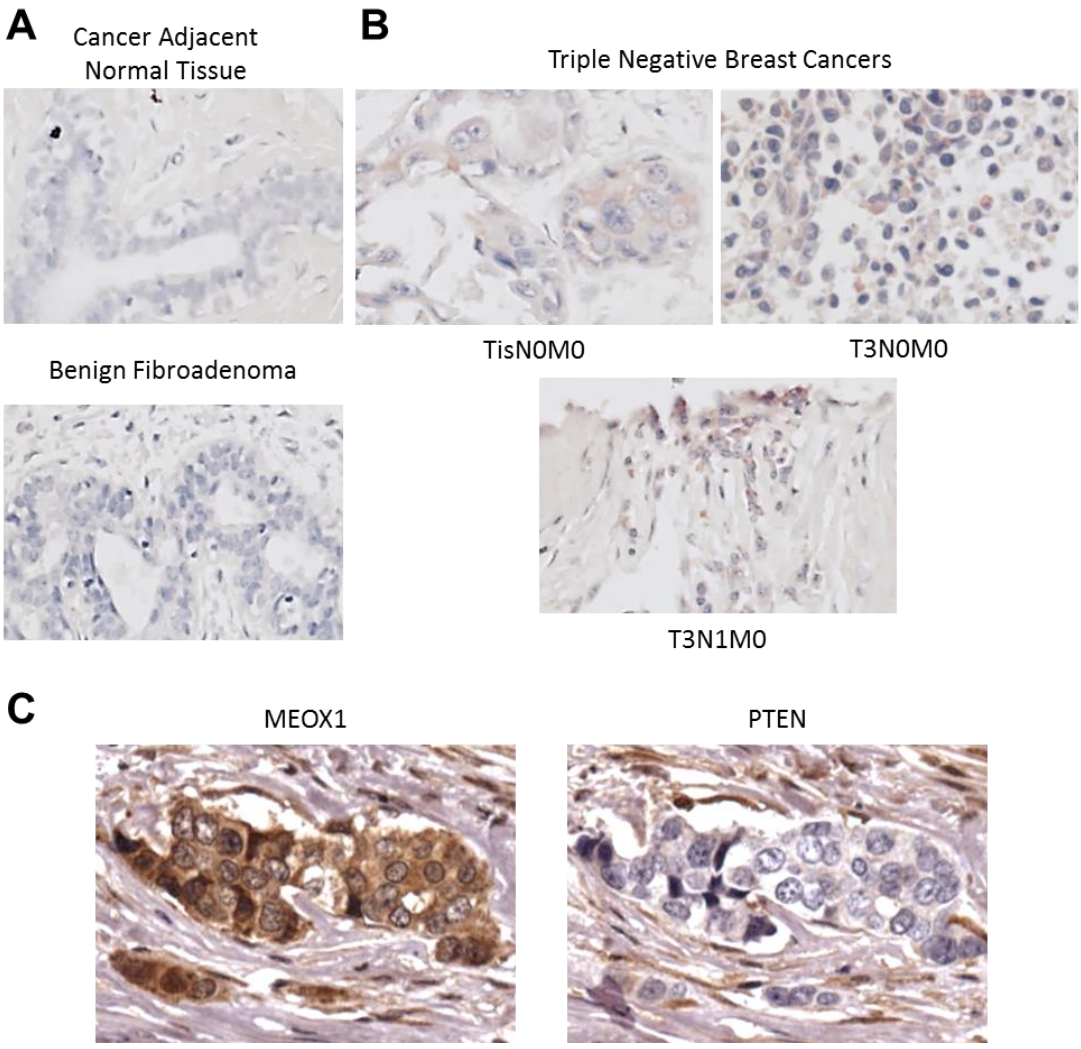

Figure 4.6 MEOX1 is present in a subset of TNBCs and is inversely correlated with PTEN expression. A) Representative immunohistochemical (IHC) staining of MEOX1 in cancer adjacent normal tissue and benign fibro adenomas in a 75 patients tissue microarray. No obvious staining was observed in these types of tissue. B) Representative image of 3/7 breast cancer tissues which stained positive for MEOX1, only TNBCs shown. T – size and invasive status of primary tumor, N – metastasis to regional lymph nodes, M – distant metastasis. C) Representative image of IHC staining in the same tissue for both MEOX1 and PTEN.

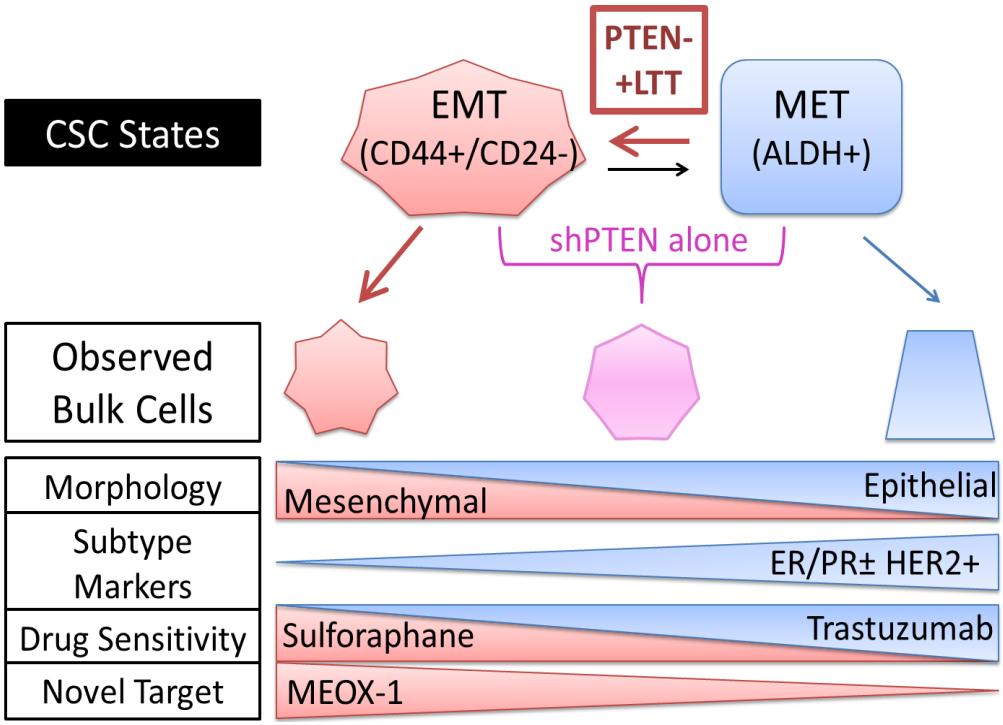

Figure 4.7 Proposed model of alterations in BT474 cells during generation of trastuzumab resistance. The parental trastuzumab sensitive BT474 (HER2+/PTEN+) cell line exhibits primarily epithelial morphology and are derived from an MET-like BCSC (ALDH+) (Blue). PTEN inactivation results in both EMT-like (CD44+/CD24-) and MET-like BCSC (ALDH+) that give rise to heterogeneous cell populations with both epithelial and mesenchymal characteristics (Pink). Trastuzumab treatment (to generate complete resistance) in the BT474 shPTEN cell line drives BCSCs to the EMT-like state that differentiate giving rise to a mesenchymal TNBC cell line (Red). These trastuzumab-resistant PTEN- breast cancers are sensitive to sulforaphane and upregulate MEOX1 to regulate bulk cell line proliferation and BCSCs.

Chapter 5

Conclusions

Summary of Findings and Clinical Implications

Due to advances in early diagnosis, surgical techniques, and the development of novel targeted therapeutic agents, overall survival of breast cancer patients has been steadily improving since the late 1980s (1). Advances in targeted therapies have also improved the quality of life for patients by reducing symptoms associated with conventional cytotoxic chemotherapies (2). However, in spite of all these improvements metastatic breast cancer is still largely an incurable disease. While targeted therapies have greatly benefited patients with Luminal A, Luminal B, and HER2+ breast cancers, no such therapies exist for the treatment of triple negative breast cancers (TNBCs) (3). Unfortunately for patients with advanced stage disease, once a malignancy becomes resistant to primary treatment relapse in additional lines of therapy often occur more rapidly (4). Throughout this dissertation it has been proposed that resistance after primary therapy can be predominantly explained by the expansion of breast cancer stem cells (BCSCs); in the case of trastuzumab resistance, this may actually alter the molecular subtype of the cancer.

In Chapter 2 of this dissertation we identify that cytotoxic chemotherapy with docetaxel increases CD44+/CD24-/EpCAM+ and ALDH+ BCSCs in TNBCs. This observation is proposed to occur through induced expression of IL-6 following therapy, which is known

to expand BCSCs (5, 6). Following a comprehensive evaluation of the efficacy of the natural product sulforaphane (SF) in the four major subtypes of breast cancer, we identify that SF preferentially inhibits TNBCs and HER2+ breast cancers with a concomitant activation of AKT (PI3K activating mutation of PTEN inactivation). Further, SF is capable of inhibiting ALDH+ BCSCs across breast cancer subtypes at concentrations >5-fold lower than the respective bulk cell line IC50. Inhibition of NF-kB by SF is evident by blockade of intracellular translocation following TNF-α stimulation and, at the transcriptional level, by reduction in an NF-kB reporter system and endogenous target IL-6. In combination SF potentiates docetaxel's efficacy in bulk cell lines, prevents docetaxel-induced IL-6 expression, and reduces the ALDH+ BCSC population in vitro. In an advanced treatment orthotopic mouse xenograft model, docetaxel reduces bulk tumor volume, but expands BCSCs as evident by extreme limiting dilution (ELDA) analysis in secondary mice. Treatment with combination therapy is more effective at reducing bulk tumor volume and BCSCs than any single agent.

These findings raise concern for continued use of docetaxel in the neo-adjuvant setting for TNBC patients. We propose a potential explanation to, and possible solution for, the so called "triple negative breast cancer paradox." This phenomenon is named for the observation that TNBCs tend to achieve higher rates of pathologic complete response (pCR) than other breast cancer subtypes, but those who do not exhibit pCR have worse overall survival following primary chemotherapy (7-9). In these patients docetaxel may increase BCSCs, leading to rapid recurrence at local and metastatic sites and ultimately reducing overall patient survival. By demonstrating that SF is capable of preventing this

phenomenon, we provide a convenient pharmacologic intervention which can supplement current clinical practice for more effective treatment of TNBCs.

In Chapter 3 of this dissertation we confirm previous studies demonstrating that generation of trastuzumab resistance in HER2+/PTEN- breast cancers induces the epithelial to mesenchymal transition (EMT) and expands CD44+/CD24- BCSCs (6, 10-12). Following induction of EMT trastuzumab-resistant, PTEN-deficient, cells adopt a triple negative phenotype in vitro and in vivo. This subtype switching from HER2+ to TNBC is associated with reduced expression of major ERBB family receptors and ligands, and activation of the IL-6/STAT3/NF-kB positive feedback loop. As in the case of TNBC from Chapter 2, we further demonstrate the ability of SF to inhibit NF-kB activity across breast cancer subtypes. We hypothesized that the efficacy of SF is determined by the relative dependence of a given cell line on NF-kB signaling for survival. While SF fails to eliminate HER2+/PTEN+ breast cancers in vitro it becomes increasingly effective as trastuzumab resistance develops, to the same extent as observed in the most sensitive cell lines from Chapter 2. Much like the efficacy in TNBCs docetaxel significantly reduces bulk tumor volume of trastuzumab-resistant breast cancer cell lines grown as xenografts, whereas for negative control xenografts trastuzumab has no effect on tumor volume. Interestingly, in this setting SF reduces bulk tumor volume to the same extent as docetaxel. Utilizing ELDA in secondary mice, we show that trastuzumab significantly increases the frequency of BCSCs whereas SF significantly reduces them. In trastuzumab-sensitive BT474 xenografts, SF only modestly reduces bulk tumor volume; this result is comparable to our observations of SF efficacy in the in vitro MTS assay. In an early treatment xenograft model, SF prevents the engraftment of

tumors in a dose-dependent manner for trastuzumab-resistant breast cancer; those tumors which do form progress at a dramatically slower rate. This phenomenon is persistent even after SF treatment is discontinued, confirming SF effectively reduces BCSCs in vivo.

These results have critical implications for the treatment of HER2+ breast cancers in late stage patients who exhibit PTEN inactivation. While in current practice the functional activity of PTEN is not considered when prescribing trastuzumab, our results suggest that in these patients trastuzumab treatment will ultimately lead to worse patient prognoses. We propose that this would be a result of EMT induction, expansion of BCSCs, and conversion of the disease to a triple negative phenotype. If this is ultimately true in trastuzumab-resistant PTEN- patients, it would imply that traditional second-line targeted therapies such as pertuzumab, TDM-1, and lapatinib would provide little benefit in the long run because they all rely on binding to HER2 (and EGFR in the case of lapatinib) and its expression would no longer be present. Due to the reliance of the transformed cells on the IL-6/NF-kB positive feedback loop we demonstrate that SF has a marked increase in efficacy after drug resistance has developed. Therefore, in the event that trastuzumab resistance develops in PTEN deficient patients, we have provided a rational therapy which can be exploited for further treatment.

In Chapter 4 of this dissertation we explore the possibility that trastuzumab-resistant breast cancers with PTEN inactivation may be dependent on more than just the IL-6/STAT3/NF-kB positive feedback loop. Strikingly, nearly 4,000 genes are differentially expressed between parental HER2+ BT474 and the trastuzumab-resistant BT474 generated by stable PTEN knockdown and long term culture with trastuzumab. We show

that the drug-resistant cell line has dramatically reduced expression of the ALDH enzymes which serve as markers for MET-like BCSCs, and higher expression of CD44 (with a concomitant reduction in CD24) which serves as a marker for EMT-like BCSCs. This suggests that the dynamics of BCSCs (13) may play a role in the generation of a TNBC phenotype, observed in Chapter 3, following trastuzumab resistance. In order to evaluate which genes are critical to proliferation and regulation of BCSCs in this model we exploit the fact that the trastuzumab-resistant cell line is remarkably more sensitive to SF. By RNA-sequencing analysis we identify that SF preferentially inhibits homeobox transcription factors in the drug-resistant cell line in both a time- and dose-dependent manner. Of these genes, MEOX1 was selected as the top candidate for further study. In order to demonstrate the SF-mediated suppression of MEOX1 at the protein level, we perform immunofluorescent staining in vitro and immunohistochemical staining of tumors from xenograft-bearing mice. Further, with siRNA knockdown we demonstrate that MEOX1 is functionally capable of regulating bulk cell line proliferation as well as BCSCs in vitro. Finally, knowing that SF is capable of inhibiting BCSCs across breast cancer subtypes and that MEOX1 was discovered in a TNBC cell line (generated by trastuzumab resistance), we expanded our search for potential applications of MEOX1-based therapies. Using confocal microscopy we demonstrate that MEOX1 is correlated with ALDH expression in an additional epithelial-like cell line harboring a PTEN inactivation mutation. Further, using a tissue micro array of patient samples we identify that MEOX1 is expressed in a subset of TNBCs and is inversely correlated with PTEN expression.

Using this unbiased approach we confirm our previous results in Chapter 3, indicating that trastuzumab resistance indeed results in the EMT, expands BCSCs, and converts HER2+ breast cancer to a TNBC subtype. If true in patients the use of trastuzumab in late stage HER2+ breast cancer patients with PTEN inactivation would ultimately be counterproductive in terms of improving long term survival. However, by coupling bulk cell line gene expression changes with those resulting from specific inhibition of the trastuzumab-resistant cell line we identify MEOX1 as a novel potential drug target for these patients. With MEOX1 capable of regulating both bulk cell line proliferation and BCSCs it may be unnecessary to use combination treatment strategies, such as those in Chapter 1, in these patients. Ultimately additional studies would be necessary to truly validate MEOX1 signaling as a bona fide drug target for the development of novel therapeutics. However, these studies provide a framework for future drug discovery efforts aimed at the treatment of trastuzumab resistance and potentially a subset of TNBCs.

References

1. Edwards BK, *et al.* (2014) Annual Report to the Nation on the status of cancer, 1975-2010, featuring prevalence of comorbidity and impact on survival among persons with lung, colorectal, breast, or prostate cancer. *Cancer* 120(9):1290-1314.
2. Lewis Phillips GD, *et al.* (2008) Targeting HER2-Positive Breast Cancer with Trastuzumab-DM1, an Antibody–Cytotoxic Drug Conjugate. *Cancer Research* 68(22):9280-9290.
3. Cardoso F, Castiglione M, & Group ObotEGW (2009) Locally recurrent or metastatic breast cancer: ESMO Clinical Recommendations for diagnosis, treatment and follow-up. *Annals of Oncology* 20(suppl 4):iv15-iv18.
4. Kassam F, *et al.* (2009) Survival Outcomes for Patients with Metastatic Triple-Negative Breast Cancer: Implications for Clinical Practice and Trial Design. *Clinical Breast Cancer* 9(1):29-33.

5. Kim S-Y, *et al.* (2013) Role of the IL-6-JAK1-STAT3-Oct-4 pathway in the conversion of non-stem cancer cells into cancer stem-like cells. *Cellular Signalling* 25(4):961-969.
6. Korkaya H, *et al.* (2012) Activation of an IL6 Inflammatory Loop Mediates Trastuzumab Resistance in HER2+ Breast Cancer by Expanding the Cancer Stem Cell Population. *Molecular Cell* 47(4):570-584.
7. Huober J, *et al.* (2010) Effect of neoadjuvant anthracycline–taxane-based chemotherapy in different biological breast cancer phenotypes: overall results from the GeparTrio study. *Breast Cancer Res Treat* 124(1):133-140.
8. Carey LA, *et al.* (2007) The Triple Negative Paradox: Primary Tumor Chemosensitivity of Breast Cancer Subtypes. *Clinical Cancer Research* 13(8):2329-2334.
9. von Minckwitz G, *et al.* (2012) Definition and Impact of Pathologic Complete Response on Prognosis After Neoadjuvant Chemotherapy in Various Intrinsic Breast Cancer Subtypes. *Journal of Clinical Oncology* 30(15):1796-1804.
10. Oliveras-Ferraros C, *et al.* (2012) Epithelial-to-mesenchymal transition (EMT) confers primary resistance to trastuzumab (Herceptin). *Cell Cycle* 11(21):4020-4032.
11. Bai W-D, *et al.* (2014) MiR-200c suppresses TGF-β signaling and counteracts trastuzumab resistance and metastasis by targeting ZNF217 and ZEB1 in breast cancer. *International Journal of Cancer* 135(6):1356-1368.
12. Lesniak D, *et al.* (2013) Spontaneous Epithelial-Mesenchymal Transition and Resistance to HER-2-Targeted Therapies in HER-2-Positive Luminal Breast Cancer. *PLoS ONE* 8(8):e71987.
13. Liu S, *et al.* (2014) Breast Cancer Stem Cells Transition between Epithelial and Mesenchymal States Reflective of their Normal Counterparts. *Stem Cell Reports* 2(1):78-91.